

AFATL-TR-85-12

A Fully Viscous Two-Dimensional Unsteady Flow Analysis Applied to Detonation Transition in Porous Explosives

Herman Krier
Laurence S Samuelson

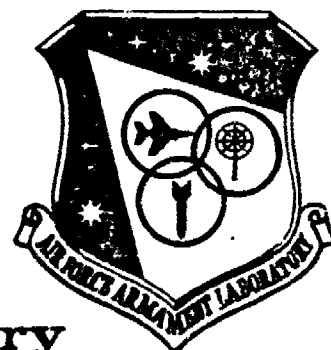
DEPARTMENT OF MECHANICAL AND INDUSTRIAL ENGINEERING
UNIVERSITY OF ILLINOIS AT URBANA-CHAMPAIGN

JUNE 1985

FINAL REPORT FOR PERIOD MAY 1982 - MARCH 1985

DTIC
ELECTE
JUL 15 1985
S **D**
G

Approved for public release; distribution unlimited



Air Force Armament Laboratory
AIR FORCE SYSTEMS COMMAND • UNITED STATES AIR FORCE • EGLIN AIR FORCE BASE, FLORIDA

85 06 21 01

AD-A157 794

DTIC FILE COPY

NOTICE

Please do not request copies of this report from the Air Force Armament Laboratory.
Additional copies may be purchased from:

National Technical Information Service
5285 Port Royal Road
Springfield, Virginia 22161

Federal Government agencies and their contractors registered with Defense Technical
Information Center should direct requests for copies of this report to:

Defense Technical Information Center
Cameron Station
Alexandria, Virginia 22314

Accession For	
NTIS GRA&I	<input checked="" type="checkbox"/>
DTIC TAB	<input type="checkbox"/>
Unannounced	<input type="checkbox"/>
Justification	
By _____	
Distribution/	
Availability Codes	
Dist	Avail and/or Special
A/1	



REPORT DOCUMENTATION PAGE				
1a. REPORT SECURITY CLASSIFICATION Unclassified AD-A 157 -794		1b. RESTRICTIVE MARKINGS None		
2a. SECURITY CLASSIFICATION AUTHORITY		3. DISTRIBUTION/AVAILABILITY OF REPORT Approved for Public Release; Distribution Unlimited		
2b. DECLASSIFICATION/DOWNGRADING SCHEDULE				
4. PERFORMING ORGANIZATION REPORT NUMBER(S) UILLU-ENG-84-4009		5. MONITORING ORGANIZATION REPORT NUMBER(S) AFATL-TR-85-12		
6a. NAME OF PERFORMING ORGANIZATION University of Illinois at Urbana-Champaign	6b. OFFICE SYMBOL (If applicable)	7a. NAME OF MONITORING ORGANIZATION Air Force Armament Laboratory		
6c. ADDRESS (City, State and ZIP Code) Urbana, Illinois 61801		7b. ADDRESS (City, State and ZIP Code) Eglin AFB FL 32542-5000		
8a. NAME OF FUNDING/SPONSORING ORGANIZATION Air Force Armament Laboratory	8b. OFFICE SYMBOL (If applicable) DLVY	9. PROCUREMENT INSTRUMENT IDENTIFICATION NUMBER F08635-82-K-0321		
8c. ADDRESS (City, State and ZIP Code) Eglin AFB FL 32542-5000		10. SOURCE OF FUNDING NOS.		
		PROGRAM ELEMENT NO. 62602F	PROJECT NO. 2543	TASK NO. 19
				WORK UNIT NO. 64
11. TITLE (Include Security Classification) (Over) A Fully Viscous Two-Dimensional Unsteady				
12. PERSONAL AUTHOR(S) Herman Krier and Martin R. Dahm				
13a. TYPE OF REPORT Final	13b. TIME COVERED FROM 5/82 TO 3/85	14. DATE OF REPORT (Yr., Mo., Day) 1984 Feb	15. PAGE COUNT 115	
16. SUPPLEMENTARY NOTATION The availability of this report is specified on verso of front cover.				
17. COSATI CODES			18. SUBJECT TERMS (Continue on reverse if necessary and identify by block number)	
FIELD	GROUP	SUB GR.		
06	21		Two-Dimensional Flow Porous Explosives	
19	04		Fully Viscous Unsteady Flow Warhead Damage	
			Detonation Transition Warhead Deflagrations	
19. ABSTRACT (Continue on reverse if necessary and identify by block number) This report describes significant new progress towards solving the two-dimensional fully viscous unsteady flow in a reactive solid/gas mixture. The results demonstrate that it may be possible to predict whether a warhead with case failure (and filled with fragmented high explosive) will produce a low order detonation which is weaker than the one required to damage a structure. The loss of mass, momentum, and energy through a warhead case opening is a multi-dimensional problem even though the reaction front may progress axially through the damaged explosive. Mass is ejected in a basically radial direction and necessitates a multi-dimensional problem formulation in order to model the deflagration to detonation transition event accurately enough to make meaningful predictions. The appropriate equations of state and continuity equations are formulated and are solved by a finite differencing scheme. Run-up length to detonation in the fragmented explosive bed from a case opening through which mass is ejected should be married with a model of probabilistic case failure on impact to predict warhead lethality.				
20. DISTRIBUTION/AVAILABILITY OF ABSTRACT UNCLASSIFIED/UNLIMITED <input checked="" type="checkbox"/> SAME AS RPT. <input type="checkbox"/> DTIC USERS <input type="checkbox"/>			21. ABSTRACT SECURITY CLASSIFICATION Unclassified	
22a. NAME OF RESPONSIBLE INDIVIDUAL Mark A. Amend			22b. TELEPHONE NUMBER (Include Area Code) (904) 882-8302	22c. OFFICE SYMBOL AFATL/DLYV

Unclassified

SECURITY CLASSIFICATION OF THIS PAGE

Item 11, Continued: Flow Analysis Applied To Detonation Transition In Porous Explosives

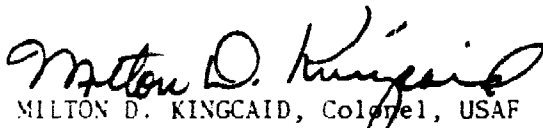
PREFACE

This report documents work performed during the period May 1982 to March 1985 by the University of Illinois, Urbana-Champaign, Illinois, under Research Contract F08635-82-K-0321 with the Air Force Armament Laboratory, Eglin Air Force Base, Florida. Mr Mark Amend monitored the program for the Armament Laboratory.

The Public Affairs Office has reviewed this report, and it is releasable to the National Technical Information Service (NTIS), where it will be available to the general public, including foreign nationals.

This technical report has been reviewed and is approved for publication.

FOR THE COMMANDER



MILTON D. KINGCAID, Colonel, USAF
Chief, Analysis & Strategic Defense Division

TABLE OF CONTENTS

Section	Title	Page
I	INTRODUCTION.....	1
II	FUNDAMENTAL CONCEPTS FOR THE TWO DIMENSIONAL MODEL.....	5
	Introduction.....	5
	Assumptions.....	5
	Domain of the Model.....	7
	Conservation Equations.....	8
	Constitutive Equations (Closure).....	13
	Boundary Conditions.....	14
	Initial Conditions.....	17
III	DERIVATION OF THE TWO DIMENSIONAL AXISYMMETRIC CONSERVATION EQUATIONS.....	18
IV	NUMERICAL INTEGRATION TECHNIQUE.....	39
	Introduction.....	39
	Domain Discretization.....	39
	The Finite Difference Equations.....	43
	Boundary Conditions.....	43
	Stability.....	53

TABLE OF CONTENTS (CONCLUDED)

Section	Title	Page
V	PRELIMINARY COMPUTATIONS.....	57
	The Computer Program.....	57
	The Baseline Case.....	59
	Test Computations.....	62
	Possible Follow Up.....	65
	REFERENCES.....	68
APPENDIX		
A	AUXILIARY DATA BASE AND CONSTITUTIVE RELATIONS.....	70
B	FINITE DIFFERENCE FORM OF THE CONSERVATION EQUATIONS.....	74
C	COMPUTER CODE LISTING.....	79

LIST OF FIGURES

Figure	Title	Page
1	Damage to GP Warhead from Impact with Hardened Target [Notice the assumed metal case failure and internal high explosive fracture.].....	2
2	Schematic Representation of the Two Dimensional Domain with a Ring-Shaped Opening.....	9
3	Boundary Conditions Imposed on the Two Dimensional Domain ($0 \leq r \leq R$ and $0 \leq z \leq L$).....	15
4	Typical Two Dimensional Finite Difference Cell Utilizing the Staggered Grid.....	40
5	The Staggered Grid Applied to the Two Dimensional Domain [Heavy border indicates the location of the boundaries while dashed border represents the opening in the container wall.].....	42
6	Symmetry Boundary Conditions Applied at the Center Line, $r = 0$	45
7	Implementation of Symmetry Boundary Conditions at the Near End Wall, $z = 0$	45
8	Application of the Radiative Boundary Conditions to the Far End Wall, $z = L$	47
9	No-Slip Boundary Condition Employed Along with the Circumferential Wall, $r = R$, for $0 \leq z \leq z_c$ and $z_c + \Delta z_c \leq z \leq L$	47
10	Boundary Conditions Applied at the Opening in the Circumferential Wall, $r = R$ for $z_c \leq z \leq z_c + \Delta z_c$	52
11	Two Dimensional Baseline Case Initial Temperature Profile.....	61
12	Two Dimensional Baseline Case Initial Pressure Profile.....	61
13	Comparison of the Flame Front Locations Predicted by Inviscid One Dimensional Simulations.....	63

LIST OF FIGURES (concluded)

- 14 Flame Front Locus Showing the Transition from a
Two-Dimensional Initiation to One Dimensional Flow....64

- 15 Viscous Gas Radial Velocity Profile at $t = 11.33 \mu s$
[Notice the severe oscillations which occur ahead of
the steep gradient.].....66

SECTION I

INTRODUCTION

General purpose (G:) warheads applied against enemy installations can produce devastating effects. The best results are obtained through maximum reliability of conventional explosive penetration and detonation. However, advances in target hardening technology have created conditions where such warheads may fail to meet this goal. Prior to fuze initiation, metal containment wall failure and fragmentation of the high explosive can result from the impact forces between the warhead and a hardened target as shown in Figure 1. The detonation that is expected to occur under totally confined conditions may be reduced to an unsteady, rapid deflagration with much less damage to the target. The principal motivation for the work presented here is the development of a model which can be used to predict whether detonation will occur within the ruptured warhead filled with fragmented high explosives.

Understanding the fluid mechanics of flame spreading through a porous reactive solid medium has been the subject of considerable research at the University of Illinois at Urbana-Champaign. Under the direction of Dr. Herman Krier, much work has been done in the analysis of these complex flows. A strong background for the research presented in this report was provided by the earlier efforts of: Van Tassell and Krier (Reference 1); Krier and Gokhale (Reference 2); Krier, Rajan, and Van Tassell (Reference 3); Dimitstein (Reference 4); Krier, Dimitstein, and Gokhale (Reference 5); Krier, Gokhale, and Hughes (Reference 6); Krier and Kezerle (Reference 7); Butler, Krier, and Lembeck (Reference 8); and Krier, Dahm, and Butler (Reference 9).

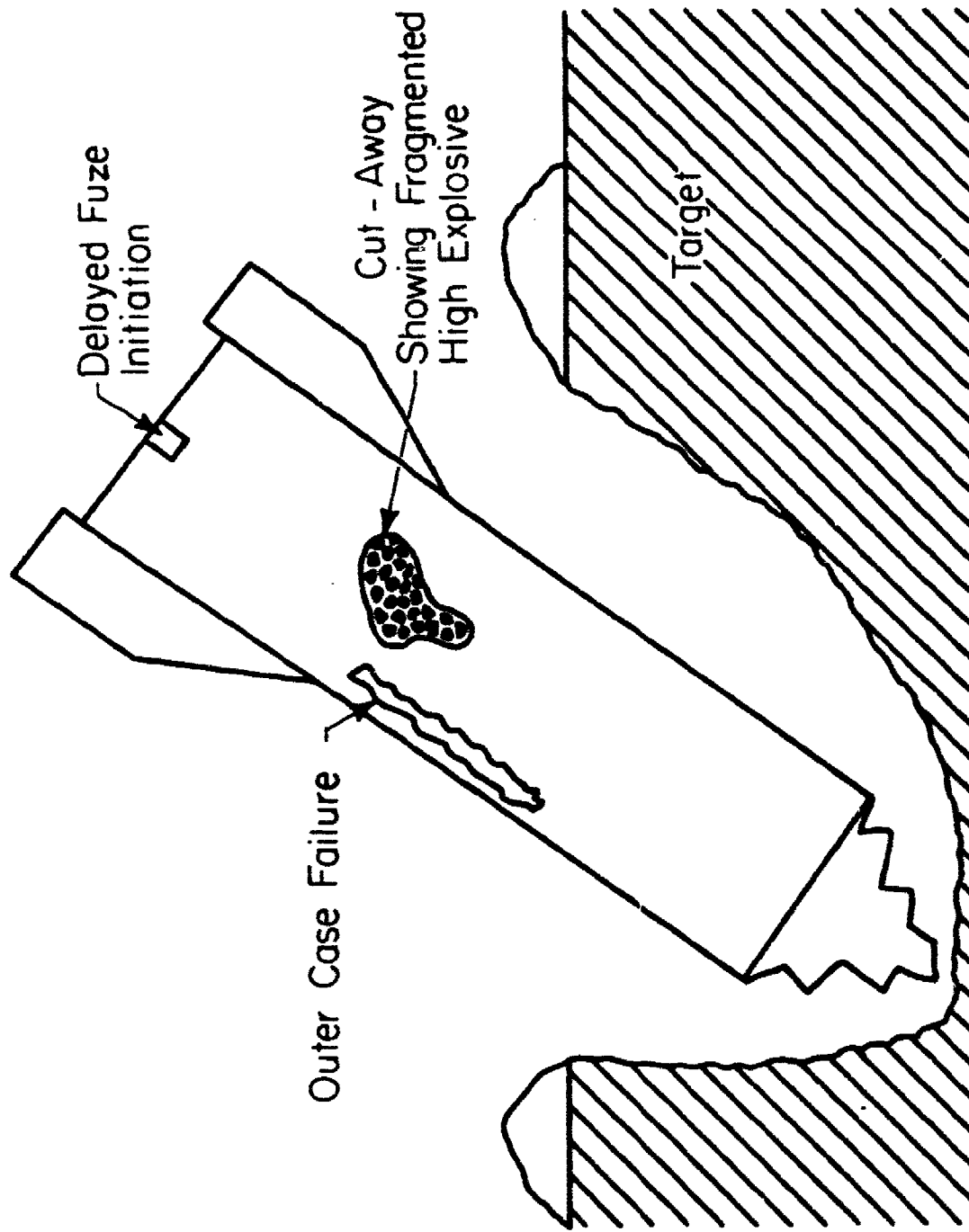


Figure 1. Damage to GP Warhead from Impact with Hardened Target
[Notice the assumed metal case failure and internal high explosive fracture.]

The culmination of these previous studies has been the development of one dimensional, numerical models of the transient events of deflagration to detonation transition. The computational representation solves the inviscid conservation equations using finite difference techniques. The codes developed in References 7-9 can accurately simulate shock formation within the fragmented propellant or explosives, and are used to depict DDT-deflagration to detonation transition. The delay of DDT resulting from the loss of mass through the container walls was modeled by a quasi one-dimensional analysis by including sink terms in the mass and momentum conservation equations (Reference 9). Significant detonation delays for a variety of input conditions have been calculated from this quasi one-dimensional code (Reference 8, 9).

However, the loss of mass, momentum, and energy through an opening in the casing is a multi-dimensional phenomenon. Even though the reaction front progresses axially through the damaged warhead, the mass is basically ejected in the radial direction. This turning of the flow is accomplished by changes in momentum and energy which cannot be described accurately by a one-dimensional representation. A multi-dimensional model is therefore needed to provide a much more accurate description of the effects of mass loss prior to the prediction of any steady detonation. The research described in the following chapters is intended to provide the foundation for such an analysis.

Three-dimensional flame spreading analyses are now being investigated in great detail by Dahm (Reference 10) and have been reported by Markatos and Kirkcaldy (Reference 11). The Dahm version simulates flow through a fragmented solid explosive inside a container by solving all the inviscid conservation equations. These relations are a coupled set of non-linear, hyperbolic partial differential equations which are solved using finite difference

techniques. However, and as expected, the numerical scheme requires enormous amounts of computer memory due to the fine grid resolution needed and other intricacies of the problem. Consequently, computation costs are very high. The Markatos and Kirkcaldy model attempts to simulate flame spreading in a bed of solid propellant grains used as a gun charge. That study utilized many of the concepts presented in Reference 3, and lacks the complexities associated with radial venting.

This study presents the analysis for the two dimensional flow inside a ruptured bed of granulated high explosive. Although requiring the assumption of a circumferential crack, the model does account for radial components of the flow. Therefore, it will be possible to describe the turning transitions taking place as mass vents through the rip in the casing surrounding the explosive bed. True non-planar burn initiation and early flame spreading transients can also be modeled, but most importantly, the two dimensional model features will also include viscous gas effects. This creates a more realistic flow simulation by satisfying the no-slip velocity boundary condition at the gas-wall interface, a process not considered by either Dahm (Reference 10) or Markatos and Kirkcaldy (Reference 11). This greatly complicates the differential equations representing momentum and energy conservation, because new second derivative terms must be numerically differenced.

The complete two-dimensional model is presented in the following section. Included are the necessary assumptions, boundary conditions, and conservation equations for the problem. The detailed derivation of these governing relations is analyzed in Section III. Section IV deals with the manner in which these equations are solved, by describing the numerical integration scheme. The computer code, preliminary results, and topics for possible future work are presented in Section V.

SECTION II

FUNDAMENTAL CONCEPTS FOR THE TWO-DIMENSIONAL MODEL

INTRODUCTION

The two-dimensional model described below is a mathematical representation of the two-phase (solid-gas) fluid mechanics within an impact-damaged warhead. First, initial and boundary conditions are imposed on the problem. Then, partial differential equations and algebraic relations describing the flow are applied to all points in the domain. Finally, a numerical differencing method is utilized to solve the system. This section will present the formulation of the two dimensional model, while a derivation of the governing conservation equations is examined in the next chapter.

ASSUMPTIONS

Before attempting the representation of two dimensional flame spreading, it is necessary to make several assumptions about the flow conditions. These are:

1. Warhead damage occurs prior to fuze initiation.

The model presented here simulates the fluid mechanics in a ruptured bomb only and does not include any treatment of the time-dependent case failure. The impact with the target, case fracture, and fragmentation of the high explosive take place prior to time $t=0$.

2. A circumferential crack is produced by the force of the concussion.

A ring-shaped opening must be considered in order to yield a two-dimensional representation of the damaged weapon. While this effectively slices the casing into two portions, it must be assumed that structural integrity is still maintained, and the size of the crack remains constant.

3. The explosive particles are treated as uniform spheres.

The shock of the warhead's impact causes granulation of the solid explosive. The resulting fragments have a high surface-to-volume ratio, and can be considered to be millimeter or sub-millimeter spheres.

4. The separated two-phase analysis is used.

This formulation considers each component as an individual fluid, with the particles treated as a pseudo-fluid (Reference 7). Each phase has its own set of conservation equations, with coupling terms to account for interactions between the solid and the gas.

5. The particles are uniformly distributed at time $t=0$.

It is assumed that the spherical particles are initially packed in a modified face centered cubic arrangement, with porosity (the ratio of gas volume to total volume) typically ranging from 0.2 to 0.3. However, porosity will change with time, due to combustion and rapid pressure increases which compress the granules.

6. The particles burn in compliance with an assumed ignition criteria and combustion rate law.

If a particle exceeds a specified input energy (or temperature), it ignites and starts producing gas. The burning rate of the explosive is described by $\dot{r} = bP^n$ with b and n being material constants. When the porosity reaches approximately 0.99, the particles are assumed to be burned out and gas production ceases. The fuse initiation at time $t=0$ is simulated by a zone of particles with temperatures already high enough to satisfy the ignition condition.

7. The gas phase obeys a non-ideal equation of state.

The two dimensional model utilizes a co-volume approach to account for molecular interactions of the gas.

8. Interphase heat transfer is accomplished through convection only.

Energy transport due to conduction and radiation effects is neglected in this analysis. Heat transfer takes place solely through convection. (See Reference 7.)

9. The flow through the damaged warhead is generally laminar.

The major source of turbulence is the two-phase nature of the flow. Gas moves around the spherical granules creating local disturbances and instabilities in its wake. However, the fluid properties are averaged over the entire control volume, and the turbulent fluctuations cancel out.

DOMAIN OF THE MODEL

The domain of the two dimensional model is prescribed by the geometry of the damaged warhead. The warhead is presented as a right circular cylinder

having solid, closed ends. The circumferential wall is also impermeable, except at the opening where mass can be ejected. This crack in the casing must be ring-shaped in order to preserve the two-dimensional nature of the problem.

The domain is axisymmetric as illustrated in Figure 2. The radial coordinate ranges from $r=0$ at the center line to $r=R$ at the circumferential container wall. The axial coordinate extends from the near end, at $z=0$, to the far end, at $z=L$. The crack begins at $z=z_c$ and its length is Δz_c .

CONSERVATION EQUATIONS

The fundamental relations needed for the analysis of fluid motion in the ruptured bomb are presented here and are derived in Section III. These equations which govern the conservation of mass, momentum, and energy must be satisfied at all points in the domain. Separated flow concepts require that a complete set of these relations be written for each phase with coupling terms added to represent particle-gas interaction. If viscous gas effects are also included, this forms a system of eight second order nonlinear partial differential equations.

The relations listed below were derived in cylindrical coordinates due to the axisymmetric geometry of the problem. The necessary interphase coupling terms (see Reference 7) are represented by:

Γ_c - the gas production rate from the burning particles,

D - the interphase drag,

and \dot{Q} - the convective heat transfer between the two constituents.

2-DIMENSIONAL MODEL

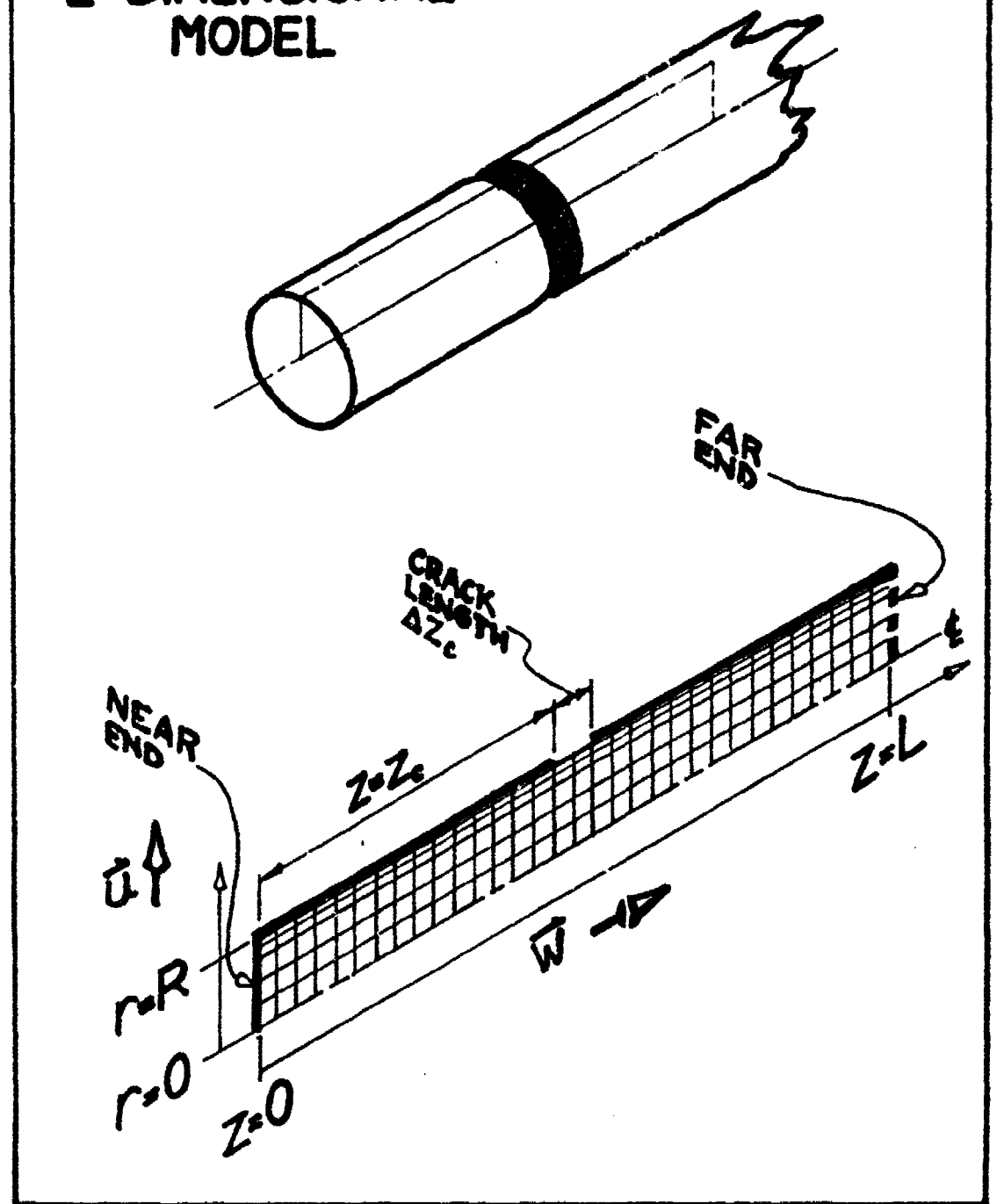


Figure 2. Schematic Representation of the Two Dimensional Domain with a Ring-Shaped Opening

Subscripts g and p indicate the gas and particle phases respectively, while r and z denote radial and axial directions. Bulk densities are defined as:

$$\rho_1 = \phi \rho_g \quad (1)$$

$$\rho_2 = (1 - \phi) \rho_p \quad (2)$$

where the porosity, ϕ , as stated earlier, represents the ratio of the gas volume to the total volume. The two-dimensional conservation equations are (see Section III):

Conservation of Mass (Gas Phase)

$$\frac{\partial \rho_1}{\partial t} = - \frac{1}{r} \frac{\partial}{\partial r} (\rho_1 r u_g) - \frac{\partial}{\partial z} (\rho_1 w_g) + r_c \quad (3)$$

Conservation of Mass (Particle Phase)

$$\frac{\partial \rho_2}{\partial t} = - \frac{1}{r} \frac{\partial}{\partial r} (\rho_2 r u_p) - \frac{\partial}{\partial z} (\rho_2 w_p) - r_c \quad (4)$$

Conservation of Momentum (Gas Phase)

Radial Direction

$$\begin{aligned} \frac{\partial}{\partial t} (\rho_1 u_g) = & - \frac{1}{r} \frac{\partial}{\partial r} (\rho_1 r u_g^2) - \frac{\partial}{\partial z} (\rho_1 u_g w_g) \\ & + \mu_g \left\{ \frac{\partial}{\partial r} \left[\frac{1}{r} \frac{\partial}{\partial r} (r u_g) \right] + \frac{\partial^2 u_g}{\partial z^2} + \frac{1}{3} \frac{\partial}{\partial r} \left[\frac{1}{r} \frac{\partial}{\partial r} (r u_g) \right] \right\} \end{aligned} \quad (5)$$

$$+ \frac{\partial w_g}{\partial z} \}} + r_c u_p - D_r - \frac{\partial}{\partial r} (p_g \phi)$$

Axial Direction

$$\begin{aligned} \frac{\partial}{\partial t} (\rho_1 w_g) &= - \frac{1}{r} \frac{\partial}{\partial r} (\rho_1 r u_g w_g) - \frac{\partial}{\partial z} (\rho_1 w_g^2) \\ &+ u_g \left\{ \frac{1}{r} \frac{\partial}{\partial r} (r \frac{\partial w_g}{\partial r}) + \frac{\partial^2 w_g}{\partial z^2} + \frac{1}{3} \frac{\partial}{\partial z} \left[\frac{1}{r} \frac{\partial}{\partial r} (r u_g) + \frac{\partial w_g}{\partial z} \right] \right\} \\ &+ r_c w_p - D_z - \frac{\partial}{\partial z} (p_g \phi) \end{aligned} \quad (6)$$

Conservation of Momentum (Particle Phase)

Radial Direction

$$\begin{aligned} \frac{\partial}{\partial t} (\rho_2 u_p) &= - \frac{1}{r} \frac{\partial}{\partial r} (\rho_2 r u_p^2) - \frac{\partial}{\partial z} (\rho_2 u_p w_p) \\ &- r_c u_p + D_r - \frac{\partial}{\partial r} [p_p (1 - \phi)] \end{aligned} \quad (7)$$

Axial Direction

$$\begin{aligned} \frac{\partial}{\partial t} (\rho_2 w_p) &= - \frac{1}{r} \frac{\partial}{\partial r} (\rho_2 r u_p w_p) - \frac{\partial}{\partial z} (\rho_2 w_p^2) \\ &- r_c w_p + D_z - \frac{\partial}{\partial z} [p_p (1 - \phi)] \end{aligned} \quad (8)$$

Conservation of Energy (Gas Phase)

$$\begin{aligned}
 \frac{\partial}{\partial t} (\rho_1 E_g) = & - \frac{1}{r} \frac{\partial}{\partial r} [\rho_1 r u_g (E_g + \frac{P_g}{\rho_g})] - \frac{\partial}{\partial z} [\rho_1 w_g (E_g + \frac{P_g}{\rho_g})] \\
 & + u_g \{ 2 [(\frac{\partial u_g}{\partial r})^2 + (\frac{u_g}{r})^2 + (\frac{\partial w_g}{\partial z})^2] - \frac{2}{3} (\frac{\partial u_g}{\partial r} + \frac{u_g}{r} + \frac{\partial w_g}{\partial z})^2 \\
 & + (\frac{\partial w_g}{\partial r} + \frac{\partial u_g}{\partial z})^2 + u_g \frac{\partial}{\partial r} [\frac{1}{r} \frac{\partial}{\partial r} (r u_g)] + u_g \frac{\partial^2 u_g}{\partial z^2} \\
 & + \frac{u_g}{3} \frac{\partial}{\partial r} [\frac{1}{r} \frac{\partial}{\partial r} (r u_g) + \frac{\partial w_g}{\partial z}] + \frac{w_g}{r} \frac{\partial}{\partial r} (r \frac{\partial w_g}{\partial r}) + w_g \frac{\partial^2 w_g}{\partial z^2} \\
 & + \frac{w_g}{3} \frac{\partial}{\partial z} [\frac{1}{r} \frac{\partial}{\partial r} (r u_g) + \frac{\partial w_g}{\partial z}] \} - \dot{Q} - D_r u_p \\
 & - D_z w_p + r_c (E_g^{\text{chem}} + \frac{u_p^2}{2} + \frac{w_p^2}{2})
 \end{aligned} \tag{9}$$

Conservation of Energy (Particle Phase)

$$\begin{aligned}
 \frac{\partial}{\partial t} (\rho_2 E_p) = & - \frac{1}{r} \frac{\partial}{\partial r} [\rho_2 r u_p (E_p + \frac{P_p}{\rho_p})] - \frac{\partial}{\partial z} [\rho_2 w_p (E_p + \frac{P_p}{\rho_p})] \\
 & + \dot{Q} + D_r u_p + D_z w_p \\
 & + r_c (E_p^{\text{chem}} - \frac{u_p^2}{2} - \frac{w_p^2}{2})
 \end{aligned} \tag{10}$$

In Equations (9) and (10), the total energies are defined as:

$$E_g = C_{v_g} T_g + \frac{u_g^2}{2} + \frac{w_g^2}{2} \quad (11)$$

$$E_p = C_{v_p} T_p + \frac{u_p^2}{2} + \frac{w_p^2}{2} \quad (12)$$

CONSTITUTIVE EQUATIONS (Closure)

The conservation of mass, momentum, and energy, in the two dimensional model is described by eight nonlinear partial differential equations containing eleven unknown quantities, namely: ρ_g , ρ_p , u_g , u_p , w_g , w_p , P_g , P_p , T_g , T_p , and ϕ . Consequently, three additional relations are required to provide closure for the system:

1. An equation of state for the gas phase
2. An equation of state for the particle phase
3. A procedure for determining porosity as a function of local stress conditions.

In addition, several constitutive relations are necessary in order to accurately represent the source/sink terms. These include:

1. An equation determining the gas production rate from the burning explosive
2. An equation for the gas viscosity coefficient
3. A relation describing the interphase drag
4. A gas-particle convective heat transfer equation.

The specific relations which were used in this work were taken from Reference 8 and are described in Appendix A.

BOUNDARY CONDITIONS

The conservation relations presented in Section II are nonlinear partial differential equations. In general, there are a very large number of entirely different possible solutions for such a system*. Finding a unique solution for these equations requires specific knowledge of the physical characteristics of the problem. This information is provided by the boundary conditions.

For the two dimensional model shown in Figure 3, five conditions must be specified. These are:

1. At the Center Line ($r=0$, $0 \leq z \leq L$)

Since the damaged warhead is depicted as a right circular cylinder with a ring shaped opening, the domain is symmetric about the center line. Consequently, there can be no flux across this border, although the flow can move parallel to it. All radial velocity components are set equal to zero, as are all gradients taken across this boundary.

* For example, the functions

$u = x^2 - y^2$ $u = e^x \cos y$ $u = \ln(x^2 + y^2)$
are all possible solutions of the second order Laplace equation,

$$\partial^2 u / \partial x^2 + \partial^2 u / \partial y^2 = 0$$

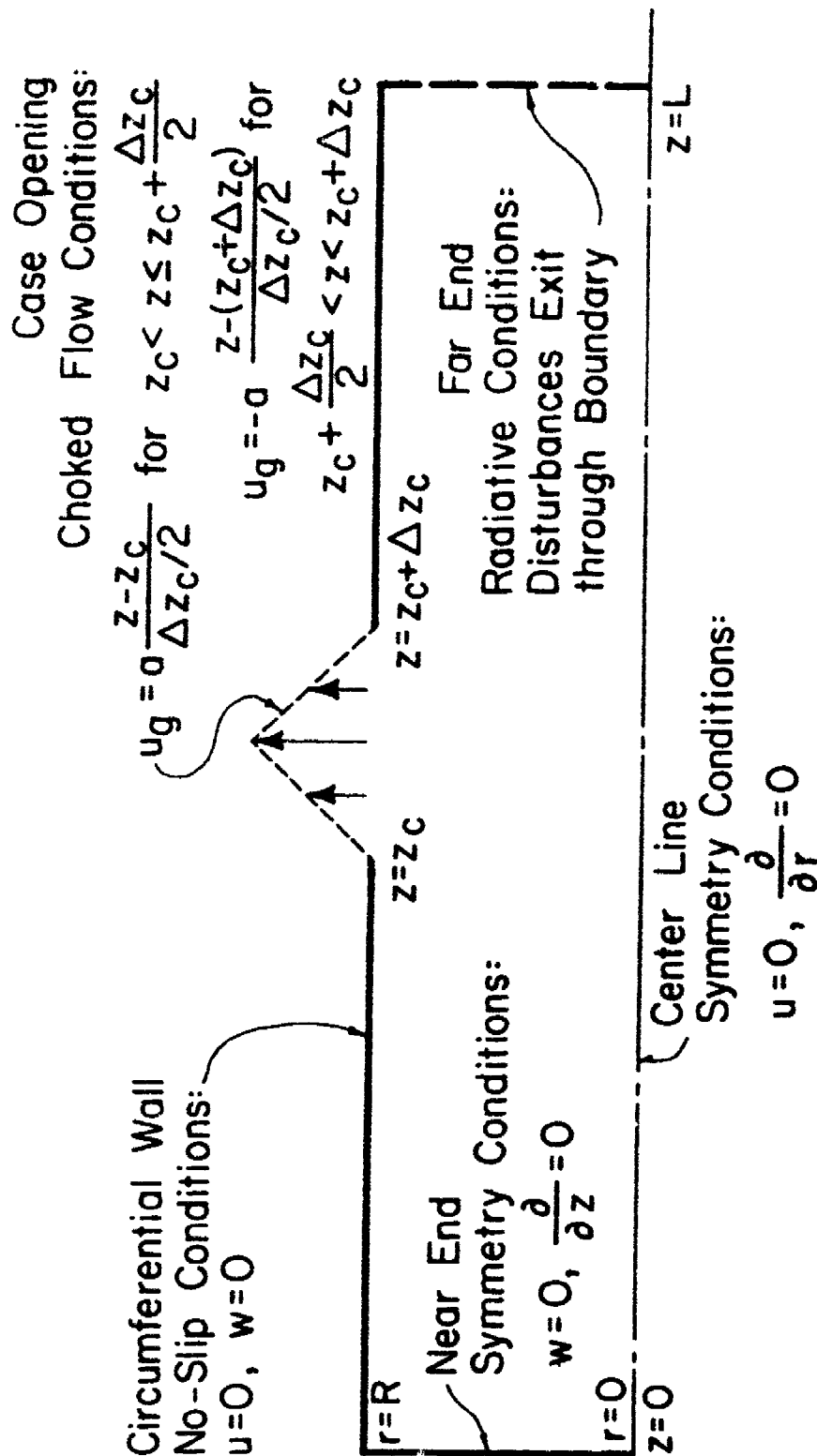


Figure 3. Boundary Conditions Imposed on the Two Dimensional Domain
($0 \leq r \leq R$ and $0 \leq z \leq L$)

2. At the Near End ($z=0, 0 \leq r \leq R$)

It is assumed that symmetry conditions also prevail along this boundary. While this would actually require the inclusion of an additional crack located outside the domain, these conditions will also be used to represent a solid wall where slip is allowed. Flow can move along the boundary but cannot pass through it, since axial velocity components and gradients are equal to zero.

3. At the Far End ($z=L, 0 \leq r \leq R$)

Here a radiative boundary condition is applied, allowing all disturbances to pass through the wall as if it did not exist. The solid end is assumed to be farther downstream outside the domain.

4. At the Circumferential Wall ($r=R, 0 \leq z \leq z_c \quad z_c + \Delta z \leq z \leq L$)

This is a solid wall, requiring the radial velocity component to be set equal to zero. However, the no-slip condition is also applied at this boundary. Note that now the axial velocities are forced to zero as well.

5. At the Opening ($r=R, z_c \leq z \leq z_c + \Delta z_c$)

It is very difficult to define a boundary condition applicable at the crack due to the unknown status of the flow beyond the opening. The radial velocity of the gas at the hole is determined by assuming the flow is choked. This maximum value is located at the center of the crack, and a linear profile is assumed, in order to lower the velocity to zero at the edges

of the opening. The radial component of the particle velocity can then be found by applying the interphase drag constitutive relation as described by Krier, Dahm, and Samuelson (Reference 12). The drag force on the solids produces a change in momentum which is used to predict a particle velocity at the tear.

The specific details of how these boundary conditions are included in the two dimensional model are explained in Chapter Four which deals with the numerical methods employed to solve the problem.

INITIAL CONDITIONS

Initial conditions represent boundaries with respect to time and are applied at the start of the simulation. Initially, all velocities are set equal to zero. Above-ambient temperatures and pressures are determined from polynomial profiles, with several particles assumed to exceed the ignition temperature criteria and thus burning. Initial gas density values are computed from the equation of state, while the solid phase density is an input parameter. The porosity and particle radius are also initially prescribed and assumed constant throughout the bed at time $t=0$.

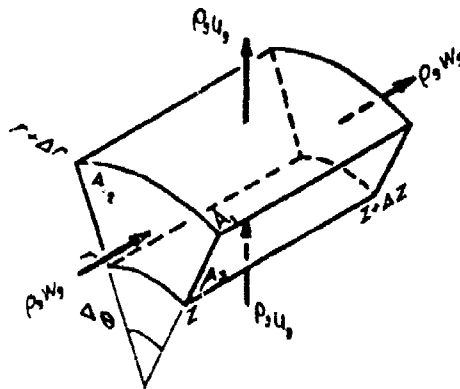
SECTION III

DERIVATION OF THE TWO DIMENSIONAL AXISYMMETRIC CONSERVATION EQUATIONS

The relations describing the conservation of mass, momentum, and energy in the two-dimensional model were presented in the previous section as Equations (3) - (10). The derivation of these governing equations is discussed here, and follows much of the logic used by Krier and Kezerle (Reference 7) for the one-dimensional flow process. But additional complexities due to the treatment of a viscous gas and the cylindrical geometry of the domain will now be incorporated into the analysis. The resulting system consists of eight second order, coupled, nonlinear partial differential equations.

1. CONSERVATION OF MASS

a. Gas Phase Continuity



Consider the control volume shown, with gas flowing through the control surfaces

Since,

$$\begin{array}{ccccccc} \text{Rate of Mass} & & \text{Rate of} & & \text{Rate of} & & \text{Rate of Mass} \\ \text{Accumulation} & = & \text{Mass in} & - & \text{Mass out} & + & \text{Generation} \end{array}$$

Then,

$$\begin{aligned} \frac{a(\rho_g V_g)}{\partial t} &= (\rho_g u_g A_{1g})_r - (\rho_g u_g A_{1g})_{r+\Delta r} + (\rho_g w_g A_{2g})_z \\ &\quad - (\rho_g w_g A_{2g})_{z+\Delta z} + r_c V \end{aligned} \quad (13)$$

where: ρ_g = gas density
 A_{1g} = cross sectional area of gas-radial direction
 A_{2g} = cross sectional area of gas-axial direction
 V_g = volume of gas within control volume
 V = total volume of control volume
 u_g = radial velocity of gas
 w_g = axial velocity of gas
 r_c = gas generation due to combustion of solid particles

From the geometry of the control volume:

$$\begin{aligned} V &= r \Delta r \Delta \theta \Delta z \\ A_1 &= r \Delta \theta \Delta z \\ A_2 &= r \Delta r \Delta \theta \end{aligned} \quad (14)$$

Now with the definition of porosity $\phi = \frac{V_g}{V}$

$$\begin{aligned}
V_g &= \phi r \Delta r \Delta \theta \Delta z \\
A_{1g} &= \phi r \Delta \theta \Delta z \\
A_{2g} &= \phi r \Delta r \Delta \theta
\end{aligned}
\tag{15}$$

Substitute back for A_{1g} , A_{2g} , V_g , and V to get

$$\begin{aligned}
\frac{\partial (\rho_g \phi r \Delta r \Delta \theta \Delta z)}{\partial t} &= (\rho_g u_g \phi r \Delta \theta \Delta z)_r - (\rho_g u_g \phi r \Delta \theta \Delta z)_{r+\Delta r} \\
&\quad + (\rho_g w_g \phi r \Delta r \Delta \theta)_z - (\rho_g w_g \phi r \Delta r \Delta \theta)_{z+\Delta z} + \Gamma_c r \Delta r \Delta \theta \Delta z
\end{aligned}
\tag{16}$$

Letting $\phi \rho_g = \rho_1$ and dividing by $r \Delta r \Delta \theta \Delta z$ gives

$$\frac{\partial \rho_1}{\partial t} = \frac{1}{r} \left[\frac{(\rho_1 u_g r)_r - (\rho_1 u_g r)_{r+\Delta r}}{\Delta r} \right] + \left[\frac{(\rho_1 w_g)_z - (\rho_1 w_g)_{z+\Delta z}}{\Delta z} \right] + \Gamma_c
\tag{17}$$

Now take the limit as $\Delta r, \Delta z \rightarrow 0$ to get the final form of the gas continuity equation

$$\frac{\partial \rho_1}{\partial t} = - \frac{1}{r} \frac{\partial}{\partial r} (\rho_1 u_g r) - \frac{\partial}{\partial z} (\rho_1 w_g) + \Gamma_c
\tag{18}$$

b. Solid Phase Continuity

From a control volume analysis similar to that used for the gas phase, one can write:

$$\begin{aligned} \frac{\partial(\rho_p V_p)}{\partial t} = & (\rho_p u_p A_{1p})_r - (\rho_p u_p A_{1p})_{r+\Delta r} \\ & + (\rho_p w_p A_{2p})_z - (\rho_p w_p A_{2p})_{z+\Delta z} - r_c V \end{aligned} \quad (19)$$

Here ρ_p = solid particle density
 A_{1p} = cross sectional area of particles-radial direction
 A_{2p} = cross sectional area of particles-axial direction
 V_p = volume of solid particles within control volume
 u_p = radial velocity of particles
 w_p = axial velocity of particles

Notice that the $r_c V$ term is negative here, since the mass of particles decreases as gas is generated. Since

$$V_p = V - V_g \quad \frac{V_p}{V} = \frac{V - V_g}{V} = 1 - \frac{V_g}{V} = 1 - \phi \quad (20)$$

Therefore

$$\begin{aligned} V_p &= (1 - \phi) r \Delta r \Delta \theta \Delta z \\ A_{1p} &= (1 - \phi) r \Delta \theta \Delta z \\ A_{2p} &= (1 - \phi) r \Delta r \Delta \theta \end{aligned} \quad (21)$$

Now substitute for A_{1p} , A_{2p} , V_p and V to get

$$\begin{aligned} \frac{\partial [\rho_p (1 - \phi) r \Delta r \Delta \theta \Delta z]}{\partial t} &= [\rho_p u_p (1 - \phi) r \Delta \theta \Delta z]_r - [\rho_p u_p (1 - \phi) r \Delta \theta \Delta z]_{r+\Delta r} \\ &+ [\rho_p w_p (1 - \phi) r \Delta r \Delta \theta]_z - [\rho_p w_p (1 - \phi) r \Delta r \Delta \theta]_{z+\Delta z} \\ &- r_c r \Delta r \Delta \theta \Delta z \end{aligned} \quad (22)$$

letting $(1 - \phi)\rho_p = \rho_2$ and dividing by $r \Delta r \Delta \theta \Delta z$ gives,

$$\frac{\partial \rho_2}{\partial t} = \frac{1}{r} \left[\frac{(\rho_2 u_p r)_r - (\rho_2 u_p r)_{r+\Delta r}}{\Delta r} \right] + \left[\frac{(\rho_2 w_p)_z - (\rho_2 w_p)_{z+\Delta z}}{\Delta z} \right] - r_c \quad (23)$$

Again taking the limit as $\Delta r, \Delta z \rightarrow 0$, the final form of the solid phase continuity equation is:

$$\frac{\partial \rho_2}{\partial t} = - \frac{1}{r} \frac{\partial}{\partial r} (\rho_2 u_p r) - \frac{\partial}{\partial z} (\rho_2 w_p) - r_c \quad (24)$$

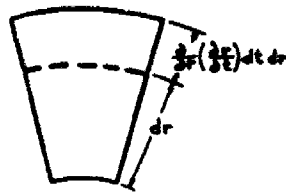
2. CONSERVATION OF MOMENTUM

a. Gas Phase Momentum

In order to include the gas viscous effects, it will first be necessary to consider the distortion of a moving fluid volume in three dimensions. The reader is referenced to any of a number of graduate level textbooks on fluid mechanics for detail.

Extension Strain:

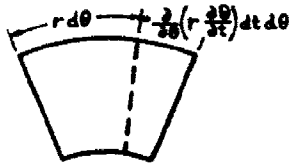
Radial Direction



$$\epsilon_{rr} dt = \frac{dr + \frac{\partial}{\partial r} \left(\frac{\partial r}{\partial t} \right) dt dr - dr}{dr} = \frac{\partial}{\partial r} \left(\frac{\partial r}{\partial t} \right) dt$$

$$\epsilon_{rr} = \frac{\partial}{\partial r} \left(\frac{\partial r}{\partial t} \right) = \frac{\partial u}{\partial r} \quad (25)$$

Azimuthal Direction



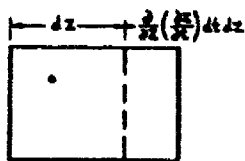
$$\epsilon_{\theta\theta} dt = \frac{r d\theta + \frac{\partial}{\partial \theta} \left(r \frac{\partial \theta}{\partial t} \right) dt d\theta - r d\theta}{r d\theta}$$

$$= \frac{1}{r} \frac{\partial}{\partial \theta} \left(r \frac{\partial \theta}{\partial t} \right) dt$$

$$\epsilon_{\theta\theta} = \frac{1}{r} \frac{\partial}{\partial \theta} \left(r \frac{\partial \theta}{\partial t} \right) = \frac{1}{r} \left(\frac{\partial r}{\partial \theta} \frac{\partial \theta}{\partial t} + r \frac{\partial^2 \theta}{\partial \theta \partial t} \right)$$

$$= \frac{u}{r} + \frac{1}{r} \frac{\partial v}{\partial \theta} \quad (26)$$

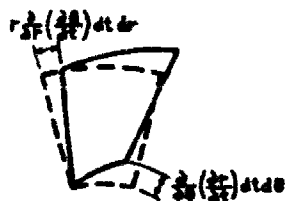
Axial Direction



$$\epsilon_{zz} dt = \frac{dz + \frac{\partial}{\partial z} \left(\frac{\partial z}{\partial t} \right) dt dz - dz}{dz} = \frac{\partial}{\partial z} \left(\frac{\partial z}{\partial t} \right) dt$$

$$\epsilon_{zz} = \frac{\partial}{\partial z} \left(\frac{\partial z}{\partial t} \right) = \frac{\partial w}{\partial z} \quad (27)$$

Shear Strain:



$r - \theta$ Strain

$$\epsilon_{r\theta} dt = \frac{1}{2} \left[\tan^{-1} \frac{r \frac{\partial}{\partial r} \left(\frac{\partial \theta}{\partial t} \right) dt dr}{dr} \right]$$

$$+ \text{TAN}^{-1} \frac{\frac{\partial}{\partial \theta} \left(\frac{\partial r}{\partial t} \right) dt d\theta}{r d\theta}]$$

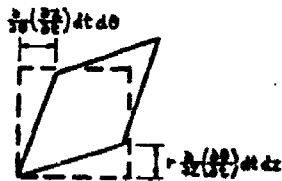
$$\epsilon_{r\theta} = \frac{1}{2} \left[r \frac{\partial}{\partial r} \left(\frac{v}{r} \right) + \frac{1}{r} \frac{\partial u}{\partial \theta} \right] \quad (28)$$

$\theta - z$ Strain

$$\epsilon_{\theta z} dt = \frac{1}{2} \left[\text{TAN}^{-1} \frac{\frac{\partial}{\partial \theta} \left(\frac{\partial z}{\partial t} \right) dt d\theta}{r d\theta} \right.$$

$$\left. + \text{TAN}^{-1} \frac{r \frac{\partial}{\partial z} \left(\frac{\partial \theta}{\partial t} \right) dt dz}{dz} \right]$$

$$\epsilon_{\theta z} = \frac{1}{2} \left[\frac{1}{r} \frac{\partial w}{\partial \theta} + \frac{\partial v}{\partial z} \right] \quad (29)$$

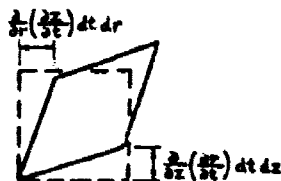


$z - r$ Strain

$$\epsilon_{rz} dt = \frac{1}{2} \left[\text{TAN}^{-1} \frac{\frac{\partial}{\partial z} \left(\frac{\partial r}{\partial t} \right) dt dz}{dz} \right.$$

$$\left. + \text{TAN}^{-1} \frac{\frac{\partial}{\partial r} \left(\frac{\partial z}{\partial t} \right) dt dr}{dr} \right]$$

$$\epsilon_{rz} = \left[\frac{\partial u}{\partial z} + \frac{\partial w}{\partial r} \right] \quad (30)$$



Since it is assumed that the gas phase behaves as a Newtonian viscous fluid, the stress tensor can be written as:

$$\tau_{ij} = -2 \mu \epsilon_{ij} - \lambda \epsilon_{kk} \delta_{ij} \quad (31)$$

where $\lambda = -\frac{2}{3} \mu$ by Stoke's hypothesis and δ_{ij} is the Kronecker delta.

Consequently the components of the stress tensor are:

$$\tau_{rr} = -\mu \left[2 \frac{\partial u}{\partial r} - \frac{2}{3} \left(\frac{1}{r} \frac{\partial(ru)}{\partial r} + \frac{1}{r} \frac{\partial v}{\partial \theta} + \frac{\partial w}{\partial z} \right) \right]$$

$$\tau_{\theta\theta} = -\mu \left[2 \left(\frac{u}{r} + \frac{1}{r} \frac{\partial v}{\partial \theta} \right) - \frac{2}{3} \left(\frac{1}{r} \frac{\partial(ru)}{\partial r} + \frac{1}{r} \frac{\partial v}{\partial \theta} + \frac{\partial w}{\partial z} \right) \right]$$

$$\tau_{zz} = -\mu \left[2 \frac{\partial w}{\partial z} - \frac{2}{3} \left(\frac{1}{r} \frac{\partial(ru)}{\partial r} + \frac{1}{r} \frac{\partial v}{\partial \theta} + \frac{\partial w}{\partial z} \right) \right]$$

$$\tau_{r\theta} = \tau_{\theta r} = -\mu \left[r \frac{\partial}{\partial r} \left(\frac{v}{r} \right) + \frac{1}{r} \frac{\partial u}{\partial \theta} \right]$$

$$\tau_{\theta z} = \tau_{z\theta} = -\mu \left[\frac{\partial v}{\partial z} + \frac{1}{r} \frac{\partial w}{\partial \theta} \right]$$

$$\tau_{zr} = \tau_{rz} = -\mu \left[\frac{\partial w}{\partial r} + \frac{\partial u}{\partial z} \right] \quad (32)$$

Now for the two-dimensional model, the azimuthal gradients and velocity coefficient are zero. Hence the stress components reduce to:

$$\tau_{rr} = -\mu \left[2 \frac{\partial u}{\partial r} - \frac{2}{3} \left(\frac{1}{r} \frac{\partial(ru)}{\partial r} + \frac{\partial w}{\partial z} \right) \right]$$

$$\tau_{\theta\theta} = -\mu \left[2 \frac{u}{r} - \frac{2}{3} \left(\frac{1}{r} \frac{\partial(ru)}{\partial r} + \frac{\partial w}{\partial z} \right) \right]$$

$$\tau_{zz} = -\mu \left[2 \frac{\partial w}{\partial z} - \frac{2}{3} \left(\frac{1}{r} \frac{\partial(ru)}{\partial r} + \frac{\partial w}{\partial z} \right) \right]$$

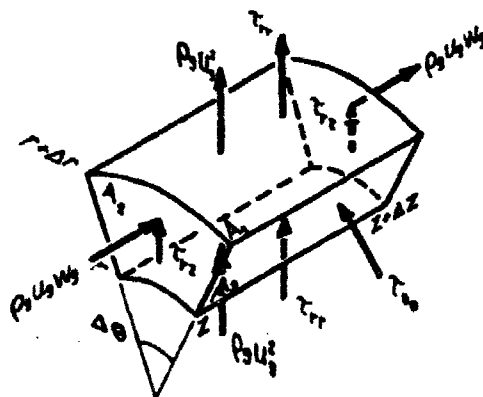
$$\tau_{r\theta} = \tau_{\theta r} = 0$$

$$\tau_{\theta z} = \tau_{z\theta} = 0$$

$$\tau_{zr} = \tau_{rz} = -\mu \left[\frac{\partial w}{\partial r} + \frac{\partial u}{\partial z} \right] \quad (33)$$

(1) Gas Phase Momentum-Radial Direction

To determine the changes in momentum in the radial direction, consider the forces acting on the control volume:



Rate of Momentum Accumulation	=	Rate of Momentum In	-	Rate of Momentum Out	+	Sum of forces acting on the control volume including: Shear Forces Gas-Particle Interaction Forces Pressure Gradient Forces Forces associated with mass addition or loss
-------------------------------------	---	---------------------------	---	----------------------------	---	--

$$\begin{aligned}
\frac{\partial(\rho_g V_g u_g)}{\partial t} = & (\rho_g u_g^2 A_{1g}) - (\rho_g u_g^2 A_{1g})_{r+\Delta r} + (\rho_g u_g w_g A_{2g})_z - (\rho_g u_g w_g A_{2g})_{z+\Delta z} \\
& + (\tau_{rr} A_1)_r - (\tau_{rr} A_1)_{r+\Delta r} + 2(\tau_{\theta\theta} A_3) \sin\left(\frac{\Delta\theta}{2}\right) \\
& + (\tau_{rz} A_2)_z - (\tau_{rz} A_2)_{z+\Delta z} - D_r V \\
& + (P_g A_{1g})_r - (P_g A_{1g})_{r+\Delta r} + 2(P_g A_{3g}) \sin\left(\frac{\Delta\theta}{2}\right) + r_c u_p V
\end{aligned} \tag{34}$$

Introduced here are: P_g = gas phase pressure

D_r = radial component of interphase drag

A_{3g} = cross sectional area of gas-azimuthal direction

It is assumed that the pressure gradient force acts through the area of the gas only. It is also envisioned that combustion takes place at the particle velocity, imparting momentum to the product gases. This is accounted for by the $r_c u_p V$ term.

Like the earlier analysis of the geometry done in Equations (14) and (15)

$$A_3 = \Delta r \Delta z \quad (35)$$

$$A_{3g} = \phi \Delta r \Delta z \quad (36)$$

Now since $\Delta\theta$ is small, then $\sin\left(\frac{\Delta\theta}{2}\right) \approx \frac{\Delta\theta}{2}$. Substituting this and the relations in Equations (14), (15), (35), and (36) into the momentum Equation (34) yields:

$$\begin{aligned} \frac{\partial(\rho_g \phi r \Delta r \Delta \theta \Delta z u_g)}{\partial t} &= (\rho_g u_g^2 \phi r \Delta \theta \Delta z)_r - (\rho_g u_g^2 \phi r \Delta \theta \Delta z)_{r+\Delta r} \\ &+ (\rho_g u_g w_g \phi r \Delta r \Delta \theta)_z - (\rho_g u_g w_g \phi r \Delta r \Delta \theta)_{z+\Delta z} \\ &+ (\tau_{rr} r \Delta \theta \Delta z)_r - (\tau_{rr} r \Delta \theta \Delta z)_{r+\Delta r} \\ &+ 2 (\tau_{\theta\theta} \Delta r \Delta z) \frac{\Delta\theta}{2} + (\tau_{rz} r \Delta r \Delta \theta)_r \\ &- (\tau_{rz} r \Delta r \Delta \theta)_{r+\Delta r} - D_r r \Delta r \Delta \theta \Delta z \\ &+ (P_g \phi r \Delta \theta \Delta z)_r - (P_g \phi r \Delta \theta \Delta z)_{r+\Delta r} + 2 (P_g \phi \Delta r \Delta z) \frac{\Delta\theta}{2} \\ &+ r_c u_p r \Delta r \Delta \theta \Delta z \end{aligned} \quad (37)$$

Rewriting Equation (37) in terms of bulk density $\rho_1 = \phi \rho_p$ and dividing by volume $r \Delta r \Delta \theta \Delta z$ gives:

$$\frac{\partial(\rho_1 u_g)}{\partial t} = \frac{1}{r} \left[\frac{(\rho_1 r u_g^2)_r - (\rho_1 r u_g^2)_{r+\Delta r}}{\Delta r} \right] + \left[\frac{(\rho_1 w_g u_g)_z - (\rho_1 w_g u_g)_{z+\Delta z}}{\Delta z} \right]$$

$$\begin{aligned}
& + \frac{1}{r} \left[\frac{(\tau_{rr}r)_r - (\tau_{rr}r)_{r+\Delta r}}{\Delta r} \right] + \frac{\tau_{\theta\theta}}{r} + \left[\frac{(\tau_{rz})_z - (\tau_{rz})_{z+\Delta z}}{\Delta z} \right] \\
& - D_r + \frac{1}{r} \left[\frac{(p_{g\phi}r)_r - (p_{g\phi}r)_{r+\Delta r}}{\Delta r} \right] + \frac{p_{g\phi}}{r} + r_c u_p
\end{aligned} \tag{38}$$

Now take the limit as $\Delta r, \Delta z \rightarrow 0$ and simplify the pressure terms:

$$\begin{aligned}
\frac{\partial(\rho_1 u_g)}{\partial t} &= - \frac{1}{r} \frac{\partial}{\partial r} (\rho_1 u_g^2 r) - \frac{\partial}{\partial z} (\rho_1 u_g w_g) - \left[\frac{1}{r} \frac{\partial}{\partial r} (\tau_{rr}r) - \frac{\tau_{\theta\theta}}{r} + \frac{\partial \tau_{rz}}{\partial z} \right] \\
&- D_r - \frac{\partial}{\partial r} (p_{g\phi}) + r_c u_p
\end{aligned} \tag{39}$$

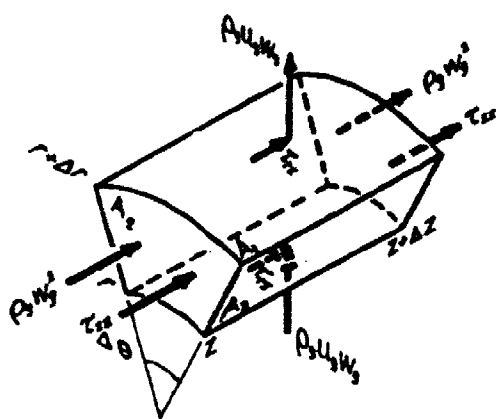
Substituting the results from (33) for the stress terms and rearranging yields the final form of the radial direction gas momentum equation:

$$\begin{aligned}
\frac{\partial(\rho_1 u_g)}{\partial t} &= - \frac{1}{r} \frac{\partial}{\partial r} (\rho_1 u_g^2 r) - \frac{\partial}{\partial z} (\rho_1 u_g w_g) + u_g \left\{ \frac{\partial}{\partial r} \left[\frac{1}{r} \frac{\partial}{\partial r} (r u_g) \right] + \frac{\partial^2 u_g}{\partial z^2} \right. \\
&\left. + \frac{1}{3} \frac{\partial}{\partial r} \left[\frac{1}{r} \frac{\partial}{\partial r} (r u_g) + \frac{\partial w_g}{\partial z} \right] \right\} + r_c u_p - D_r - \frac{\partial}{\partial r} (p_{g\phi})
\end{aligned} \tag{40}$$

(2) Gas Phase Momentum-Axial Direction

Again consider a control volume but now examine the forces acting axially on it. (See figure on following page.)

$$\frac{\partial(\rho_g V_g w_g)}{\partial t} = (\rho_g u_g w_g A_{1g})_r - (\rho_g u_g w_g A_{1g})_{r+\Delta r} + \dots$$



$$\begin{aligned}
 & (\rho_g w_g^2 A_{2g})_z - (\rho_g w_g^2 A_{2g})_{z+\Delta z} + (\tau_{rz} A_1)_r \\
 & - (\tau_{rz} A_1)_{r+\Delta r} + (\tau_{zz} A_2)_z - (\tau_{zz} A_2)_{z+\Delta z} \\
 & - D_z V + (P_g A_{2g})_z - (P_g A_{2g})_{z+\Delta z} \\
 & + \Gamma_c w_p V
 \end{aligned} \quad (41)$$

where: D_z = axial component of interphase drag

As done previously for the radial momentum component, substitute geometric relations Equations (14) and (15), divide by the volume $r \Delta r \Delta \theta \Delta z$, and let $\rho_1 = \phi \rho_g$ to get:

$$\begin{aligned}
 \frac{\partial (\rho_1 w_g)}{\partial t} &= \frac{1}{r} \left[\frac{(\rho_1 u_g w_g r)_r - (\rho_1 u_g w_g r)_{r+\Delta r}}{\Delta r} \right] + \left[\frac{(\rho_1 w_g^2)_z - (\rho_1 w_g^2)_{z+\Delta z}}{\Delta z} \right] \\
 &+ \frac{1}{r} \left[\frac{(\tau_{rz} r)_r - (\tau_{rz} r)_{r+\Delta r}}{\Delta r} \right] + \left[\frac{(\tau_{zz})_z - (\tau_{zz})_{z+\Delta z}}{\Delta z} \right] \\
 &- D_z + \left[\frac{(P_g \phi)_z - (P_g \phi)_{z+\Delta z}}{\Delta z} \right] + \Gamma_c w_p
 \end{aligned} \quad (42)$$

Again let $\Delta r, \Delta z \rightarrow 0$

$$\begin{aligned}
 \frac{\partial (\rho_1 w_g)}{\partial t} &= - \frac{1}{r} \frac{\partial}{\partial r} (\rho_1 u_g w_g r) - \frac{\partial}{\partial z} (\rho_1 w_g^2) - \left[\frac{1}{r} \frac{\partial}{\partial r} (\tau_{rz} r) + \frac{\partial \tau_{zz}}{\partial z} \right] \\
 &- D_z - \frac{\partial}{\partial z} (P_g \phi) + \Gamma_c w_p
 \end{aligned} \quad (43)$$

Now substitute in the stress terms from Equation (33) and rearrange to get the final form of the axial direction gas momentum equation:

$$\begin{aligned} \frac{\partial(\rho_1 w_g)}{\partial t} = & -\frac{1}{r} \frac{\partial}{\partial r} (\rho_1 u_g w_g r) - \frac{\partial}{\partial z} (\rho_1 w_g^2) + \mu_g \left\{ \frac{1}{r} \frac{\partial}{\partial r} \left(r \frac{\partial w_g}{\partial r} \right) + \frac{\partial^2 w_g}{\partial z^2} \right. \\ & \left. + \frac{1}{3} \frac{\partial}{\partial z} \left[\frac{1}{r} \frac{\partial}{\partial r} (r u_g) + \frac{\partial w_g}{\partial z} \right] \right\} + \Gamma_c w_p - D_z - \frac{\partial}{\partial z} (P_{g\phi}) \end{aligned} \quad (44)$$

b. Solid Phase Momentum

The derivations of the solid phase momentum equations are very similar to those done earlier for the gas phase, but the complexities of viscous shear are not included. Instead, interphase drag forces become source terms while combustion effects are now momentum sinks. Finally, assume that solid phase pressure acts through the particle area only.

(1) Solid Phase Momentum-Radial Direction

From a control volume approach similar to that used for the gas phase:

$$\begin{aligned} \frac{\partial(\rho_p v_p u_p)}{\partial t} = & (\rho_p u_p^2 A_{1p})_r - (\rho_p u_p^2 A_{1p})_{r+\Delta r} + (\rho_p u_p w_p A_{2p})_z \\ & - (\rho_p u_p w_p A_{2p})_{z+\Delta z} + D_r v + (P_p A_{1p})_r \\ & - (P_p A_{1p})_{r+\Delta r} + 2 (P_p A_{3p}) \sin\left(\frac{\Delta\theta}{2}\right) - \Gamma_c u_p v \end{aligned} \quad (45)$$

with: P_p = particle phase pressure

As in the geometry analysis done in Equations (20) and (21)

$$A_{3p} = (1 - \phi) \Delta r \Delta z \quad (46)$$

Now substitute for A_{1p} , A_{2p} , A_{3p} , V_p , and V . Let $\sin(\frac{\Delta\theta}{2}) \approx \frac{\Delta\theta}{2}$ to obtain:

$$\begin{aligned} \frac{\partial [\rho_p (1-\phi) r \Delta r \Delta \theta \Delta z u_p]}{\partial t} &= [\rho_p u_p^2 (1-\phi) r \Delta \theta \Delta z]_r - [\rho_p u_p^2 (1-\phi) r \Delta \theta \Delta z]_{r+\Delta r} \\ &+ [\rho_p u_p w_p (1-\phi) r \Delta \theta \Delta r]_z - [\rho_p u_p w_p (1-\phi) r \Delta \theta \Delta r]_{z+\Delta z} \\ &+ D_r r \Delta r \Delta \theta \Delta z + [P_p (1-\phi) r \Delta \theta \Delta z]_r - [P_p (1-\phi) r \Delta \theta \Delta z]_{r+\Delta r} \\ &+ 2 [P_p (1-\phi) \Delta r \Delta z] \frac{\Delta \theta}{2} - r_c u_p r \Delta r \Delta \theta \Delta z \end{aligned} \quad (47)$$

Rewrite Equation (47) in terms of bulk density $\rho_2 = (1-\phi)\rho_p$ and divide by $r \Delta r \Delta \theta \Delta z$:

$$\begin{aligned} \frac{\partial (\rho_2 u_p)}{\partial t} &= \frac{1}{r} \left[\frac{(\rho_2 u_p^2 r)}{\Delta r} \right]_r - \left[\frac{(\rho_2 u_p^2 r)}{\Delta r} \right]_{r+\Delta r} + \left[\frac{(\rho_2 u_p w_p)}{\Delta z} \right]_z - \left[\frac{(\rho_2 u_p w_p)}{\Delta z} \right]_{z+\Delta z} \\ &+ D_r + \frac{1}{r} \left\{ \frac{[P_p (1-\phi) r]}{\Delta r} \right\}_r - \left[\frac{P_p (1-\phi)}{r} \right]_{r+\Delta r} + \frac{P_p (1-\phi)}{r} - r_c u_p \end{aligned} \quad (48)$$

Now take the limit as $\Delta r, \Delta z \rightarrow 0$ and simplify the pressure term to get the final form of the radial direction solid phase momentum equation:

$$\frac{\partial (\rho_2 u_p)}{\partial t} = \frac{1}{r} \frac{\partial}{\partial r} (\rho_2 u_p^2 r) - \frac{\partial}{\partial z} (\rho_2 u_p w_p) - r_c u_p + D_r - \frac{\partial}{\partial r} [P_p (1-\phi)] \quad (49)$$

(2) Solid Phase Momentum-Axial Direction

Again using the control volume approach, the axial momentum equation is written as:

$$\begin{aligned} \frac{\partial(\rho_p V_p w_p)}{\partial t} = & (\rho_p u_p w_p A_{1p})_r - (\rho_p u_p w_p A_{1p})_{r+\Delta r} + (\rho_p w_p^2)_z - (\rho_p w_p^2)_{z+\Delta z} \\ & + D_z V + (P_p A_{2p})_z - (P_p A_{2p})_{z+\Delta z} - r_c w_p V \end{aligned} \quad (50)$$

Substitute geometric relations Equations (14) and (21), divide by the volume $r\Delta r\Delta\theta\Delta z$, and let $\rho_2 = (1-\phi)\rho_p$ to get:

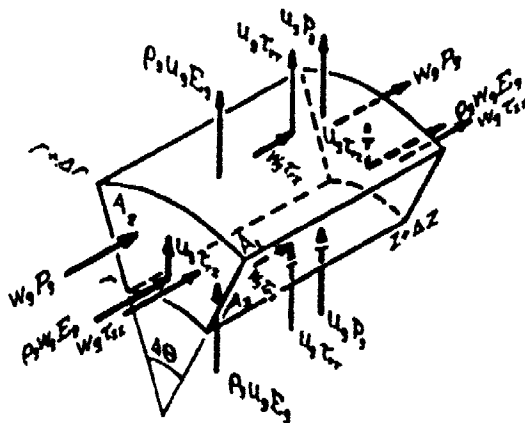
$$\begin{aligned} \frac{\partial(\rho_2 w_p)}{\partial t} = & \frac{1}{r} \left[\frac{(\rho_2 u_p w_p r)_r - (\rho_2 u_p w_p r)_{r+\Delta r}}{\Delta r} \right] + \left[\frac{(\rho_2 w_p^2)_z - (\rho_2 w_p^2)_{z+\Delta z}}{\Delta z} \right] \\ & + D_z + \left\{ \frac{[P_p(1-\phi)]_z - [P_p(1-\phi)]_{z+\Delta z}}{\Delta z} \right\} - r_c w_p \end{aligned} \quad (51)$$

Take the limit as $\Delta r, \Delta z \rightarrow 0$ to arrive at the final form of the axial direction solid phase momentum equation:

$$\frac{\partial(\rho_2 w_p)}{\partial t} = -\frac{1}{r} \frac{\partial}{\partial r} (\rho_2 u_p w_p r) - \frac{\partial}{\partial z} (\rho_2 w_p^2) - r_c w_p + D_z - \frac{\partial}{\partial z} [P_p(1-\phi)] \quad (52)$$

3. CONSERVATION OF ENERGY

a. Gas Phase Energy



From the first law of thermodynamics for a viscous gas passing through the control surfaces, we know that:

$$\begin{array}{ccccc} \text{Rate of Energy} & & \text{Rate of Energy} & & \text{Rate of Energy} \\ \text{Accumulation} & = & \text{In} & - & \text{Out} \end{array}$$

$$\begin{array}{ccccc} & \text{Heat addition} & & \text{Work done by the} & \\ & \text{from} & + & \text{surroundings including:} & \\ & \text{combustion or} & & \text{pressure, viscous shear,} & \\ & \text{convection} & & \text{and interphase drag} & \end{array}$$

Thus,

$$\begin{aligned} \frac{\partial(\rho_g V_g E_g)}{\partial t} &= (\rho_g u_g A_{1g} E_g)_r - (\rho_g u_g A_{1g} E_g)_{r+\Delta r} \\ &+ (\rho_g w_g A_{2g} E_g)_z - (\rho_g w_g A_{2g} E_g)_{z+\Delta z} - QV \end{aligned}$$

$$\begin{aligned}
& + r_c (E_g^{\text{chem}} + \frac{u_g^2}{2} + \frac{w_g^2}{2}) V + (P_g A_{1g} u_g)_r \\
& - (P_g A_{1g} u_g)_{r+\Delta r} + (P_g A_{2g} w_g)_z - (P_g A_{2g} w_g)_{z+\Delta z} \\
& + (\tau_{rr} A_{1g} u_g)_r - (\tau_{rr} A_{1g} u_g)_{r+\Delta r} + (\tau_{zz} A_{2g} w_g)_z - (\tau_{zz} A_{2g} w_g)_{z+\Delta z} \\
& + (\tau_{rz} A_{1g} w_g)_r - (\tau_{rz} A_{1g} w_g)_{r+\Delta r} + (\tau_{rz} A_{2g} u_g)_z - (\tau_{rz} A_{2g} u_g)_{z+\Delta z} \\
& - D_r u_p V - D_z w_p V
\end{aligned} \tag{53}$$

where: E_g = total gas energy $C_{vg} T_g + \frac{u_g^2}{2} + \frac{w_g^2}{2}$
 \dot{Q} = rate of convective heat transfer from gas to solid
 E_g^{chem} = gas chemical energy released during combustion

Now substitute in the geometry relations of Equations (14) and (15) and divide by the volume. If $\rho_1 = \rho_g \phi$, energy Equation (53) becomes:

$$\begin{aligned}
\frac{\partial(\rho_1 E_g)}{\partial t} &= \frac{1}{r} \left[\frac{(\rho_1 u_g E_g)_r - (\rho_1 u_g E_g)_{r+\Delta r}}{\Delta r} \right] + \left[\frac{(\rho_1 w_g E_g)_z - (\rho_1 w_g E_g)_{z+\Delta z}}{\Delta z} \right] \\
&- \dot{Q} + r_c (E_g^{\text{chem}} + \frac{u_g^2}{2} + \frac{w_g^2}{2}) + \frac{1}{r} \left[\frac{(P_g \phi u_g)_r - (P_g \phi u_g)_{r+\Delta r}}{\Delta r} \right] \\
&+ \left[\frac{(P_g \phi w_g)_z - (P_g \phi w_g)_{z+\Delta z}}{\Delta z} \right] + \frac{1}{r} \left[\frac{(\tau_{rr} u_g)_r - (\tau_{rr} u_g)_{r+\Delta r}}{\Delta r} \right] \\
&+ \left[\frac{(\tau_{zz} w_g)_z - (\tau_{zz} w_g)_{z+\Delta z}}{\Delta z} \right] + \frac{1}{r} \left[\frac{(\tau_{rz} w_g)_r - (\tau_{rz} w_g)_{r+\Delta r}}{\Delta r} \right]
\end{aligned}$$

$$+ \left[\frac{(\tau_{rz} u_g)_z - (\tau_{rz} u_g)_{z+\Delta z}}{\Delta z} \right] - D_r u_p - D_z w_p \quad (54)$$

Combine energy and pressure terms and take the limit as $\Delta r, \Delta z \rightarrow 0$ to get:

$$\begin{aligned} \frac{\partial(\rho_1 E_g)}{\partial t} = & -\frac{1}{r} \frac{\partial}{\partial r} [\rho_1 r u_g (E_g + \frac{p_g}{\rho_g})] - \frac{\partial}{\partial z} [\rho_1 w_g (E_g + \frac{p_g}{\rho_g})] \\ & - \left[\frac{1}{r} \frac{\partial}{\partial r} (\tau_{rr} u_g r) + \frac{\partial}{\partial z} (\tau_{zz} w_g) + \frac{1}{r} \frac{\partial}{\partial r} (\tau_{rz} w_g r) + \frac{\partial}{\partial z} (\tau_{rz} u_g) \right] \\ & - \dot{Q} - D_r u_p - D_z w_p + r_c (E_g^{\text{chem}} + \frac{u_p^2}{2} + \frac{w_p^2}{2}) \end{aligned} \quad (55)$$

Substitute Equation (33) for the stress terms and take the derivatives.

Rearrange to get the final form of the gas energy equation:

$$\begin{aligned} \frac{\partial(\rho_1 E_g)}{\partial t} = & -\frac{1}{r} \frac{\partial}{\partial r} [\rho_1 r u_g (E_g + \frac{p_g}{\rho_g})] - \frac{\partial}{\partial z} [\rho_1 w_g (E_g + \frac{p_g}{\rho_g})] \\ & + u_g \{ 2 [(\frac{\partial u_g}{\partial r})^2 + (\frac{u_g}{r})^2 + (\frac{\partial w_g}{\partial z})^2] - \frac{2}{3} (\frac{\partial u_g}{\partial r} + \frac{u_g}{r} + \frac{\partial w_g}{\partial z})^2 \\ & + (\frac{\partial w_g}{\partial r} + \frac{\partial u_g}{\partial z})^2 + u_g \frac{\partial}{\partial r} [\frac{1}{r} \frac{\partial}{\partial r} (r u_g)] + u_g \frac{\partial^2 u_g}{\partial z^2} \\ & + \frac{u_g}{3} \frac{\partial}{\partial r} [\frac{1}{r} \frac{\partial}{\partial r} (r u_g) + \frac{\partial w_g}{\partial z}] + \frac{w_g}{r} \frac{\partial}{\partial r} (r \frac{\partial w_g}{\partial r}) + w_g \frac{\partial^2 w_g}{\partial z^2} \\ & + \frac{w_g}{3} \frac{\partial}{\partial z} [\frac{1}{r} \frac{\partial}{\partial r} (r u_g) + \frac{\partial w_g}{\partial z}] \} - \dot{Q} - D_r u_p - D_z w_p \\ & + r_c (E_g^{\text{chem}} + \frac{u_p^2}{2} + \frac{w_p^2}{2}) \end{aligned} \quad (56)$$

b. Solid Phase Energy

The solid phase energy equation is derived using a control volume analysis similar to the one used for the gas phase. Once again, complications from particle viscosity are neglected as they were in solid phase momentum equations.

$$\begin{aligned} \frac{\partial(\rho_p V E_p)}{\partial t} = & (\rho_p u_p A_{1p} E_p)_r - (\rho_p u_p A_{1p} E_p)_{r+\Delta r} + (\rho_p w_p A_{2p} E_p)_z \\ & - (\rho_p w_p A_{2p} E_p)_{z+\Delta z} + \dot{Q}V + r_c (E_p^{\text{chem}} - \frac{u_p^2}{2} - \frac{w_p^2}{2}) V \\ & + (P_p A_{1p} u_p)_r - (P_p A_{1p} u_p)_{r+\Delta r} + (P_p A_{2p} w_p)_z \\ & - (P_p A_{2p} w_p)_{z+\Delta z} + D_r u_p V + D_z w_p V \end{aligned} \quad (57)$$

where: E_p = total particle energy $C_v T_p + \frac{u_p^2}{2} + \frac{w_p^2}{2}$
 E_p^{chem} = particle chemical energy released during combustion

Substitute in the geometry Equations (20) and (21) divide by the volume, and let $\rho_2 = \rho_p(1-\phi)$ to get:

$$\begin{aligned} \frac{\partial(\rho_2 E_p)}{\partial t} = & \frac{1}{r} \left[\frac{(\rho_2 u_p E_p)_r - (\rho_2 u_p E_p)_{r+\Delta r}}{\Delta r} \right] + \left[\frac{(\rho_2 w_p E_p)_z - (\rho_2 w_p E_p)_{z+\Delta z}}{\Delta z} \right] \\ & + \dot{Q} + r_c (E_p^{\text{chem}} - \frac{u_p^2}{2} - \frac{w_p^2}{2}) + \frac{1}{r} \left[\frac{[P_p(1-\phi)u_p]_r - [P_p(1-\phi)u_p]_{r+\Delta r}}{\Delta r} \right] \end{aligned}$$

$$+ \left\{ \frac{[\rho_p(1-\phi)w_p]_z - [\rho_p(1-\phi)w_p]_{z+\Delta z}}{\Delta z} \right\} + D_r u_p + D_z w_p \quad (58)$$

Combine pressure and energy terms and take the limit as $\Delta r, \Delta z \rightarrow 0$ to yield the final form of the solid phase energy equation

$$\begin{aligned} \frac{\partial(\rho_2 E_p)}{\partial t} = & - \frac{1}{r} \frac{\partial}{\partial r} [\rho_2 r u_p (E_p + \frac{p}{\rho_p})] - \frac{\partial}{\partial z} [\rho_2 w_p (E_p + \frac{p}{\rho_p})] \\ & + \dot{Q} + D_r u_p + D_z w_p + r_c (E_p^{\text{chem}} - \frac{u_p^2}{2} - \frac{w_p^2}{2}) \end{aligned} \quad (59)$$

SECTION IV

NUMERICAL INTEGRATION TECHNIQUE

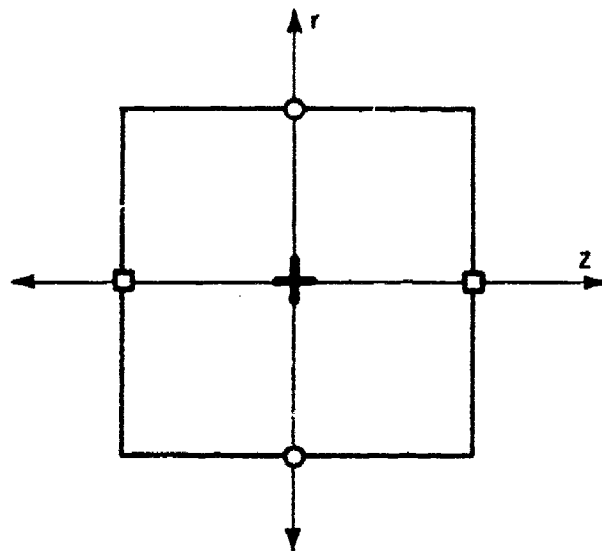
INTRODUCTION

In the previous sections, the mathematical foundations of the two-dimensional model were derived and discussed in great detail. The system of partial differential equations, constitutive relations, initial conditions, and boundary conditions form the basis of a well-posed problem, indicating that a solution is possible. However, analytical methods for solving this set of complex, coupled, non-linear partial differential equations do not currently exist. Therefore, a computational numeric method must be utilized in order to determine the solution of the system. The implementation of such a finite differencing scheme is discussed here.

DOMAIN DISCRETIZATION

Before a numerical integration technique can be used to solve a system of partial differential equations, the domain of the problem must be re-defined. The continuous region is replaced by a set of control cells, which represent locations where values of dependent variables are stored. These discrete nodes make it possible to approximate derivatives which would ordinarily be unknown.

The two-dimensional model utilizes a staggered grid to represent the domain which was described in Section II. In this arrangement, velocity components are calculated at points that lie on the edges of the control cells while scalar quantities are defined at the centers. As shown in Figure 4,



- Radial Velocity (\hat{u}) Node
- Axial Velocity (\hat{w}) Node
- + Pressure, Temperature, Density,
Porosity Node

Figure 4. Typical Two Dimensional Finite Difference Cell Utilizing the Staggered Grid

radial velocities are determined at the sides that are normal to the r direction, and axial velocities are calculated at faces perpendicular to the z direction.

Figure 5 illustrates how the staggered grid is implemented in the two-dimensional model. The mass continuity equations (Equations (3) and (4)) which are used to determine ρ_1 and ρ_2 , and the energy equations (Equations (9) and (10)) which are used to find E_g and E_p , are solved at the scalar nodes. The radial momentum equations (Equations (5) and (7)) which solve for u_g and u_p are applied at the displaced radial velocity nodes while the axial momentum equations (Equations (6) and (8)) that determine w_g and w_p are employed at the staggered axial velocity nodes. The grid is arranged so that the boundaries of the domain pass through sites containing normal velocity components, although the entire mesh extends beyond these borders. These exterior nodes will be shown to be very useful in dealing with the boundary conditions in finite difference form.

There are three important advantages to be gained by using a staggered grid instead of a conventional one. First, it provides second-order accuracy for the centered space finite differencing used here. Because flow information is known at more locations, due to the displaced velocity nodes, derivative approximations can be made over smaller distance, as explained by Dahm, Samuelson, and Krier (Reference 12). The second advantage is that the pressure difference between two adjacent nodes becomes the natural driving force for the velocity component located between these grid points. According to Patankar (Reference 13) this feature eliminates the problems which can arise in the momentum equation due to a wavy pressure field. Finally, as will be shown, the staggered grid makes the necessary boundary conditions much easier to implement in finite difference form.

O RADIAL VELOCITY NODE
 □ AXIAL VELOCITY NODE
 + SCALAR NODE

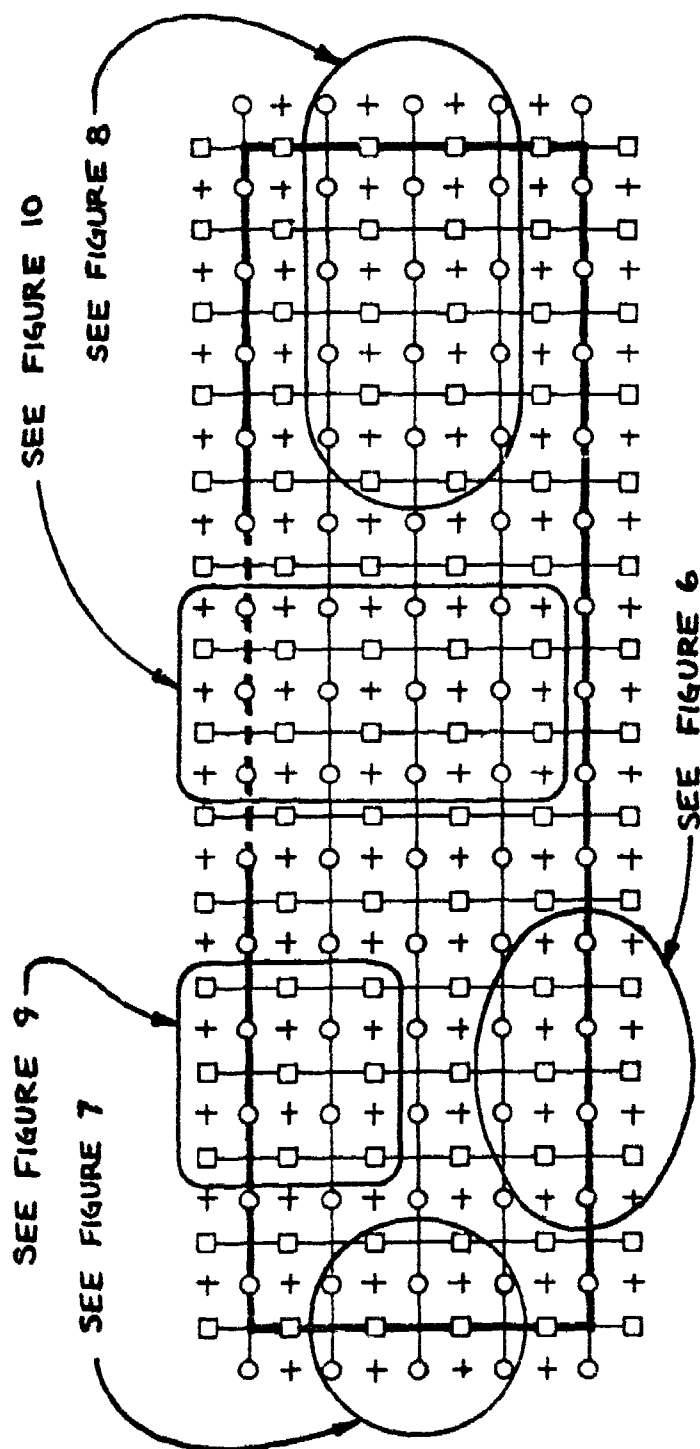


Figure 5. The Staggered Grid Applied to the Two Dimensional Domain
 [Heavy border indicates the location of the boundaries while
 dashed border represents the opening in the container wall.]

THE FINITE DIFFERENCE EQUATIONS

Once the domain has been discretized, the continuous conservation equations (3) - (10) are cast into finite difference form using the "leapfrog" scheme (Reference 14). This centered time, centered space, explicit method evaluates unsteady terms at time levels $t + \Delta t$ and $t - \Delta t$, while the fluxes, sources, and sinks are determined at the current time t . Spatial derivatives are taken in a similar manner, by evaluating properties at grid sites adjacent to the location in question and dividing by the distance between the nodes. The finite difference forms of the conservation of mass, momentum, and energy are listed in Appendix B.

The leapfrog scheme was chosen for the two dimensional model based upon the successful results reported by other authors. Kurihara (Reference 14) showed that this method could be used to integrate the time dependent wave equation. Williams (Reference 15) applied this scheme to the three dimensional conservation equations for an incompressible, single-phase, viscous fluid. In addition, Dahm (Reference 10) is currently obtaining successful results by employing this technique to solve the two-phase, reactive flow equations in three dimensions, a problem similar to the one being investigated here.

BOUNDARY CONDITIONS

When partial differential equations are applied at a boundary of the domain, special conditions must be defined in order to yield a unique solution. This is also true when dealing with the finite difference form of the equations. Hence the boundary conditions must now be stated in a finite difference configuration.

Recall from Section II that there are five boundary conditions which must be specified for the two dimensional model. Each one is considered separately:

1. At the center line (Figure 6)

The symmetry conditions applied along this boundary specify that all radial velocity components and derivatives in the radial direction must vanish at the center line. Consequently, the staggered grid is applied so that the u-velocity nodes are positioned on the boundary with their values initialized to zero. Since only the radial momentum equations are evaluated at these points, halting the integration prior to reaching the center line leaves the u-velocity components unchanged. Their values remain at zero and thus satisfy the boundary condition. Note that this procedure eliminates the problems of evaluating the $1/r$ terms as $r \rightarrow 0$. The singularities which normally occur at the center line do not have to be dealt with, since no computations are performed on the nodes at this location. The values at these grid points are preset to zero and then left alone.

It is also necessary to be able to evaluate the continuity, energy, and axial momentum equations along the boundary, although the nodes containing the axial velocities and the scalar quantities do not lie directly on the border at $r = 0$. Consequently, the symmetry conditions are applied by using reflection points about the centerline. Recall from Paragraph 2 and Figure 5, that the mesh of grid points extends beyond the limits of the domain. The values stored in these exterior nodes are set equal to their adjacent counterpart directly across the boundary. Therefore, all derivatives taken radially at $r = 0$ are equal to zero and satisfy the boundary condition.

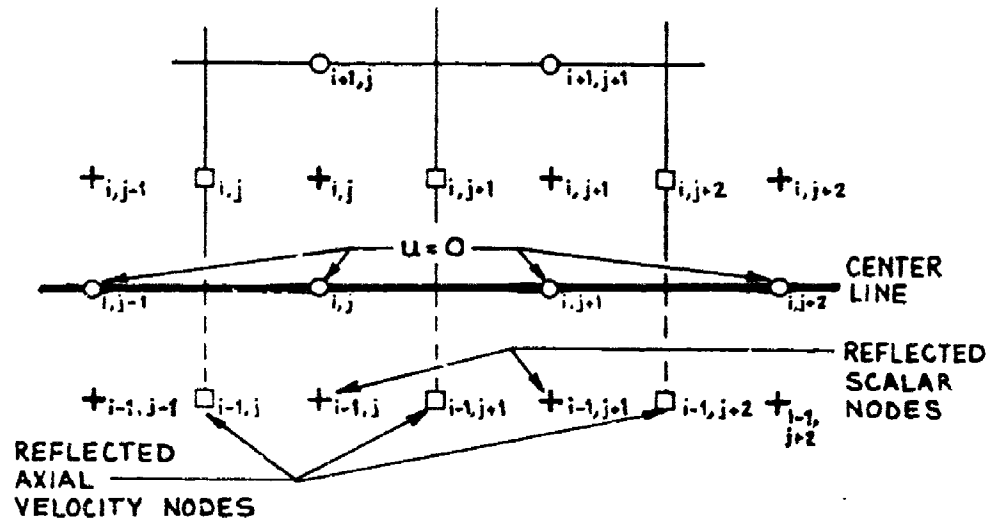


Figure 6. Symmetry Boundary Conditions Applied at the Center Line, $r = 0$

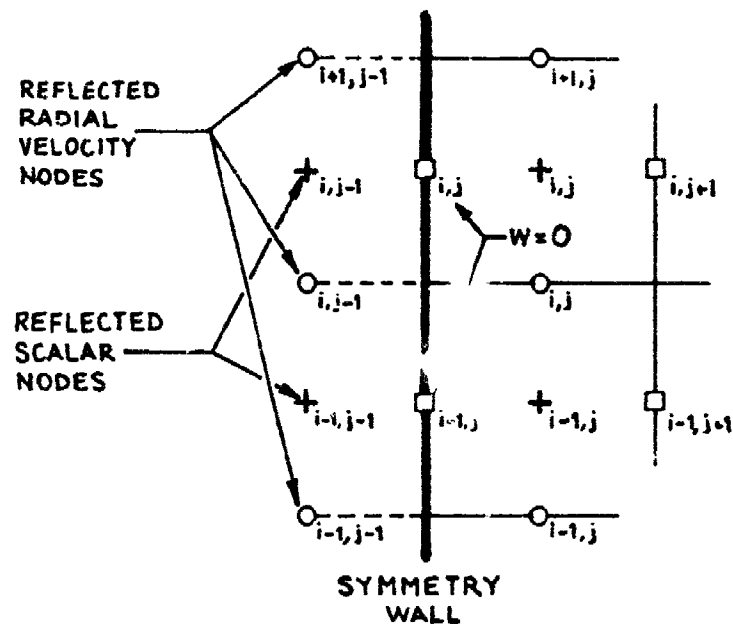


Figure 7. Implementation of Symmetry Boundary Conditions at the Near End Wall, $z = 0$

It should be pointed out that the two dimensional model requires that the values stored in the reflected nodes consistently match those located within the domain. This is due to the existence of the second derivative, viscous force terms in the gas phase momentum equations. Dahm (Reference 10) explains how the radial flux terms are automatically set to zero when a staggered grid is applied. However, because he is solving inviscid conservation equations containing only fluxes, sources, and sinks, he can store arbitrary values in his external nodes, since eventually they get multiplied by radial velocities known to be equal to zero. But viscous gas effects are due to forces rather than fluxes, and the second derivatives are not multiplied by these velocity components. Consequently, the symmetry of the reflected nodes must be maintained in order to provide an adequate boundary condition for these higher order terms.

2. At the near end wall (Figure 7)

Symmetry conditions are also applied along this end wall. Here the axial velocity components are set equal to zero, as are all gradients taken across the boundary. The displaced w-velocity nodes lie directly on the wall and are initialized to zero. These values remain unchanged since the axial momentum equations are not applied at these grid points. Reflected external nodes are again implemented to provide symmetry conditions for the second derivative terms.

3. At the far end (Figure 8)

In order to allow flow disturbances to propagate through this boundary, a radiative end condition was utilized. This involved using a Taylor series

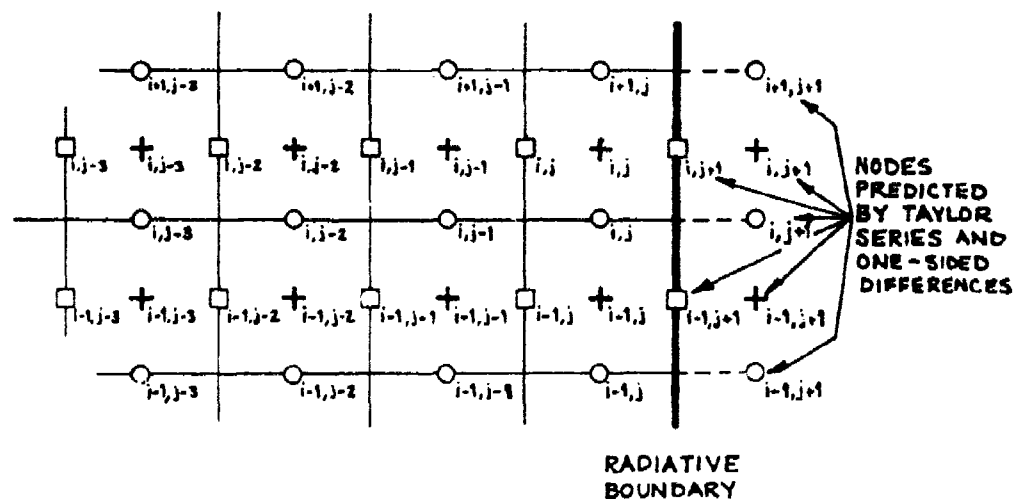


Figure 8. Application of the Radiative Boundary Conditions to the Far End Wall, $z = L$

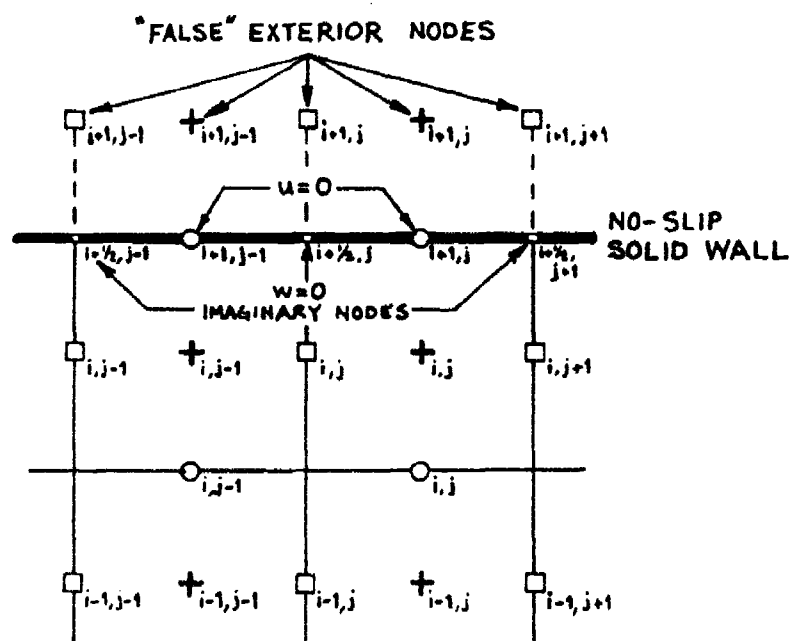


Figure 9. No-Slip Boundary Condition Employed Along with the Circumferential Wall, $r = R$, for $0 \leq a \leq z_c$ and $z_c + \Delta z_c \leq z \leq L$

expansion with one-sided finite differences to determine the quantities to be stored in the external nodes. These predicted results are then used in the conservation equations to calculate values inside the domain.

For example, assume that "A" represents a generalized dependent variable which is stored in either a scalar or a velocity node. As illustrated in Figure 8, the nodes at (j), (j-1), (j-2), and (j-3) are located inside the domain while (j+1) is an external grid point. Using a Taylor series expansion, the value of A at the outside node is:

$$A_{j+1} = A_j + \Delta z \frac{\partial A}{\partial z} \Big|_j + \frac{(\Delta z)^2}{2} \frac{\partial^2 A}{\partial z^2} \Big|_j \quad (60)$$

One-sided differencing is used to evaluate the derivatives in this approximation:

$$\frac{\partial A}{\partial z} \Big|_j = \frac{3A_j - 4A_{j-1} + A_{j-2}}{2\Delta z} \quad (61)$$

$$\frac{\partial^2 A}{\partial z^2} \Big|_j = \frac{2A_j - 5A_{j-1} + 4A_{j-2} - A_{j-3}}{(\Delta z)^2} \quad (62)$$

which when substituted into Equation (60) yields the predicted value to be stored in the exterior node:

$$A_{j+1} = \frac{7A_j - 9A_{j-1} + 3A_{j-2} - A_{j-3}}{2} \quad (63)$$

4. At the circumferential wall (Figure 9)

Recall that this is a solid wall where the no-slip condition is imposed upon the flow. Once again the normal, radial velocity nodes are positioned on the boundary and the values are initialized to zero. Integration of the radial momentum equation is halted prior to reaching these points, in order to leave the u-velocity components unchanged during the numerical simulation.

However, the no-slip requirement can not be imposed through the staggered grid, but must be incorporated into the finite difference scheme. While the boundary conditions force the axial velocities to be equal to zero at the wall, the grid points which store these quantities are located elsewhere, as illustrated in Figure 9. Hence the axial velocity nodes can not simply be initialized to zero and then left alone. Instead, their values must be determined from the discretized z-momentum equation, with special considerations made for the solid wall and the no-slip conditions. This is done by using "lopsided" finite differences for approximating the radial derivatives representing viscous gas effects.

For example, assume that the axial velocity gradient $\frac{\partial w}{\partial r}$ must be determined at node (i) as shown in Figure 9. At any other boundary, the derivative could be determined by utilizing the centered difference of:

$$\frac{\partial w}{\partial r} \Big|_i = \frac{w_{i+1} - w_{i-1}}{\Delta r} \quad (64)$$

This type of approximation is possible because the velocities stored outside the domain at (i+1) are known from symmetry or predicted by a Taylor series. However, the values in the exterior nodes along the solid wall are unknown, so

center differencing can not be applied. Instead, an imaginary axial velocity node is created on the boundary at $(i + 1/2)$, and a lopsided approximation is used such that:

$$\frac{\partial w}{\partial r} \Big|_i = \frac{4w_{i+1/2} - 3w_i - w_{i-1}}{3\Delta r} \quad (65)$$

A derivation of this formula can be found in a variety of textbooks dealing with numerical integration methods. Now the no-slip condition can be implemented by setting the value of $w_{i+1/2}$ equal to zero to get:

$$\frac{\partial w}{\partial r} \Big|_i = \frac{-3w_i - w_{i-1}}{3\Delta r} \quad (66)$$

Following a similar line of reasoning, second derivative values are approximated at the solid wall as:

$$\frac{\partial^2 w}{\partial r^2} \Big|_i = \frac{-12w_i + 4w_{i-1}}{3(\Delta r)^2} \quad (67)$$

Viscous gas terms, consisting of gradients evaluated in the axial direction, require no special treatment at the solid wall. Centered space differencing is used to approximate these derivatives, since all the necessary grid points are located inside the domain.

The radial flux terms in the conservation equations are satisfied at the boundary by utilizing "false" exterior nodes, as described by Dahm (Reference 10). Recall that grid points located beyond the solid wall were not required for the evaluation of the gas viscosity terms, since lopsided differencing was employed. In addition, when a flux is determined across the boundary, the

quantities stored in these exterior nodes are multiplied by radial velocity components, which are known to be equal to zero. Consequently, arbitrary values can be stored in these false exterior nodes in order to facilitate the integration scheme.

5. At the opening (Figure 10)

The flow conditions imposed at the rip in the circumferential wall are based upon an assumed linear profile for the radial component of the gas velocity. These values are stored in the boundary nodes at (i+1) shown in Figure 10:

$$\begin{aligned} u_{g_{i+1}} &= a_i \frac{z - z_c}{\Delta z_c / 2} & \text{FOR } z_c < z \leq z_c + \frac{\Delta z_c}{2} \\ u_{g_{i+1}} &= -a_i \frac{z - (z_c + \Delta z_c)}{\Delta z_c / 2} & \text{FOR } z_c + \frac{\Delta z_c}{2} < z < z_c + \Delta z_c \end{aligned} \quad (68)$$

Here a_i is the gas speed of sound, which is a function of local temperature and pressure below the hole:

$$a_i = \sqrt{\frac{C_{v_g} (1 + 2b_1 \rho_{g_i}) + R(1 + b_1 \rho_{g_i})}{C_{v_g} \rho_{g_i} (1 + b_1 \rho_{g_i})} P_{g_i}} \quad (69)$$

This formula is derived from the non-ideal equation of state in the paper by Dahm, Samuelson, and Krier (Reference 12).

In order to predict the values of the particle velocity components normal to the opening, the interphase drag constitutive relation was utilized. It was assumed that this force acts to pull the particles through the hole, such that:

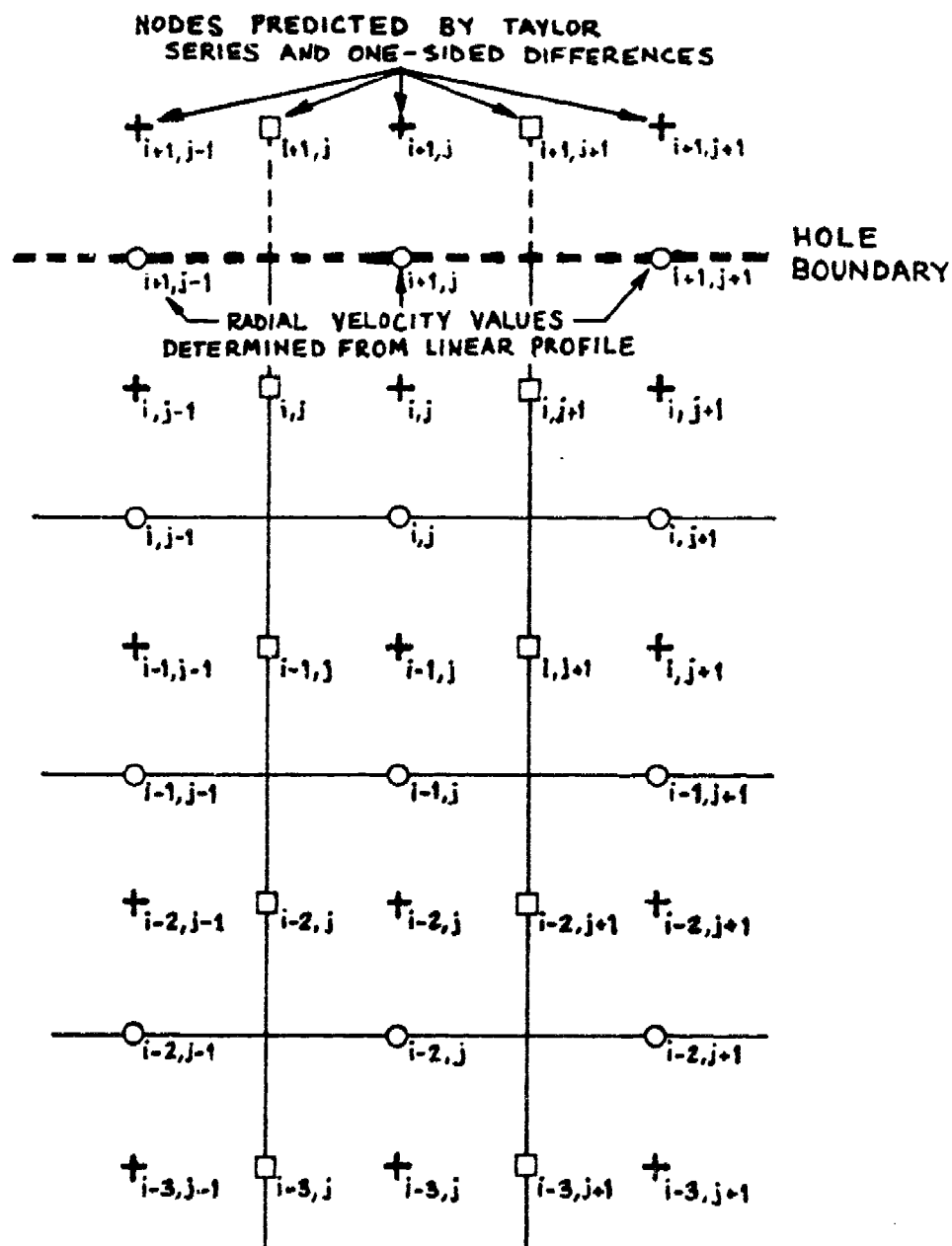


Figure 10. Boundary Conditions Applied at the Opening in the Circumferential Wall, $r = R$ for $z_c \leq z \leq z_c + \Delta z_c$

$$(\rho_2 u_p)^{t+\Delta t} = 2\Delta t D_r (2\pi r_p^2) + (\rho_2 u_p)^{t-\Delta t} \quad (70)$$

The reader is again referred to Reference 12 for a derivation of this relation.

The remaining scalar quantities and the axial velocity components are determined by using a Taylor series predictor, similar to the one derived for the end wall radiative boundary conditions. If "A" is a generalized dependent variable, then

$$A_{i+1} = \frac{7A_i - 9A_{i-1} + 3A_{i-2} - A_{i-3}}{2} \quad (71)$$

These predicted values are stored in the exterior nodes at (i+1) as shown in Figure 10. The conservation equations are then applied to the grid points at (i) using the standard centered differencing techniques.

STABILITY

The stability of the finite difference scheme is always a problem when using numerical methods to integrate partial differencing equations. Solutions which oscillate or grow without bound can develop due to the necessary mathematical approximations required to discretize the system. But steps can be taken to minimize the effects of these inherent instabilities. The methodology used for the two dimensional model is discussed below.

Recall from Section I!I that the explicit, centered time, centered space, leapfrog technique was used to cast the conservation equations into finite difference form. In any scheme such as this, a bound exists on the maximum

size of the time step. If this limit is exceeded, oscillations will soon develop and the predicted solution will become unstable. The conditions which determine this maximum time step can be found from the Von Neumann criteria which is described by Richtmeyer and Morton (Reference 16). However, the complexity of the governing system of equations makes a complete analysis of this kind extremely unwieldy and difficult. Consequently, a trial and error method was utilized to find a suitable time step, although a Von Neumann stability condition should probably be derived in the future.

Another source of instabilities is called time splitting. Although this is a direct consequence of the centered time differencing used in the leapfrog scheme, this method was selected because Kurihara (Reference 14) showed that it provided less damping of the kinetic energy. If "A" is a generalized dependent variable and $f(r,z)$ represents the fluxes, sources, sinks, and viscous gas terms, centered time differencing can be represented schematically as:

$$\frac{A^{t+\Delta t} - A^{t-\Delta t}}{2\Delta t} = f(r,z)^t \quad (72)$$

Rearranging the terms gives:

$$A^{t+\Delta t} = 2\Delta t f(r,z)^t + A^{t-\Delta t} \quad (73)$$

Notice that oscillations can develop if the value of $A^{t+\Delta t}$ is less than the value of A^t . These instabilities grow until eventually, two separate solutions form at the even and odd time steps. However, this problem can be controlled through the use of an intermediate smoothing step. The time filter developed by Robert (Reference 17) was used for the two-dimensional model:

$$A^{*t+\Delta t} = 2\Delta t f(r,z)^{*t} + A^{t-\Delta t} \quad (74)$$

$$A^t = A^{*t} + \epsilon(A^{*t+\Delta t} - 2A^{*t} + A^{t-\Delta t}) \quad (75)$$

where the starred terms represent unsmoothed quantities, and ϵ is the filter parameter. First, Equation (74) is used to predict values at time $t + \Delta t$, by employing centered differencing and the unfiltered quantities at time t . Then, the smoothing step of (75) is implemented to produce a filtered value at t . Finally, the iteration moves to the next time level and the process repeats. This method has been shown to provide excellent damping of the time splitting oscillations of the leapfrog scheme (Reference 18).

Instability due to the finite differencing of non-linear partial differential equations appears through the mechanism of aliasing. This misinterpretation of the high frequency waves is explained in the paper by Krier, Dahm, and Samuelson (Reference 12). Aliasing is controlled by evaluating the conservation equations as derived, in their flux form (as opposed to the convective form with expanded derivatives) (Reference 19).

The development of shocks in the computational domain is another source of instability in the numerical integration. The extremely steep gradients produced in the vicinity of the wave can cause explosive growth of the solution. The viscous gas effects do help to reduce the shock discontinuities, however, the second derivatives cannot provide sufficient damping of these strong perturbations. Therefore, artificial diffusion terms are introduced into the conservation equations in a manner similar to the one described by Sod (Reference 20). In order to ensure stability, it is necessary to evaluate

these quantities based upon values calculated at the previous time step (Reference 21). The magnitude of the artificial diffusion terms is determined by numerical experimentation.

SECTION V

PRELIMINARY COMPUTATIONS

THE COMPUTER PROGRAM

The fluid dynamics concepts and numerical integration techniques which are described in the previous chapters were incorporated into a FORTRAN-V computer program called DDT2D. This algorithm features:

1. An external data file

This enables a user to vary the input parameters without having to re-compile the entire program, resulting in a lower overall computation cost.

2. A variable time step

For each integration, the distance between two adjacent grid points is divided by the local sound speed in the solid phase. That result is then multiplied by an input factor to yield the size of the next time increment. This feature provides added stability and produces better results when steep gradients develop. The DDT2D program automatically reduces the time step so that the rapid changes occurring near a disturbance can be accurately represented without generating oscillations in the solution.

3. A choice of one or two dimensional burn initiation

The user can select from two polynomial profiles for the initial temperature distribution in the solid phase. One option leads to a one dimensional

initiation, by producing an area of burning particles along the entire near end wall. The alternative generates a localized ignition zone at the $r = 0$, $z = 0$ corner of the domain, resulting in a two dimensional problem.

4. The ability to switch off the viscous gas effects

The viscous force and dissipation terms in the gas momentum and energy equations can be set to zero by simply changing the value of an input parameter. This feature is particularly useful when examining the effects of gas viscosity on the flow near the opening in the outer wall. An identical but inviscid case could be used to highlight these aspects by providing contrasting results.

These features make DDT2D a versatile program which should be easy to use. A listing of the current version of this code is given in Appendix C.

The DDT2D program requires a great deal of computer memory due to the complex nature of the fluid dynamics problem. At each node, it is necessary to store the values of eight primary variables at three time levels, as well as the values of 18 secondary variables at a single time level. For the CDC CYBER-175 computer currently in use at the University of Illinois at Urbana-Champaign, the maximum core memory available is 131,000 words. After allowing enough space for the program itself, the remaining storage limits the size of the computational domain to under 3000 nodes. While this should be sufficient for most cases, additional memory can be obtained by using the more expensive, off-line storage techniques.

THE BASELINE CASE

All the tests described in this chapter were conducted for a single set of fluid characteristics and initial conditions. These input parameters for the two-dimensional baseline case are listed in Table 1.

Recall from Section II that the initial temperature and pressure conditions were prescribed by polynomial profiles imposed over the domain. The ones utilized for the two-dimensional baseline case are shown in Figures 11 and 12. Notice that at several points located near $r = 0$, $z = 0$ the temperatures satisfy the ignition criteria and the particles are assumed to be burning. If a one-dimensional initiation is desired, a similar set of profiles are used, with variation occurring only in the axial direction.

The baseline case does not include any mass loss through the container walls. This was done in order to simplify the problem during the computer program evaluation stage. When the computer code can accurately simulate flame spreading in a totally confined bed, the opening in the circumferential wall can be re-introduced into the problem.

TABLE 1. BASELINE CASE INPUT PARAMETERS

<u>Parameter</u>	<u>Symbol</u>	<u>Nominal Value</u>
Length of bed	L	3.0 cm
Radius of bed	R	0.5 cm
Particle radius	r_{p0}	100 μm
Porosity	ϕ	0.30
Particle density	ρ_{p0}	1.675 g/cm ³
Ambient gas temperature	T_{g0}	300 K
Ambient particle temperature	T_{p0}	300 K
Ambient gas pressure	P_{g0}	100 kPa
Ambient particle pressure	P_{p0}	100 kPa
Particle ignition energy	E_{ign}	4.621×10^9 erg/g
Gas viscosity	μ_{g0}	1.8×10^{-4} poise
Prandtl Number	Pr	0.7
Gas constant	R^*	2967.9 erg/K \cdot gmol
Gas phase specific heat	C_{vg}	1.51×10^7 erg/g \cdot K
Particle phase specific heat	C_{vp}	1.51×10^7 erg/g \cdot K
Particle chemical energy	E^{chem}	5.74×10^{10} erg/g \cdot K
Burning rate index	n	1.0
Burning rate coefficient	b	$36.8 [\text{cm/s}]/[\text{dyne/cm}^2]^n$
Gas equation of state coefficient	b_1	4.0 cm ³ /g
Axial space increment	Δz	1 mm
Radial space increment	Δr	1 mm
Time filter coefficient	c	0.25

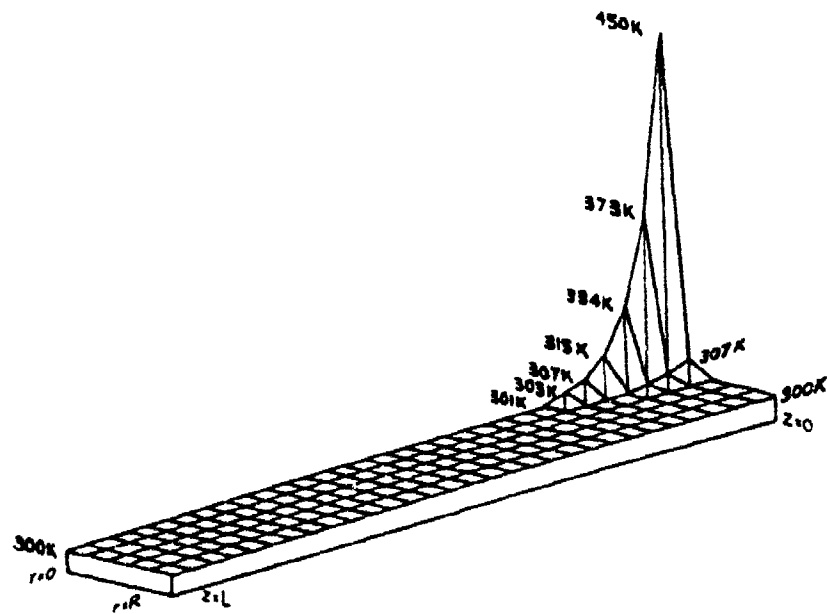


Figure 11. Two Dimensional Baseline Case Initial Temperature Profile

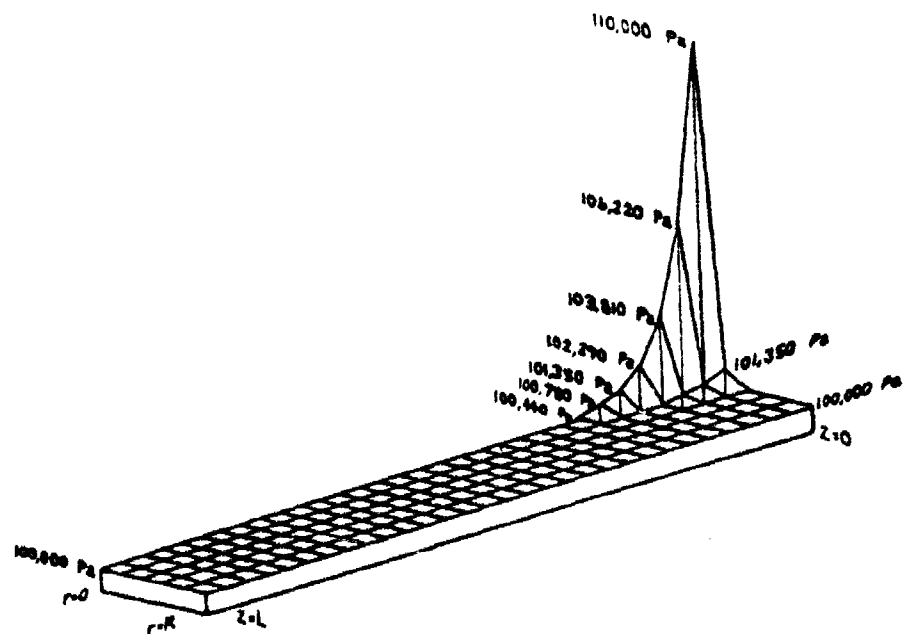


Figure 12. Two Dimensional Baseline Case Initial Pressure Profile

TEST COMPUTATIONS

Before any results can be obtained from the two dimensional model, the computer program should be able to successfully reproduce the solutions of other simpler cases. The failure to do so may indicate the need for some numerical fine tuning or variations of input parameters. (On the other hand, the inability to duplicate previous results may be symptomatic of a more serious problem with the code.) For these reasons, comparisons with other models are essential for the development of a viable two dimensional representation of the viscous gas flow in the damaged warhead.

The first case which was examined was the one dimensional inviscid, two-phase, reactive flow problem described by Butler, Lembeck, and Krier (Reference 8). In order to model these flow characteristics, viscous gas effects were switched off and initiation was fixed to take place in one dimension. The resulting propagation of the flame front is plotted in Figure 13. Notice the excellent correlation between the three different versions of the same problem. The Dahm (Reference 10) three dimensional code (run with a one dimensional initiation) predicts almost identical flame front locations while the purely one dimensional model produces slightly lower values. These results indicate that the DDT2D computer code can accurately model one dimensional, inviscid flows.

However, this is not the case for the more complicated two dimensional problems. This time the DDT2D program produced the locus of ignition fronts shown in Figure 14. Note that initially the flame front location varies in both the axial and radial directions. As time progresses, the variations in the r-direction become less and less, until the flow is nearly one dimensional, after $t = 1.97 \mu s$. While this result is qualitatively correct, the

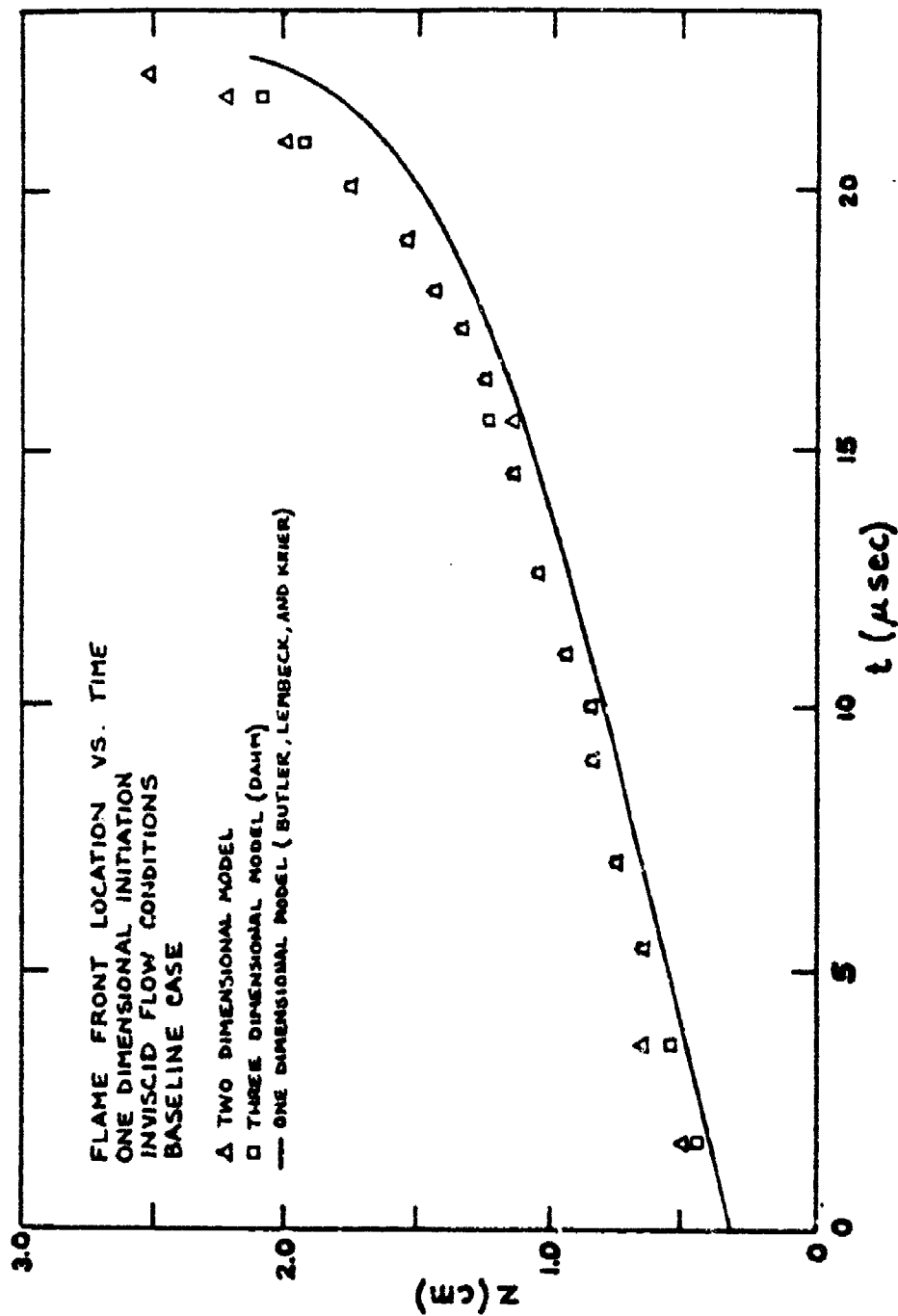


Figure 13. Comparison of the Flame Front Locations Predicted by Inviscid One Dimensional Simulations

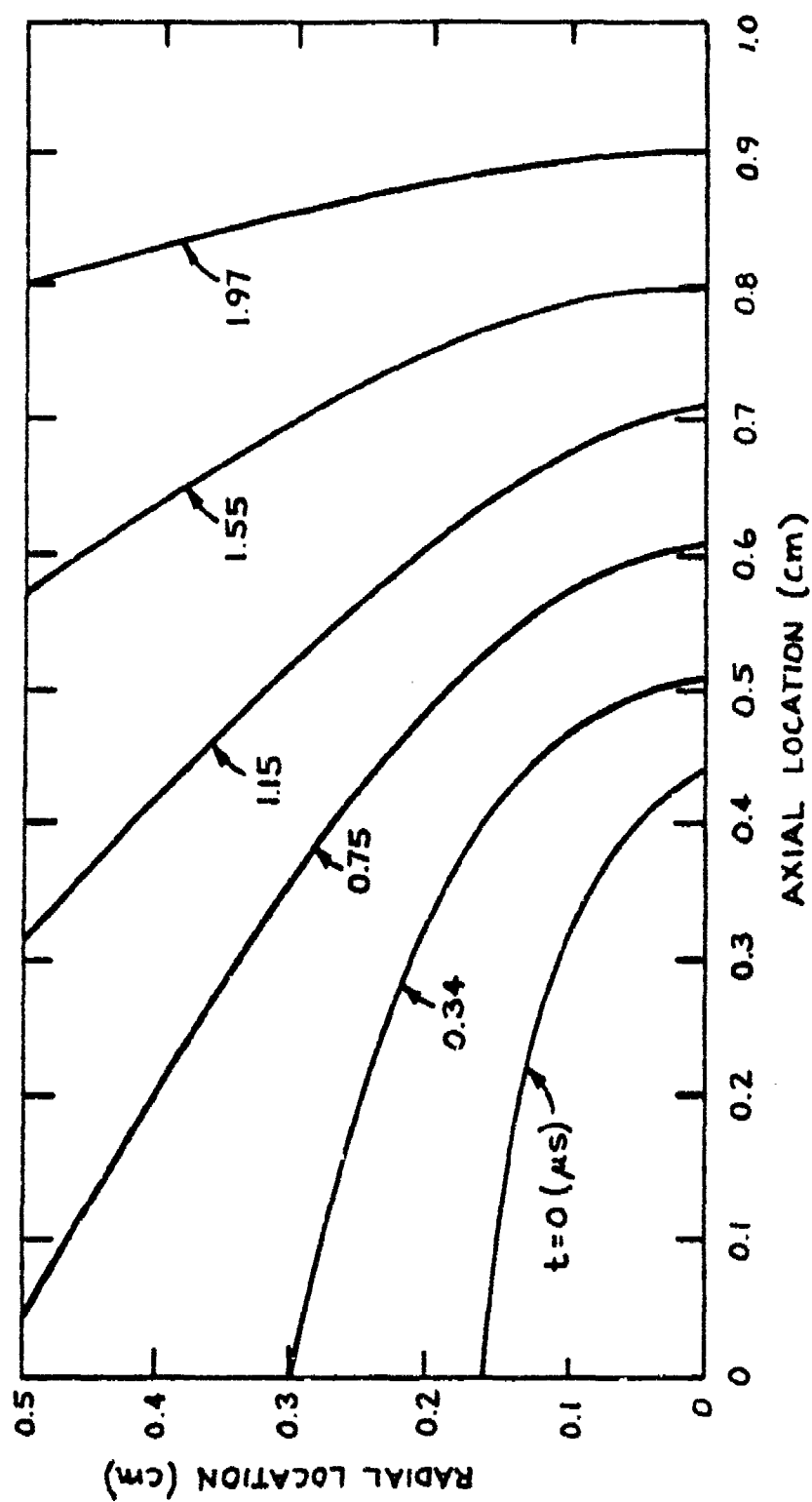


Figure 14. Flame Front Locus Showing the Transition from a Two-Dimensional Initiation to One Dimensional Flow

event takes place much too fast. Based upon results obtained by Dahm (Reference 10), the transition to one dimensional flow should not occur until nearly 50 μ s. Obviously, there is too much energy in the system causing the particles to ignite prematurely.

Therefore, it was decided to attempt to run a case with a two dimensional initiation and gas viscosity effects. It was assumed that the inclusion of the viscous dissipation terms in the gas energy equation would slow the advance of the flame front. Unfortunately, no meaningful results could be obtained since almost immediately, spatial oscillations developed. These wild swings in the radial velocity components (shown in Figure 15) eventually forced the program to stop after 11.33 μ s. Despite numerous attempts at damping these numerical oscillations with adjustments to the input parameters, no significant progress was made.

POSSIBLE FOLLOW UP

Although the current algorithm used in the DDT2D code may not be entirely free from all errors, the foundations are correct and work on this two-dimensional, viscous gas model should be continued. Reasonable results have been obtained for an inviscid one dimensional analysis. For this reason, it is felt that this program can eventually be used to solve the two-dimensional viscous flow problem without major alterations. Suggested areas for possible changes in DDT2D are,

1. Provide better initial conditions

The initial temperature and pressure profiles which are currently used in the two dimensional model actually do not satisfy the conservation equations

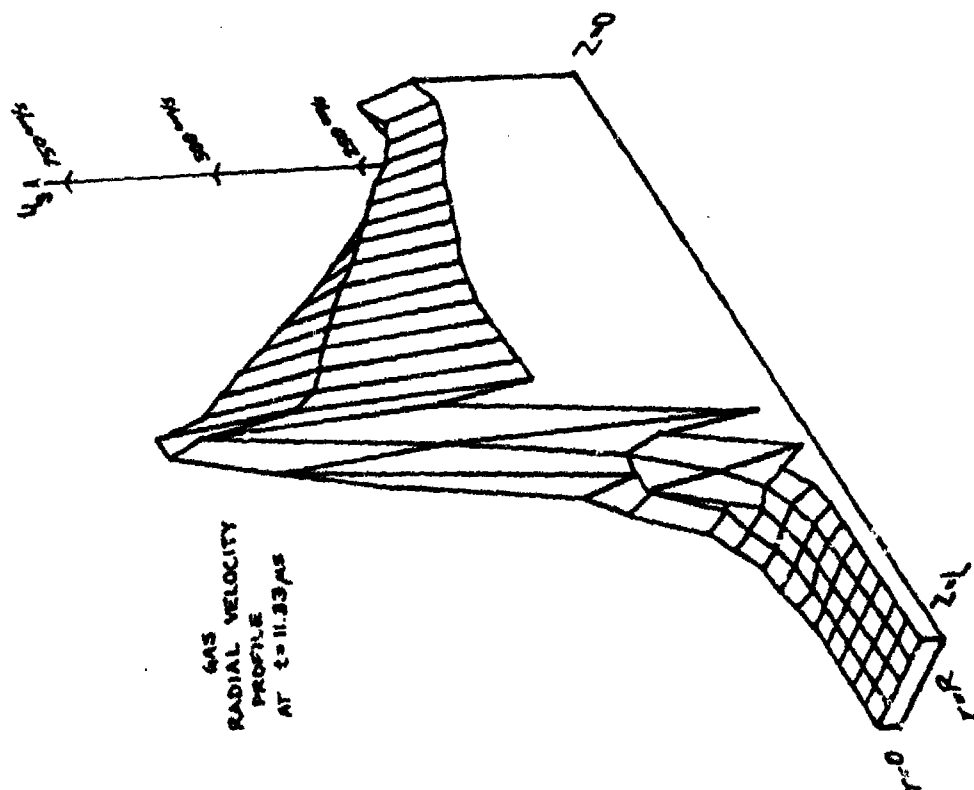


Figure 15. Viscous Gas Radial Velocity Profile at $t = 11.33 \mu s$
 [Notice the severe oscillations which occur ahead of
 the steep gradient.]

at time $t = 0$. Consequently, the flow must quickly adjust in order to meet the requirements of these governing relations. This momentary instability may be the trigger which touches off the oscillations which develop downstream. Therefore, better results may be obtained from initial conditions based upon established flows from inviscid models, such as a two-dimensional version of the Dahm code, given in Reference 10.

2. Determine an optimal time step

It may be advantageous to use a Von Neumann stability analysis (Reference 16) to determine the formula for the optimal size time step. This could then be incorporated into the computer program, enabling it to determine the ideal time increment for each integration, and insuring the stability of the differencing scheme.

3. Change the finite differencing scheme

The inviscid conservation relations form a set of hyperbolic partial differential equations which can be solved numerically by using the leapfrog scheme. However, when the second derivative terms representing viscous forces are included, the nature of the governing equations may become parabolic or elliptic. If this is the case, then a different finite differencing scheme must be implemented.

REFERENCES

1. Krier, H. and Van Tassel, W. F., "Combustion and Flame Spreading Phenomena in Gas Permeable Explosive Material," International Journal of Heat and Mass Transfer, Vol. 8, pp. 1377-1386, 1975.
2. Krier, H. and Gokhale, S., "Vigorous Ignition of Granulated Propellant Beds by Blast Impact," International Journal of Heat and Mass Transfer, Vol. 19, pp. 915-923, 1976.
3. Krier, H., Rajan, S., and Van Tassel, W. F., "Flame Spreading and Combustion in Packed Beds of Propellant Grains," AIAA Journal, Vol. 14, pp. 301-309, 1976.
4. Dimitstein, M., "A Separated-Flow Model for Predicting the Pressure Dynamics in Highly Loaded Beds of Granulated Propellant," MS Thesis, Dept. of Aero/Astro Engineering, University of Illinois at Urbana-Champaign, 1976.
5. Krier, H., Dimitstein, M., and Gokhale, S., "Reactive Two Phase Flow Models Applied to the Prediction of Detonation Transition in Granulated Solid Propellant," Technical Report AAE 76-3, UIUC-Eng 76-0503, UIUC, Dept. of Aero/Astro Engineering, July 1971.
6. Krier, H., Gokhale, S., and Hughes, E. D., "Modeling of Convective Mode Combustion Through Granulated Solid Propellant to Predict Possible Detonation Transition," AIAA paper 77-857, Presented at the 19th, AIAA/SAE, Propulsion Conference, Orlando, FL, July 1977.
7. Krier, H., and Kezerle, J. A., Seventeenth Combustion Symposium, The Combustion Institute, pp. 23-24, 1979.
8. Butler, P. B., Lembeck, M. F., and Krier, H., "Modeling of Shock Development and Transition to Detonation Initiated by Burning in Porous Propellant Beds," Combustion and Flame, Vol. 46, pp. 75-93, 1982.
9. Krier, H., Dahm, M. R., and Butler, P. B., "Modeling the Burn-to-Violent Reaction to Simulate Impact Damaged GP Warheads," Proceedings of the First Symposium on the Interactions of Non-Nuclear Munitions with Structures, U.S. Air Force Academy, Colorado, pp. 37, May 1983.
10. Dahm, M. R., "Numerical Integration of the Unsteady Two-Phase Conservation Equations to Predict Multi-Dimensional Flame Spreading in Partially Confined Porous Propellant Beds," MS Thesis, Dept. of Mechanical and Industrial Engineering, University of Illinois at Urbana-Champaign, 1984.
11. Markatos, N. C., and Kircaldy, D., "Analysis and Computation of Three-Dimensional, Transient Flow and Combustion Through Granulated Propellants," International Journal of Heat and Mass Transfer, Vol. 26, No. 7, pp. 1037-1053, 1983.

12. Krier, H., Dahm, M. R., and Samuelson, L. S., "Multi-Dimensional Reactive Flows to Simulate Detonation Delays in Damaged Warheads," Technical Report to Air Force Armament Laboratory (to be published September 1984).
13. Patankar, S. V., Numerical Heat Transfer and Fluid Flow, Washington: Hemisphere Publishing Co., pp. 118-120, 1980.
14. Kurihara, Y., "On the Use of Implicit and Iterative Methods for the Time Integration of the Wave Equation," Monthly Weather Report, Vol. 93, No. 1, pp. 33, June 1965.
15. Williams, G., "Numerical Integration of the Three-Dimensional Navier-Stokes Equations for Compressible Flow," Journal of Fluid Mechanics, Vol. 37, Part 4, pp. 727-750, 1969.
16. Richtmeyer, R. D., and Morton, K. W., Difference Methods for Initial Value Problems, New York: Interscience Publishers, 1967.
17. Robert, A. J., "The Intergration of a Low Order Spectral Form of the Primitive Meteorological Equations," Journal of the Meteorological Society of Japan, Ser. 2, Vol. 44, No. 5, pp. 237-245, Tokyo, October 1966.
18. Asselin, R., "Frequency Filter for Time Integrations," Monthly Weather Review, Vol. 100, No. 6, pp. 487-490, June 1972.
19. Arakawa, A., "Computation Design for Long Term Numerical Integration of the Equations of Fluid Motion, Two-Dimensional Incompressible Flow. Part 1," Journal of Computational Physics, Vol. 1, pp. 119, 1966.
20. Sod, G. A., "A Survey of Several Finite Difference Methods for Systems of Nonlinear Hyperbolic Conservation Laws," Journal of Computational Physics, Vol. 27, pp. 1-37, 1978.
21. Wilhelmson, R., ATMOS 405-A, Numerical Methods in Fluid Dynamics: Lecture Notes, University of Illinois. Dept. of Atmospheric Sciences, Fall 1983.
22. Butler, P. B., "Analysis of Deflagration to Detonation Transition in High-Energy Solid Propellants," Ph.D. Thesis, Dept. of Mechanical and Industrial Engineering, University of Illinois at Urbana-Champaign, 1984.
23. Coyne, D. W., Butler, P. B., and Krier, H., "Shock Development from Compression Waves Due to Confined Burning in Porous Solid Propellants and Explosives," AIAA Paper 83-0480, Presented at the 21st Aerospace Sciences Meeting, Reno, NV, January 1983.
24. Jones, D. P., and Krier, H., "Gas Flow Resistance Measurements Through Packed Beds at High Reynolds Numbers," Journal of Fluids Engineering, Vol. 105, pp. 168-173, June 1983.

APPENDIX A

AUXILIARY DATA BASE AND CONSTITUTIVE RELATIONS

The eight conservation equations presented in Section II contain 11 unknown quantities. Determining the values of these parameters requires the addition of three state relations, thereby providing closure to the system. Moreover, constitutive equations are needed to describe the gas viscosity and the interactions between phases. This appendix details these necessary supplemental relations which were used for this report.

1. Gas Phase Equation of State

A non-ideal equation of state was utilized:

$$P_g = RT_g \rho_g (1 + b_1 \rho_g) \quad (A-1)$$

The value of the coefficient b_1 is based upon a fit of CJ detonation data produced by the TIGER code (Reference 22) and is assumed to remain constant.

2. Solid Phase Equation of State

The density of the explosive particles was specified by applying the Tait equation (see Coyne, Butler, and Krier, Reference 23):

$$\rho_p = \rho_{p_0} \left[\frac{3P}{K_0} + 1 \right]^{1/3} \quad (A-2)$$

3. Porosity-Stress Relation

There are actually no suitable correlations for the dynamic porosity-stress relation for a packed bed of compressible solid particles over the range of conditions imposed by this problem. Consequently, an approximate numerical predictor method was used. At each time step, an equilibrium condition is applied, setting the particle pressure equal to that of the gas. Porosity is then determined by dividing the particle density from the previous step into the current value of the solid phase bulk density (predicted by Equation (4)). Since the time steps are small, and the changes in particle density are very gradual, the errors resulting from this approximation are not significant.

4. Gas Production Rate

The burning particles produce gas according to:

$$\dot{r}_c = \frac{3}{r_p} (1 - \phi) \rho_p \dot{r} \quad (\text{A-3})$$

where the particle surface to volume ratio for the spheres is $\frac{3}{r_p}$ and the surface burning rate was described as:

$$\dot{r} = b p_g^n \quad (\text{A-4})$$

with b and n being known imposed constants.

5. Gas Viscosity Coefficient

The viscosity of the gas phase was assumed to be a standard function of temperature only, and was given as:

$$\mu_g = \mu_{g_0} \left(\frac{T_g}{T_{g_0}} \right)^{0.65} \quad (\text{A-5})$$

A relation which considers the coefficient as a function of both temperature and pressure would have been more desirable here because the extreme pressures will have some influence on the viscosity.

6. Interphase Drag

The equations used to predict the drag forces between the gas and particles were:

$$D_r = \frac{\mu_g}{4r_p^2} (u_g - u_p) f_{pg} \quad (\text{A-6})$$

$$D_z = \frac{\mu_g}{4r_p^2} (w_g - w_p) f_{pg} \quad (\text{A-7})$$

where the friction factor f_{pg} is defined as:

$$f_{pg} = \frac{(1-\phi)^2}{\phi^2} \left[150 + 1.75 \left(\frac{Re}{1-\phi} \right)^{0.87} \right] \quad (\text{A-8})$$

Here Re is the flow Reynolds number based upon the particle diameter:

$$Re = \frac{2r_p V_{p1}}{\mu_g} \quad (\text{A-9})$$

where V represents the relative velocity of the gas as it moves over the solids, such that:

$$V = [(u_g - u_p)^2 + (w_g - w_p)^2]^{1/2} \quad (A-10)$$

This drag relationship was derived from semi-empirical results by Jones and Krier (Reference 24) for steady flow over a packed bed of spherical beads. It assumes a constant porosity and is valid for Reynolds number ranging from 733 to 126670. Although the problem presented in this study is unsteady with variable porosity, the Jones and Krier correlation produces reasonable values for the interphase drag in the two dimensional model.

7. Convective Heat Transfer

The rate of heat transfer between the gas and the particles is described by:

$$\dot{Q} = \frac{3}{r_p} (1-\phi) (T_g - T_p) h_{pg} \quad (A-11)$$

where the heat transfer coefficient h_{pg} is the classical Denton formula also used by Krier and Kezerle (Reference 7):

$$h_{pg} = 0.58 \frac{k_g}{r_p} Re^{0.7} Pr^{0.33} \quad (A-12)$$

APPENDIX B

FINITE DIFFERENCE FORM OF THE CONSERVATION EQUATIONS

Numerical computation methods must be employed to solve the unsteady, two-phase conservation equations derived in Section III. After the domain has been divided into discrete nodes, the governing partial differential equations are rewritten in finite difference form using the explicit, centered time, centered space, leapfrog scheme. The resulting algebraic relations are applied at all node points, producing a system which can be solved by a digital computer.

The following shorthand notation is used in the finite difference equations which are presented here. If "A" is considered to be a generalized dependent variable while "x" is an independent variable, then:

$$\delta_x A = \frac{A_{x+\frac{\Delta x}{2}} - A_{x-\frac{\Delta x}{2}}}{\Delta x} \quad (B-1)$$

$$\delta_{xx} A = \frac{A_{x+\Delta x} + A_{x-\Delta x} - 2A_x}{(\Delta x)^2} \quad (B-2)$$

$$\bar{A}_x = \frac{A_{x+\frac{\Delta x}{2}} + A_{x-\frac{\Delta x}{2}}}{2} \quad (B-3)$$

Thus the conservation equations in finite difference form are:

1. Conservation of Mass
 - a. Gas Phase Continuity (applied at scalar nodes)

$$\delta_t \bar{\rho}_1^t = -\frac{1}{r} \delta_r (\bar{\rho}_1^r r u_g) - \delta_z (\bar{\rho}_1^z w_g) + r_c \quad (B-4)$$

b. Particle Phase Continuity (applied at scalar nodes)

$$\delta_t \bar{\rho}_2^t = -\frac{1}{r} \delta_r (\bar{\rho}_2^r r u_p) - \delta_z (\bar{\rho}_2^z w_p) - r_c \quad (B-5)$$

2. Conservation of Momentum

a. Gas Phase Momentum

(1) Radial Direction (applied at radial velocity nodes)

$$\begin{aligned} \delta_t (\bar{\rho}_1^r u_g)^t &= -\frac{1}{r} \delta_r (\bar{\rho}_1^r \bar{u}_g^r \bar{u}_g^r) - \delta_z (\bar{\rho}_1^z \bar{u}_g^z \bar{w}_g^r) \\ &+ \bar{u}_g^r \left\{ \delta_r \left[\frac{1}{r} \delta_r (r u_g) \right] + \delta_{zz} u_g + \frac{1}{3} \delta_r \left[\frac{1}{r} \delta_r (r u_g) + \delta_z w_g \right] \right\} \\ &+ \bar{\Gamma}_c^r u_p - D_r - \delta_r (P_g \phi) \end{aligned} \quad (B-6)$$

(2) Axial Direction (applied at axial velocity nodes)

$$\begin{aligned} \delta_t (\bar{\rho}_1^z w_g)^t &= -\frac{1}{r} \delta_r (\bar{\rho}_1^r r \bar{u}_g^z \bar{w}_g^r) - \delta_z (\bar{\rho}_2^z \bar{w}_g^z \bar{w}_g^z) \\ &+ \bar{u}_g^z \left\{ \frac{1}{r} \delta_r (r \delta_r w_g) + \delta_{zz} w_g + \frac{1}{3} \delta_z \left[\frac{1}{r} \delta_r (r u_g) + \delta_z w_g \right] \right\} \\ &+ \bar{\Gamma}_c^z w_p - D_z - \delta_z (P_g \phi) \end{aligned} \quad (B-7)$$

b. Particle Phase

(1) Radial Direction (applied at radial velocity nodes)

$$\begin{aligned} \delta_t(\overline{\rho_2^r u_p})^t &= -\frac{1}{r} \delta_r(\rho_2^r \overline{u_p^r} \overline{u_p^r}) - \delta_z(\overline{\rho_2^z} \overline{u_p^z} \overline{w_p^r}) \\ &\quad - \overline{\Gamma_c^r} u_p + D_r - \delta_r[P_p(1-\phi)] \end{aligned} \quad (B-8)$$

(2) Axial Direction (applied at axial velocity nodes)

$$\begin{aligned} \delta_t(\overline{\rho_2^z w_p})^t &= -\frac{1}{r} \delta_r(\overline{\rho_2^r} r \overline{u_p^z} \overline{w_p^r}) - \delta_z(\rho_2 \overline{w_p^z} \overline{w_p^z}) \\ &\quad - \overline{\Gamma_c^z} w_p + D_z - \delta_z[P_p(1-\phi)] \end{aligned} \quad (B-9)$$

3. Conservation of Energy

a. Gas Phase (applied at scalar nodes)

$$\begin{aligned} \delta_t(\rho_1 \overline{E_g})^t &= -\frac{1}{r} \delta_r[\rho_1^r u_g r (\overline{E_g^r} + \frac{\overline{p_g^r}}{\rho_g})] - \delta_z[\rho_1^z w_g (\overline{E_g^z} + \frac{\overline{p_g^z}}{\rho_g})] \\ &\quad + \mu_g \{2 [(\delta_r u_g)^2 + (\frac{\overline{u_g^r}}{r})^2 + (\delta_z w_g)^2] \\ &\quad - \frac{2}{3} (\delta_r u_g + \frac{\overline{u_g^r}}{r} + \delta_z w_g)^2 + (\delta_r \overline{w_g^r} + \delta_z \overline{u_g^z})^2 \\ &\quad + \overline{u_g^r} \delta_r[\frac{1}{r} \delta_r(r \overline{u_g^r})] + \overline{u_g^r} \delta_{zz} \overline{u_g^r} \\ &\quad + \frac{\overline{u_g^r}}{3} \delta_r[\frac{1}{r} \delta_r(r \overline{u_g^r}) + \delta_z \overline{w_g^r}] + \frac{\overline{w_g^z}}{r} \delta_r(r \delta_r \overline{w_g^z}) \end{aligned}$$

$$\begin{aligned}
& + \bar{w}_g^z \delta_{zz} \bar{w}_g^z + \frac{\bar{w}_g^z}{3} \delta_z \left[\frac{1}{r} \delta_r (r \bar{u}_g^z) + \delta_z \bar{w}_g^z \right] \} \\
& - \dot{Q} - \bar{D}_r^r \bar{u}_p^r - \bar{D}_z^z \bar{w}_p^z \\
& + r_c \left(E_g^{\text{chem}} + \frac{\bar{u}_p^r^2}{2} + \frac{\bar{w}_p^z^2}{2} \right)
\end{aligned} \tag{B-10}$$

b. Particle Phase (applied at scalar nodes)

$$\begin{aligned}
\overline{\delta_t(\rho_2 E_p)}^t &= -\frac{1}{r} \delta_r \left[\rho_2^r u_p^r \left(E_p^r + \frac{\bar{p}_p^r}{\rho_p^r} \right) \right] - \delta_z \left[\rho_2^z w_p^z \left(E_p^z + \frac{\bar{p}_p^z}{\rho_p^z} \right) \right] \\
& + \dot{Q} + \bar{D}_r^r \bar{u}_p^r + \bar{D}_z^z \bar{w}_p^z + r_c \left(E_p^{\text{chem}} - \frac{\bar{u}_p^r^2}{2} - \frac{\bar{w}_p^z^2}{2} \right)
\end{aligned} \tag{B-11}$$

In Equations (B-10) and (B-11) the total energies are defined as:

$$\bar{E} = C_v T + \frac{(\bar{u}^r)^2}{2} + \frac{(\bar{w}^z)^2}{2} \tag{B-12}$$

$$\bar{E}^r = C_v T^r + \frac{u^2}{2} + \frac{(\bar{w}^z)^2}{2} \tag{B-13}$$

$$\bar{E}^z = C_v T^z + \frac{(\bar{u}^r)^2}{2} + \frac{w^2}{2} \tag{B-14}$$

where a subscript is added to denote gas or particle phase. In addition, the averages of the interphase drag terms must be described as:

$$\bar{D}_r^r = \frac{\mu_g}{4r_p^2} (\bar{u}_g^r - \bar{u}_p^r) f_{pg} \quad (B-15)$$

$$\bar{D}_z^z = \frac{\mu_g}{4r_p^2} (\bar{w}_g^z - \bar{w}_p^z) f_{pg} \quad (B-16)$$

while the remainder of the source/sink terms present no significant problems resulting from discretization of the system.

APPENDIX C
COMPUTER CODE LISTING

PROGRAM DDT2DA(INPUT,OUTPUT,TAPE6,TAPE7,TAPE8)

WRITTEN BY LAURENCE S. SAMUELSON AND HERMAN KRIER
UNIVERSITY OF ILLINOIS AT URBANA-CHAMPAIGN
LATEST VERSION--AUGUST 1984

THIS IS DDT2DA, A PROGRAM WHICH MODELS A DAMAGED GENERAL PURPOSE
WARHEAD IN TWO DIMENSIONS AND INCLUDES THE EFFECTS OF GAS
VISCOSITY. THE PROGRAM USES A CENTERED TIME, CENTERED SPACE,
EXPLICIT DIFFERENCING SCHEME ON A STAGGERED GRID. TO REDUCE THE
TIME SPLITTING OSCILLATIONS INHERENT IN CENTERED TIME METHODS,
A SMOOTHING STEP IS ALSO INCLUDED.

THE MAIN PROGRAM SETS THE SIZE OF THE TIME STEPS AND CONTROLS
THE FLOW OF INFORMATION THROUGH THE SUBROUTINES.

SUBROUTINE READA READS IN THE INPUT PARAMETERS FROM AN
EXTERIOR DATAFILE CALLED DATA2D. THESE VALUES ARE THEN
PRINTED TO AN OUTPUT FILE FOR CONFIRMATION AND INDEXING
PURPOSES.

SUBROUTINE INITIAL LOADS THE VARIABLE ARRAYS WITH THE INITIAL
CONDITIONS FOR THE BURN.

SUBROUTINE VARSET RESETS AND UPDATES THE SECONDARY VARIABLES
BASED UPON THE RESULTS FROM THE PREVIOUS TIME STEP. IT ALSO
PREPARES THE PRIMARY VARIABLES FOR THE NEXT TIME STEP.

SUBROUTINE SWEEP PERFORMS THE ACTUAL FINITE DIFFERENCE
INTEGRATIONS ON THE PRIMARY VARIABLES. ALL THE CALCULATIONS
ARE PERFORMED ON A SINGLE NODE BEFORE ADVANCING TO THE NEXT
POSITION. THE SUBROUTINE SWEEPS DOWN THE LENGTH OF THE BED
BEFORE MOVING TO A NEW RADIAL POSITION.

FUNCTION AVG AVERAGES THE VALUES AT THE INPUT NODE AND THE
PREVIOUS NODE IN THE INPUT DIRECTION.

FUNCTION DBLAVG AVERAGES THE VALUES OF FOUR NODES.

SUBROUTINE DUMP CONTROLS THE FORMAT OF THE OUTPUT.

SUBROUTINE DUMP2 PRINTS RATIOS OF DRAG AND VISCOS STRESS TERMS.

C THE VARIABLES USED IN THE PROGRAM ARE:
 C PRIMARY VARIABLES
 C RHO1 BULK GAS DENSITY
 C RHO2 BULK PARTICLE DENSITY
 C UG GAS RADIAL VELOCITY COMPONENT
 C UP PARTICLE RADIAL VELOCITY COMPONENT
 C WG GAS AXIAL VELOCITY COMPONENT
 C WP PARTICLE AXIAL VELOCITY COMPONENT
 C EG GAS TOTAL ENERGY
 C EP PARTICLE TOTAL ENERGY
 C SECONDARY VARIABLES
 C RHOG GAS PHASE DENSITY
 C RHOP PARTICLE PHASE DENSITY
 C PG GAS PHASE PRESSURE
 C PP PARTICLE PHASE PRESSURE
 C PGPFI BULK GAS PRESSURE
 C PPIMP BULK PARTICLE PRESSURE
 C TG GAS TEMPERATURE
 C TP PARTICLE PRESSURE
 C PHI POROSITY
 C RADP INSTANTANEOUS PARTICLE RADIUS
 C IGN CONDITION OF PARTICLE (INTACT, BURNING, OR BURNED OUT)
 C MUG GAS VISCOSITY
 C GAMMAC GAS GENERATION RATE DURING COMBUSTION
 C DRAGR RADIAL COMPONENT GAS-PARTICLE INTERACTION DRAG
 C DRAGZ AXIAL COMPONENT GAS-PARTICLE INTERACTION DRAG
 C QDOT HEAT TRANSFER RATE FROM GAS TO PARTICLE PHASE
 C ARVISR ARTIFICIAL VISCOSITY IN THE RADIAL DIRECTION
 C ARVISZ ARTIFICIAL VISCOSITY IN THE AXIAL DIRECTION
 C OTHER VARIABLES
 C RLEN ACTUAL RADIAL LENGTH OF BED
 C ZLEN ACTUAL AXIAL LENGTH OF BED
 C DELR RADIAL DIRECTION DIFFERENCING SPACE STEP
 C DELZ AXIAL DIRECTION DIFFERENCING SPACE STEP
 C DELT DIFFERENCING TIME STEP
 C STEP INCREMENTAL TIME STEP FACTOR
 C EPS TIME SMOOTHER COEFFICIENT
 C ARV ARTIFICIAL VISCOSITY COEFFICIENT
 C TOL TRUNCATION ERROR TOLERANCE
 C R ACTUAL RADIAL POSITION
 C TIME ACTUAL TIME
 C CVG GAS SPECIFIC HEAT AT CONSTANT VOLUME
 C CVP PARTICLE SPECIFIC HEAT AT CONSTANT VOLUME
 C RO GAS CONSTANT
 C MW MOLECULAR WEIGHT OF GAS
 C B1 NON-IDEAL EQUATION OF STATE CONSTANT
 C TGO INITIAL BULK GAS TEMPERATURE
 C TPG INITIAL BULK PARTICLE TEMPERATURE
 C TCH INITIAL LOCAL MAXIMUM TEMPERATURE
 C TIGN TEMPERATURE NECESSARY TO IGNITE PARTICLES
 C B BURNING RATE PROPORTIONALITY CONSTANT
 C BNT BURNING RATE INDEX
 C EPT PROPELLANT ENERGY
 C RHOP0 INITIAL PARTICLE DENSITY

C	PHIO	INITIAL POROSITY
C	PGO	INITIAL BULK GAS PRESSURE
C	PCH	INITIAL LOCAL MAXIMUM PRESSURE
C	PWALL	MAXIMUM PRESSURE AT THE WALLS
C	RADPO	INITIAL PARTICLE RADIUS
C	KO	PARTICLE BULK MODULUS
C	MUGO	INITIAL GAS VISCOSITY
C	PR	PRANDTL NUMBER
C	INIT	DETERMINES THE TYPE OF INITIATION
C		(ONE OR TWO DIMENSIONAL)
C	TOGGLE	TOGGLES GAS VISCOSITY EFFECTS ON AND OFF
C	ENDR	BOUNDARY NODE IN THE RADIAL DIRECTION
C	ENDZ	BOUNDARY NODE IN THE AXIAL DIRECTION
C	STOPIT	WARNING FLAG FOR IMPOSSIBLE CONDITIONS OCCURING
C	COUNT	INDICATES THE NUMBER OF SWEEPS THROUGH THE BED
C	MAX	MAXIMUM NUMBER OF INTEGRATION SWEEPS PERMITTED
C	RPRINT	DETERMINES THE NUMBER OF RADIAL NODES PRINTED
C	ZPRINT	DETERMINES THE NUMBER OF AXIAL NODES PRINTED
C	TPRINT	DETERMINES THE NUMBER OF TIME STEPS BETWEEN PRINTING
C	NTGR-	NUMBER OF NODES AT INITIAL TEMPERATURES/PRESSURES
C	NPGZ	ABOVE THE INITIAL BULK TEMPERATURE/PRESSURE
C	LOCAL VARIABLES	
C	A	SPEED OF SOUND
C	BURNED	AVERAGE CONDITION OF PARTICLES AT END OF BED
C	PHIM	1-POROSITY
C	RDOT	BURNING RATE
C	V	TOTAL GAS-PARTICLE RELATIVE VELOCITY
C	RE	REYNOLDS NUMBER
C	FPG	DRAG COEFFICIENT
C	KG	GAS THERMAL CONDUCTIVITY
C	HTC	GAS TO PARTICLE HEAT TRANSFER COEFFICIENT
C	CG1-	INTERMEDIATE QUANTITIES IN
C	EP6	CONTINUITY, MOMENTUM, AND ENERGY EQUATIONS
C	UGRHO1-	INTERMEDIATE QUANTITIES IN
C	EPRHO2	TIME SMOOTHER EQUATIONS
C	EGCHEM	GAS CHEMICAL ENERGY RELEASED DURING COMBUSTION
C	EPCHEM	PARTICLE CHEMICAL ENERGY RELEASED DURING COMBUSTION
C	RLOC	ACTUAL R LOCATION FOR PRINTING
C	ZLOC	ACTUAL Z LOCATION FOR PRINTING
C	PGSI	GAS PRESSURE IN GPA
C	RADPSI	PARTICLE RADIUS IN MICRO-METERS
C	TIMOUT	TIME OF PRINTING IN MICRO-SECONDS
C	DTOUT	SIZE OF TIME STEP IN MICRO-SECONDS
C	PWALOT	MAXIMUM WALL PRESSURE IN GPA
C	I,J,K	DO LOOP COUNTERS

*** LOCAL VARIABLES ***

REAL A
 INTEGER I, J, BURNED

*** COMMON VARIABLES ***

```

C      REAL RHO1(0:6,0:61,3), RHO2(0:6,0:61,3), UG(0:6,0:61,3),
      & UP(0:6,0:61,3), WG(0:6,0:61,3), WP(0:6,0:61,3),
      & EG(0:6,0:61,3), EP(0:6,0:61,3)
      REAL RHOG(0:6,0:61), RHOP(0:6,0:61), PG(0:6,0:61), PP(0:6,0:61),
      & PGPHI(0:6,0:61), PP1MF(0:6,0:61), TG(0:6,0:61), TP(0:6,0:61),
      & PHI(0:6,0:61), RADP(0:6,0:61), MUG(0:6,0:61),
      & GAMMAC(0:6,0:61), DRAGR(0:6,0:61), DRAGZ(0:6,0:61),
      & QDOT(0:6,0:61), ARVISR(0:6,0:61), ARVISZ(0:6,0:61)
      INTEGER IGN(0:6,0:61)
      REAL RLEN, ZLEN, DELR, DELZ, DELT, STEP, EPS, ARV, TOL, R, TIME,
      & CVG, CVP, RO, MW, B1, TGO, TPO, TCH, TIGN, B, ENT, EPT, RHOPO,
      & PHIO, PGO, PCH, PWALL, RADPO, KO, MUGO, PR
      INTEGER INIT, TOGGLE, ENDR, ENDZ, STOPIT, COUNT, MAX,
      & RPRINT, ZPRINT, TPRINT, NTGR, NTGZ, NTPR, NTPZ, NPGR, NPGZ
      COMMON /PRI/ RHO1, RHO2, UG, UP, WG, WP, EG, EP
      COMMON /SEC/ RHOG, RHOP, PG, PP, PGPHI, PP1MF, TG, TP, PHI,
      & RADP, IGN, MUG, GAMMAC, DRAGR, DRAGZ, QDOT, ARVISR, ARVISZ
      COMMON // RLEN, ZLEN, DELR, DELZ, DELT, STEP, EPS, ARV, TOL, R,
      & TIME, CVG, CVP, RO, MW, B1, TGO, TPO, TCH, TIGN, B, ENT, EPT,
      & RHOPO, PHIO, PGO, PCH, PWALL, RADPO, KO, MUGO, PR, INIT, TOGGLE,
      & ENDR, ENDZ, STOPIT, COUNT, MAX,
      & RPRINT, ZPRINT, TPRINT, NTGR, NTGZ, NTPR, NTPZ, NPGR, NPGZ

C
C      CALL READA
      CALL INITIAL
      TIME=0.0
      COUNT=0
      DELT=1.0E-8
      CALL DUMP
      CALL VARSET
      DO 10 COUNT=1,MAX
        CALL SWEEP

C
C      ** CHECK FOR BURNED OUT CONDITIONS **

      BURNED=0
      DO 20 I=1,ENDR
        BURNED=BURNED+IGN(I,ENDZ-3)
20      CONTINUE
      IF ((BURNED/ENDR)*ENDR.GE.1) THEN
        CALL DUMP
        STOP
      END IF

C
      IF ((COUNT/TPRINT)*TPRINT.EQ.COUNT) CALL DUMP
      CALL VARSET
      TIME=TIME+DELT

C
C      ** COMPUTE NEW TIME STEP **

      DELT=5.0E-7
      DO 30 I=1,ENDR

```

```

DO 40 J=1,ENDZ
C      A=SQRT(PG(I,J)/RHOG(I,J)*((1.0+2.0*B1*RHOG(I,J))
C      & /((1.0+B1*RHOG(I,J))+RO/MW/CVG*(1.0+B1*RHOG(I,J))))
      A=SQRT(KO/RHO2(I,J,2))
      DTR=STEP*DEL R/A
      DTZ=STEP*DEL Z/A
      IF (DTR.LT.DELT) DELT=DTR
      IF (DTZ.LT.DELT) DELT=DTZ
40     CONTINUE
30     CONTINUE
10     CONTINUE
C
C      ** IF THIS POINT IS REACHED, THE PROGRAM HAS EXCEEDED **
C      ** THE MAXIMUM NUMBER OF TIME STEPS ALLOWED **
C
PRINT 100
100  FORMAT(' THE MAXIMUM NUMBER OF TIME STEPS HAS BEEN REACHED')
STOP
END

C
C
C      SUBROUTINE READA
C
C      ** COMMON VARIABLES **
C
      REAL RHO1(0:6,0:61,3), RHO2(0:6,0:61,3), UG(0:6,0:61,3),
& UP(0:6,0:61,3), WG(0:6,0:61,3), WP(0:6,0:61,3),
& EG(0:6,0:61,3), EP(0:6,0:61,3)
      REAL RHOG(0:6,0:61), RHOP(0:6,0:61), PG(0:6,0:61), PP(0:6,0:61),
& PGPHI(0:6,0:61), PP1MF(0:6,0:61), TG(0:6,0:61), TP(0:6,0:61),
& PHI(0:6,0:61), RADP(0:6,0:61), MUG(0:6,0:61),
& GAMMAC(0:6,0:61), DRAGR(0:6,0:61), DRAGZ(0:6,0:61),
& QDOT(0:6,0:61), ARVISR(0:6,0:61), ARVISZ(0:6,0:61)
      INTEGER ICN(0:6,0:61)
      REAL RLEN, ZLEN, DEL R, DEL Z, DELT, STEP, EPS, ARV, TOL, R, TIME,
& CVG, CVP, RO, MW, B1, TGO, TPO, TCH, TIGN, B, BMT, EPT, RHOPO,
& PHIO, PGO, PCH, PWALL, RADPO, KO, MUGO, PR
      INTEGER INIT, TOGGLE, ENDR, ENDZ, STOPIT, COUNT, MAX,
& RPRINT, ZPRINT, TPRINT, NTGR, NTGZ, NTPR, NTPZ, NPGR, NPGZ
      COMMON /PRI/ RHO1, RHO2, UG, UP, WG, WP, EG, EP
      COMMON /SEC/ RHOG, RHOP, PG, PP, PGPHI, PP1MF, TG, TP, PHI,
& RADP, ICN, MUG, GAMMAC, DRAGR, DRAGZ, QDOT, ARVISR, ARVISZ
      COMMON // RLEN, ZLEN, DEL R, DEL Z, DELT, STEP, EPS, ARV, TOL, R,
& TIME, CVG, CVP, RO, MW, B1, TGO, TPO, TCH, TIGN, B, BMT, EPT,
& RHOPO, PHIO, PGO, PCH, PWALL, RADPO, KO, MUGO, PR, INIT, TOGGLE,
& ENDR, ENDZ, STOPIT, COUNT, MAX,
& RPRINT, ZPRINT, TPRINT, NTGR, NTGZ, NTPR, NTPZ, NPGR, NPGZ
C
C
      READ 1, RLEN
      READ 2, ZLEN
      READ 3, ENDR
      READ 4, ENDZ

```

READ 5, STEP
 READ 6, EPS
 READ 7, ARV
 READ 8, TOL
 READ 9, MAX
 READ 10, CVG
 READ 11, CVP
 READ 12, RO
 READ 13, MW
 READ 14, B1
 READ 15, TGO
 READ 16, TPO
 READ 17, TCH
 READ 18, NTGR
 READ 19, NTGZ
 READ 20, NTPR
 READ 21, NTPZ
 READ 22, PGO
 READ 23, PCH
 READ 24, NPCR
 READ 25, NPGZ
 READ 26, TIGN
 READ 27, B
 READ 28, BNT
 READ 29, KO
 READ 30, EPT
 READ 31, RHOPO
 READ 32, PHIO
 READ 33, RADPO
 READ 34, MUGO
 READ 35, PR
 READ 36, TPRINT
 READ 37, RPRINT
 READ 38, ZPRINT
 READ 39, INIT
 READ 40, TOGGLE

1 FORMAT(/19X,G33.16)
 2 FORMAT(18X,G33.16)
 3 FORMAT(/19X,I3)
 4 FORMAT(18X,I3)
 5 FORMAT(29X,G33.16)
 6 FORMAT(27X,G33.16)
 7 FORMAT(33X,G33.16)
 8 FORMAT(36X,G33.16)
 9 FORMAT(37X,I5)
 10 FORMAT(/28X,G33.16)
 11 FORMAT(33X,G33.16)
 12 FORMAT(35X,G33.16)
 13 FORMAT(29X,G33.16)
 14 FORMAT(44X,G33.16)
 15 FORMAT(/33X,G33.16)
 16 FORMAT(38X,G33.16)
 17 FORMAT(38X,G33.16)
 18 FORMAT(/19X,I3)

```

19  FORMAT(19X,I3)
20  FORMAT(/19X,I3)
21  FORMAT(18X,I3)
22  FORMAT(34X,G33.16)
23  FORMAT(43X,G33.16)
24  FORMAT(/19X,I3)
25  FORMAT(18X,I3)
26  FORMAT(/46X,G33.16)
27  FORMAT(38X,G33.16)
28  FORMAT(19X,G33.16)
29  FORMAT(34X,G33.16)
30  FORMAT(24X,G33.16)
31  FORMAT(32X,G33.16)
32  FORMAT(17X,G33.16)
33  FORMAT(29X,G33.16)
34  FORMAT(30X,G33.16)
35  FORMAT(19X,G33.16)
36  FORMAT(/36X,I3)
37  FORMAT(38X,I3)
38  FORMAT(37X,I3)
39  FORMAT(/41X,I1)
40  FORMAT(45X,I1)

```

C
C

```

PRINT 100
PRINT 101, RLEN
PRINT 102, ZLEN
PRINT 103, ENDR
PRINT 104, ENDZ
PRINT 105, STEP
PRINT 106, EPS
PRINT 107, ARV
PRINT 108, TOL
PRINT 109, MAX
PRINT 110, CVG
PRINT 111, CVP
PRINT 112, RO
PRINT 113, MW
PRINT 114, B1
PRINT 115, TGO
PRINT 116, TPO
PRINT 117, TCH
PRINT 118, NTGR
PRINT 119, NTGZ
PRINT 120, NTPR
PRINT 121, NTPZ
PRINT 122, PCO
PRINT 123, PCH
PRINT 124, NPGR
PRINT 125, NPCZ
PRINT 126, TIGN
PRINT 127, B
PRINT 128, BMT
PRINT 129, KO

```

```

PRINT 130, EPT
PRINT 131, RHOPO
PRINT 132, PHIO
PRINT 133, RADPO
PRINT 134, MUOGO
PRINT 135, PR
PRINT 136, TPRINT
PRINT 137, RPRINT
PRINT 138, ZPRINT
IF(INIT.EQ.1) PRINT 139
IF(INIT.EQ.0) PRINT 239
IF(TOGGLE.EQ.1) PRINT 140
IF(TOGGLE.EQ.0) PRINT 240
100 FORMAT('I','INPUT PARAMETERS FOR DDT2DA')
101 FORMAT('O','RADIAL LENGTH (CM)=' ,G12.4)
102 FORMAT(' ','AXIAL LENGTH (CM)=' ,G12.4)
103 FORMAT(' ','NUMBER OF SCALAR NODES--'/
& ' ','RADIAL DIRECTION=' ,I3)
104 FORMAT(' ','AXIAL DIRECTION=' ,I3)
105 FORMAT(' ','INCREMENTAL TIME STEP FACTOR=' ,G12.4)
106 FORMAT(' ','TIME SMOOTHING COEFFICIENT=' ,G12.4)
107 FORMAT(' ','ARTIFICIAL VISCOSITY COEFFICIENT=' ,G12.4)
108 FORMAT(' ','TRUNCATION ERROR TOLERANCE (CM/SEC)=' ,G12.4)
109 FORMAT(' ','MAXIMUM NUMBER OF TIME STEPS ALLOWED=' ,I5)
110 FORMAT('O','GAS SPECIFIC HEAT (ERG/G/K)=' ,G12.4)
111 FORMAT(' ','PARTICLE SPECIFIC HEAT (ERG/G/K)=' ,G12.4)
112 FORMAT(' ','UNIVERSAL GAS CONSTANT (ERG/MOL/K)=' ,G12.4)
113 FORMAT(' ','GAS MOLECULAR WEIGHT (G/MOL)=' ,G12.4)
114 FORMAT(' ','NON-IDEAL EQUATION OF STATE CONSTANT (CC/G)=' ,G12.4)
115 FORMAT('O','INITIAL BULK GAS TEMPERATURE (K)=' ,G12.4)
116 FORMAT(' ','INITIAL BULK PARTICLE TEMPERATURE (K)=' ,G12.4)
117 FORMAT(' ','MAXIMUM LOCAL INITIAL TEMPERATURE (K)=' ,G12.4)
118 FORMAT(' ','NUMBER OF SCALAR NODES ABOVE BULK GAS TEMPERATURE--'/
& ' ','RADIAL DIRECTION=' ,I3)
119 FORMAT(' ','AXIAL DIRECTION=' ,I3)
120 FORMAT(' ','
& 'NUMBER OF SCALAR NODES ABOVE BULK PARTICLE TEMPERATURE--'/
& ' ','RADIAL DIRECTION=' ,I3)
121 FORMAT(' ','AXIAL DIRECTION=' ,I3)
122 FORMAT(' ','INITIAL BULK PRESSURE (DYN/CM/CM)=' ,G12.4)
123 FORMAT(' ','MAXIMUM LOCAL INITIAL PRESSURE (DYN/CM/CM)=' ,G12.4)
124 FORMAT(' ','NUMBER OF SCALAR NODES ABOVE BULK PRESSURE--'/
& ' ','RADIAL DIRECTION=' ,I3)
125 FORMAT(' ','AXIAL DIRECTION=' ,I3)
126 FORMAT('O','TEMPERATURE NECESSARY TO IGNITE PARTICLES (K)=' ,G12.4)
127 FORMAT(' ','BURNING RATE PROPORTIONALITY CONSTANT=' ,G12.4)
128 FORMAT(' ','BURNING RATE INDEX=' ,G12.4)
129 FORMAT(' ','PARTICLE BULK MODULUS (DYN/CM/CM)=' ,G12.4)
130 FORMAT(' ','PROPELLANT ENERGY (ERG)=' ,G12.4)
131 FORMAT(' ','INITIAL PARTICLE DENSITY (G/CC)=' ,G12.4)
132 FORMAT(' ','INITIAL POROSITY=' ,G12.4)
133 FORMAT(' ','INITIAL PARTICLE RADIUS (CM)=' ,G12.4)
134 FORMAT(' ','INITIAL GAS VISCOSITY (POISE)=' ,G12.4)
135 FORMAT(' ','GAS PRANDTL NUMBER=' ,G12.4)

```

```

136 FORMAT('0','NUMBER OF TIME STEPS BETWEEN OUTPUT=',I3)
137 FORMAT(' ','NUMBER OF RADIAL NODES BETWEEN OUTPUT=',I3)
138 FORMAT(' ','NUMBER OF AXIAL NODES BETWEEN OUTPUT=',I3)
139 FORMAT('-', '** INITIATION TAKES PLACE TWO-Dimensionally **')
239 FORMAT('-', '** INITIATION TAKES PLACE ONE-Dimensionally **')
140 FORMAT('0', '** VISCous GAS EFFECTS ARE INCLUDED **')
240 FORMAT('0', '** VISCous GAS EFFECTS ARE NOT INCLUDED **')
      RETURN
      END

C
C
C
      SUBROUTINE INITIAL
C
C      ** LOCAL VARIABLES **
C
      INTEGER I, J, K
C
C      ** COMMON VARIABLES **
C
      REAL RHO1(0:6,0:61,3), RHO2(0:6,0:61,3), UG(0:6,0:61,3),
& UP(0:6,0:61,3), WG(0:6,0:61,3), WP(0:6,0:61,3),
& EG(0:6,0:61,3), EP(0:6,0:61,3)
      REAL RHOG(0:6,0:61), RHOP(0:6,0:61), PG(0:6,0:61), PP(0:6,0:61),
& PGPHI(0:6,0:61), PP1MF(0:6,0:61), TG(0:6,0:61), TP(0:6,0:61),
& PHI(0:6,0:61), RADP(0:6,0:61), MUG(0:6,0:61),
& GAMMAC(0:6,0:61), DRAGR(0:6,0:61), DRAGZ(0:6,0:61),
& QDOT(0:6,0:61), ARVISR(0:6,0:61), ARVISZ(0:6,0:61)
      INTEGER IGN(0:6,0:61)
      REAL RLEN, ZLEN, DELR, DELZ, DELT, STEP, EPS, ARV, TOL, R, TIME,
& CVG, CVP, RO, MW, B1, TGO, TPO, TCH, TIGN, B, BNT, EPT, RHOPO,
& PHIO, PGO, PCH, PWALL, RADPO, KO, MUGO, PR
      INTEGER INIT, TOGGLE, ENDR, ENDZ, STOPIT, COUNT, MAX,
& RPRINT, ZPRINT, TPRINT, NTGR, NTGZ, NTPR, NTPZ, NPCR, NPGZ
      COMMON /PRI/ RHO1, RHO2, UG, UP, WG, WP, EG, EP
      COMMON /SEC/ RHOG, RHOP, PG, PP, PGPHI, PP1MF, TG, TP, PHI,
& RADP, IGN, MUG, GAMMAC, DRAGR, DRAGZ, QDOT, ARVISR, ARVISZ
      COMMON // RLEN, ZLEN, DELR, DELZ, DELT, STEP, EPS, ARV, TOL, R,
& TIME, CVG, CVP, RO, MW, B1, TGO, TPO, TCH, TIGN, B, BNT, EPT,
& RHOPO, PHIO, PGO, PCH, PWALL, RADPO, KO, MUGO, PR, INIT, TOGGLE,
& ENDR, ENDZ, STOPIT, COUNT, MAX,
& RPRINT, ZPRINT, TPRINT, NTGR, NTGZ, NTPR, NTPZ, NPCR, NPGZ
C
C
      EXTERNAL AVG
      STOPIT=0
      DELR=RLEN/ENDR
      DELZ=ZLEN/ENDZ
      DO 10 I=0,ENDR+1
        DO 20 J=0,ENDZ+1
C
C
C      ** POROSITY **
C
      PHI(I,J)=PHIO

```



```

C
C
C      ** TEMPERATURE **
      TG(I,J)=TGO
      IF(INIT.EQ.1.AND.(I.LE.NTGR.AND.J.LE.NTGZ)) THEN
C      IF(J+(1.0*NTGZ)/NTGR*I.LE.NTGZ)
C      &      TG(I,J)=(NTGZ*NTGR*TCH-NTGZ*(TCH-TGO)*(I-1)-NTGR
C      &      *(TCH-TGO)*(J-1))/(NTGZ*NTGR)
      TG(I,J)=TGO+(TCH-TGO)*((NTGR*1.0-(I-1))/NTGR*1.0)**14.0
      &      *((NTGZ*1.0-(J-1))/NTGZ*1.0)**14.0
      ELSE
      IF(J.LE.NTGZ)
C      &      TG(I,J)=TCH-(TCH-TGO)*(J-1)/NTGZ
C      &      TG(I,J)=TGO+(TCH-TGO)*((NTGZ*1.0-(J-1))/NTGZ*1.0)**14.0
      END IF
      TP(I,J)=TPO
      IF(INIT.EQ.1.AND.(I.LE.NTPR.AND.J.LE.NTPZ)) THEN
C      IF(J+(1.0*NTPZ)/NTPR*I.LE.NTPZ)
C      &      TP(I,J)=(NTPZ*NTPR*TCH-NTPZ*(TCH-TPO)*(I-1)-NTPR
C      &      *(TCH-TPO)*(J-1))/(NTPZ*NTPR)
      TP(I,J)=TPO+(TCH-TPO)*((NTPR*1.0-(I-1))/NTPR*1.0)**14.0
      &      *((NTPZ*1.0-(J-1))/NTPZ*1.0)**14.0
      ELSE
      IF(J.LE.NTPZ)
C      &      TP(I,J)=TCH-(TCH-TPO)*(J-1)/NTPZ
C      &      TP(I,J)=TPO+(TCH-TPO)*((NTPZ*1.0-(J-1))/NTPZ*1.0)**14.0
      END IF
C
C
C      ** PRESSURE **
      PG(I,J)=PGO
      IF(INIT.EQ.1.AND.(I.LE.NPGR.AND.J.LE.NPGZ)) THEN
C      IF(J+(1.0*NPGZ)/NPGR*I.LE.NPGZ)
C      &      PG(I,J)=(NPGZ*NPGR*PCH-NPGZ*(PCH-PGO)*(I-1)-NPGR
C      &      *(PCH-PGO)*(J-1))/(NPGZ*NPGR)
      PG(I,J)=PGO+(PCH-PGO)*((NPGR*1.0-(I-1))/NPGR*1.0)**14.0
      &      *((NPGZ*1.0-(J-1))/NPGZ*1.0)**14.0
      ELSE
      IF(J.LE.NPGZ)
C      &      PG(I,J)=PCH-(PCH-PGO)*(J-1)/NPGZ
C      &      PG(I,J)=PGO+(PCH-PGO)*((NPGZ*1.0-(J-1))/NPGZ*1.0)**14.0
      END IF
      PP(I,J)=PG(I,J)
      PGPHI(I,J)=PG(I,J)*PHI(I,J)
      PP1MF(I,J)=PP(I,J)*(1.0-PHI(I,J))
      PWALL=PCH
C
C
C      ** DENSITY **
      RHOP(I,J)=RHOP0
      RHOG(I,J)=(PG(I,J)*MW)/(RO*TG(I,J))
C
C
C      ** PARTICLE SIZE AND GAS PRODUCTION **

```

```

RADP(I,J)=RADPO
IGN(I,J)=0
GAMMAC(I,J)=0.0
C
C
C
** DRAG, VISCOSITY, AND HEAT TRANSFER RATE **

DRAGR(I,J)=0.0
DRAGZ(I,J)=0.0
MUG(I,J)=0.0
QDOT(I,J)=0.0
C
C
C
** PRIMARY VARIABLES **

DO 30 K=1,3
  RHO1(I,J,K)=RHOG(I,J)*PHI(I,J)
  RHO2(I,J,K)=RHOP(I,J)*(1.0-PHI(I,J))
  UG(I,J,K)=0.0
  UP(I,J,K)=0.0
  WG(I,J,K)=0.0
  WP(I,J,K)=0.0
  EG(I,J,K)=(TG(I,J)-TGO)*CVG
  EP(I,J,K)=(TP(I,J)-TPO)*CVP
30  CONTINUE
20  CONTINUE
10  CONTINUE
RETURN
END
C
C
C
SUBROUTINE VARSET
C
C
C
** LOCAL VARIABLES **

REAL PHIM, RDOT, V, RE, FPG, KG, HTC
INTEGER I, J, K
C
C
C
** COMMON VARIABLES **

REAL RHO1(0:6,0:61,3), RHO2(0:6,0:61,3), UG(0:6,0:61,3),
& UP(0:6,0:61,3), WG(0:6,0:61,3), WP(0:6,0:61,3),
& EG(0:6,0:61,3), EP(0:6,0:61,3)
REAL RHOG(0:6,0:61), RHOP(0:6,0:61), PG(0:6,0:61), PP(0:6,0:61),
& PGPHI(0:6,0:61), PP1MF(0:6,0:61), TG(0:6,0:61), TP(0:6,0:61),
& PHI(0:6,0:61), RADP(0:6,0:61), MUG(0:6,0:61),
& GAMMAC(0:6,0:61), DRAGR(0:6,0:61), DRAGZ(0:6,0:61),
& QDOT(0:6,0:61), ARVISR(0:6,0:61), ARVISZ(0:6,0:61)
INTEGER IGN(0:6,0:61)
REAL RLEN, ZLEN, DELR, DELZ, DELT, STEP, EPS, ARV, TOL, R, TIME,
& CVG, CVP, RO, MW, B1, TGO, TPO, TCH, TIGN, B, BNT, EPT, RHOPO,
& PHIO, PGO, PCH, PWALL, RADPO, KO, MUGO, PR
INTEGER INIT, TOGGLE, ENDR, ENDZ, STOPIT, COUNT, MAX,
& RPRINT, ZPRINT, TPRINT, NTGR, NTGZ, NTPR, NTPZ, NPGR, NPGZ
COMMON /PRI/ RHO1, RHO2, UG, UP, WG, WP, EG, EP

```

```

COMMON /SEC/ RHOG, RHOP, PG, PP, PGPFI, PPIMF, TG, TP, PHI,
& RADP, IGM, MUG, GAMMAC, DRAGR, DRAGZ, QDOT, ARVISR, ARVISZ
COMMON // RLEN, ZLEN, DELR, DELZ, DELT, STEP, EPS, ARV, TOL, R,
& TIME, CVG, CVP, RO, MW, B1, TGO, TPO, TCH, TIGN, B, BMT, EPT,
& RHOPO, PHIO, PGO, PCH, FWALL, RADPO, KO, MUGO, PR, INIT, TOGGLE,
& ENDR, ENDZ, STOPIT, COUNT, MAX,
& RPRINT, ZPRINT, TPRINT, NTGR, NTGZ, NTPR, NTPZ, NPCR, NPGZ

```

```

C
C
EXTERNAL AVG
DO 10 I=0,ENDR
DO 20 J=0,ENDZ

```

```

C
C
C
** POROSITY APPROXIMATION **

```

```

PHIM=RHO2(I,J,1)/RHOP(I,J)
PHI(I,J)=1.0-PHIM

```

```

C
C
C
** TEMPERATURE **

```

```

& TG(I,J)=(EQ(I,J,1)-AVG(UG,I+1,J,1,1)**2.0/2.0
& -AVG(WG,I,J+1,1,2)**2.0/2.0)/CVG+TGO
& TP(I,J)=(EP(I,J,1)-AVG(UP,I+1,J,1,1)**2.0/2.0
& -AVG(WP,I,J+1,1,2)**2.0/2.0)/CVP+TPO

```

```

C
C
C
** EQUATIONS OF STATE **

```

```

RHOG(I,J)=RHO1(I,J,1)/PHI(I,J)
PG(I,J)=(RO/MW)*TG(I,J)*RHOG(I,J)*(1.0+B1*RHOG(I,J))
PGPFI(I,J)=PG(I,J)*PHI(I,J)
PP(I,J)=PG(I,J)
PPIMF(I,J)=PP(I,J)*PHIM
RHOP(I,J)=RHOPO*(3.0*(PP(I,J)-1.0E6)/KO+1.0)**(1.0/3.0)

```

```

C
C
C
** CONTAINMENT WALL PRESSURE **

```

```

IF(PG(ENDR,J).GT.FWALL) FWALL=PG(ENDR,J)
IF(PG(I,ENDZ).GT.FWALL) FWALL=PG(I,ENDZ)

```

```

C
C
C
** GAS PRODUCTION **

```

```

IF(PHI(I,J).GT.0.985) THEN
  IGM(I,J)=2
  GAMMAC(I,J)=0.0
  IF(TP(I,J).GT.TG(I,J)) TP(I,J)=TG(I,J)
  ELSE IF(TP(I,J).GE.TIGN.OR.IGM(I,J).EQ.1) THEN
    IGM(I,J)=1
    RDOT=(B*(PG(I,J)*1.45E-5)**BMT)*2.54
    RADP(I,J)=RADP(I,J)-RDOT*DELT
    GAMMAC(I,J)=3.0/RADP(I,J)*PHIM*RHOP(I,J)*RDOT
  ELSE
    IGM(I,J)=0
    GAMMAC(I,J)=0.0
  END IF

```

```

C
C
C      ** GAS VISCOSITY **
C
C      MUG(I,J)=MUGO*((TG(I,J)/TGO)**0.65)
C
C
C      ** REYNOLDS NUMBER **
C
C      V=SQRT((UG(I,J,1)-UP(I,J,1))**2.0+(WG(I,J,1)-WP(I,J,1))**2.0)
C      RE=RHO1(I,J,1)*V*2.0*RADP(I,J)/MUG(I,J)
C
C
C      ** DRAG **
C
C      FPG=PHIM**2.0/PHI(I,J)**2.0*(150.0+3.89*(RE/PHIM)**0.87)
C      DRAGR(I,J)=MUG(I,J)/(4.0*RADP(I,J)**2.0)*FPG
C      &      *(UG(I,J,2)-UP(I,J,2))
C      DRAGZ(I,J)=MUG(I,J)/(4.0*RADP(I,J)**2.0)*FPG
C      &      *(WG(I,J,2)-WP(I,J,2))
C
C
C      ** HEAT TRANSFER RATE **
C
C      KG=MUG(I,J)*((RO/MW)+CVG)/PR
C      HTC=0.58*KG/RADP(I,J)*(RE**0.7)*(PR**0.3333)
C      IF(IGN(I,J).GT.0) THEN
C          QDOT(I,J)=0.0
C      ELSE
C          QDOT(I,J)=3.0*PHIM/RADP(I,J)*(TG(I,J)-TP(I,J))*HTC
C      END IF
C
C
C      ** ARTIFICIAL VISCOSITY **
C
C      ARVISR(I,J)=ARV*(ABS(AVG(UG,I+1,J,2,1)+0.1)+2.74E5)
C      ARVISZ(I,J)=ARV*(ABS(AVG(WG,I,J+1,2,2)+0.1)+2.74E5)
C      ARVISR(ENDR+1,J)=ARVISR(ENDR,J)
C      ARVISR(I,ENDZ+1)=ARVISR(I,ENDZ)
C      ARVISZ(ENDR+1,J)=ARVISZ(ENDR,J)
C      ARVISZ(I,ENDZ+1)=ARVISZ(I,ENDZ)
C
C
C      ** PRIMARY VARIABLE SHIFT **
C
C      DO 30 K=3,2,-1
C          RHO1(I,J,K)=RHO1(I,J,K-1)
C          RHO2(I,J,K)=RHO2(I,J,K-1)
C          UG(I,J,K)=UG(I,J,K-1)
C          WG(I,J,K)=WG(I,J,K-1)
C          UP(I,J,K)=UP(I,J,K-1)
C          WP(I,J,K)=WP(I,J,K-1)
C          EG(I,J,K)=EG(I,J,K-1)
C          EP(I,J,K)=EP(I,J,K-1)
C          CONTINUE
C      30 CONTINUE
C      20 CONTINUE
C      10 CONTINUE
C      RETURN
C      END
C

```

C
C

SUBROUTINE SWEEP

C
C
C

** LOCAL VARIABLES **

```
REAL CG1, CG2, CG3, CG4, CP1, CP2, CP3, CP4
REAL MGR1, MGR2, MGR3, MGR4, MGR5, MGR6, MGR7, MGR8, MGR9
REAL MGZ1, MGZ2, MGZ3, MGZ4, MGZ5, MGZ6, MGZ7, MGZ8, MGZ9
REAL MPR1, MPR2, MPR3, MPR4, MPR5, MPR6
REAL MPZ1, MPZ2, MPZ3, MPZ4, MPZ5, MPZ6
REAL EG1, EG2, EG3, EG4, EG5, EG6, EG7, EG8, EG9, EG10
REAL EP1, EP2, EP3, EP4, EP5, EP6
REAL EGCHEM, EPCHEM
REAL UGRHO1, WGRHO1, UPRHO2, WPRHO2, EGRHO1, EPRHO2
REAL TAUGGR(0:6,0:61), TAUGGZ(0:6,0:61)
INTEGER I, J
```

C
C
C

** COMMON VARIABLES **

```
REAL RHO1(0:6,0:61,3), RHO2(0:6,0:61,3), UG(0:6,0:61,3),
& UP(0:6,0:61,3), WG(0:6,0:61,3), WP(0:6,0:61,3),
& EG(0:6,0:61,3), EP(0:6,0:61,3)
REAL RHOG(0:6,0:61), RHOP(0:6,0:61), PG(0:6,0:61), PP(0:6,0:61),
& PGPFI(0:6,0:61), PP1MF(0:6,0:61), TG(0:6,0:61), TP(0:6,0:61),
& PHI(0:6,0:61), RADP(0:6,0:61), MUG(0:6,0:61),
& GAMMAC(0:6,0:61), DRAGR(0:6,0:61), DRAGZ(0:6,0:61),
& QDOT(0:6,0:61), ARVISR(0:6,0:61), ARVISZ(0:6,0:61)
INTEGER IGN(0:6,0:61)
REAL RLEN, ZLEN, DELR, DELZ, DELT, STEP, EPS, ARV, TOL, R, TIME,
& CVG, CVP, RO, MW, B1, TGO, TPO, TCH, TIGN, B, BNT, EPT, RHOPO,
& PHIO, PGO, PCH, PWALL, RADPO, KO, MUGO, PR
INTEGER INIT, TOGGLE, ENDR, ENDZ, STOPIT, COUNT, MAX,
& RPRINT, ZPRINT, TPRINT, NTGR, NTGZ, NTPR, NTPZ, NPGR, NPGZ
COMMON /PRI/ RHO1, RHO2, UG, UP, WG, WP, EG, EP
COMMON /SEC/ RHOG, RHOP, PG, PT, PGPFI, PP1MF, TG, TP, PHI,
& RADP, IGN, MUG, GAMMAC, DRAGR, DRAGZ, QDOT, ARVISR, ARVISZ
COMMON // RLEN, ZLEN, DELR, DELZ, DELT, STEP, EPS, ARV, TOL, R,
& TIME, CVG, CVP, RO, MW, B1, TGO, TPO, TCH, TIGN, B, BNT, EPT,
& RHOPO, PHIO, PGO, PCH, PWALL, RADPO, KO, MUGO, PR, INIT, TOGGLE,
& ENDR, ENDZ, STOPIT, COUNT, MAX,
& RPRINT, ZPRINT, TPRINT, NTGR, NTGZ, NTPR, NTPZ, NPGR, NPGZ
```

C
C

```
EXTERNAL AVG, DBLAVG
EGCHEM=0.95*EPT
EPCHEM=0.05*EPT
DO 10 I=1,ENDR
DO 20 J=1,ENDZ
```

C
C
C
C
C

```
*****
* GAS CONTINUITY EQUATION *
*****
```

```

      R=DELR*(I-0.5)
      CG1=(AVG(RHO1,I+1,J,2,1)*(R+DELR/2.0)
&      *UG(I+1,J,2)-AVG(RHO1,I,J,2,1)*(R-DELR/2.0)
&      *UG(I,J,2))/DELR
C
      CG2=(AVG(RHO1,I,J+1,2,2)*WG(I,J+1,2)
&      -AVG(RHO1,I,J,2,2)*WG(I,J,2))/DELZ
C
      CG3=(AVG(ARVISR,I+1,J,1,1)*(RHO1(I+1,J,2)-RHO1(I,J,2))
&      -AVG(ARVISR,I,J,1,1)*(RHO1(I,J,2)-RHO1(I-1,J,2)))/DELR
      CG3=0.0
C
      CG4=(AVG(ARVISZ,I,J+1,1,2)*(RHO1(I,J+1,2)-RHO1(I,J,2))
&      -AVG(ARVISZ,I,J,1,2)*(RHO1(I,J,2)-RHO1(I,J-1,2)))/DELZ
      IF(J.EQ.1) CG4=(AVG(ARVISZ,I,J+2,1,2)*(RHO1(I,J+2,2)
&      -RHO1(I,J+1,2))-AVG(ARVISZ,I,J+1,1,2)*(RHO1(I,J+1,2)
&      -RHO1(I,J,2)))/DELZ
C
      RHO1(I,J,1)=RHO1(I,J,3)+2.0*DELT*(-1.0/R*CG1-CG2+CG3+CG4
&      +GAMMAC(I,J))
C
C      *****
C      * PARTICLE CONTINUITY EQUATION *
C      *****
C
      CP1=(AVG(RHO2,I+1,J,2,1)*(R+DELR/2.0)
&      *UP(I+1,J,2)-AVG(RHO2,I,J,2,1)*(R-DELR/2.0)
&      *UP(I,J,2))/DELR
C
      CP2=(AVG(RHO2,I,J+1,2,2)*WP(I,J+1,2)
&      -AVG(RHO2,I,J,2,2)*WP(I,J,2))/DELZ
C
      CP3=(AVG(ARVISR,I+1,J,1,1)*(RHO2(I+1,J,2)-RHO2(I,J,2))
&      -AVG(ARVISR,I,J,1,1)*(RHO2(I,J,2)-RHO2(I-1,J,2)))/DELR
      CP3=0.0
C
      CP4=(AVG(ARVISZ,I,J+1,1,2)*(RHO2(I,J+1,2)-RHO2(I,J,2))
&      -AVG(ARVISZ,I,J,1,2)*(RHO2(I,J,2)-RHO2(I,J-1,2)))/DELZ
      IF(J.EQ.1) CP4=(AVG(ARVISZ,I,J+2,1,2)*(RHO2(I,J+2,2)
&      -RHO2(I,J+1,2))-AVG(ARVISZ,I,J+1,1,2)*(RHO2(I,J+1,2)
&      -RHO2(I,J,2)))/DELZ
C
      RHO2(I,J,1)=RHO2(I,J,3)+2.0*DELT*(-1.0/R*CP1-CP2+CP3+CP4
&      -GAMMAC(I,J))
C
C      *****
C      * GAS MOMENTUM EQUATION *
C      * RADIAL DIRECTION *
C      *****
C
      R=DELR*(I-1)
      IF(R.EQ.0.0) GO TO 1000
      MGR1=(RHO1(I,J,2)*(R+DELR/2.0)
&      *(AVG(UG,I+1,J,2,1))*2.0-RHO1(I-1,J,2)

```

```

C      &      *(R-DELR/2.0)*(AVG(UG,I,J,2,1))**2.0)/DELR
C
C      MGR2=(DBLAVG(RHO1,I,J+1,2)
C      &      *AVG(UG,I,J+1,2,2)*AVG(WG,I,J+1,2,1)
C      &      -DBLAVG(RHO1,I,J,2)*AVG(UG,I,J,2,2)
C      &      *AVG(WG,I,J,2,1))/DELZ
C
C      IF(TOGGLE.EQ.1) THEN
C
C          MGR3=((R+DELR)*UG(I+1,J,2)-R*UG(I,J,2))/(R+DELR/2.0)
C          &      -(R*UG(I,J,2)-(R-DELR)*UG(I-1,J,2))/(R-DELR/2.0)
C          &      /(DELR**2.0)
C
C          MGR4=(UG(I,J+1,2)+UG(I,J-1,2)-2.0*UG(I,J,2))/DELZ**2.0
C
C          MGR5=MGR3+(WG(I,J+1,2)-WG(I,J,2)-(WG(I-1,J+1,2)
C          &      -WG(I-1,J,2)))/(DELR*DELZ)
C
C      ELSE
C
C          MGR3=0.0
C
C          MGR4=0.0
C
C          MGR5=0.0
C
C      END IF
C
C      MGR6=(GAMMAC(I,J)+GAMMAC(I-1,J))/2.0*UP(I,J,2)
C
C      MGR7=(PGPHI(I,J)-PGPHI(I-1,J))/DELR
C
C      MGR8=(ARVISR(I,J)*(AVG(RHO1,I+1,J,2,1)*UG(I+1,J,2)
C      &      -AVG(RHO1,I,J,2,1)*UG(I,J,2))-ARVISR(I-1,J)
C      &      *(AVG(RHO1,I,J,2,1)*UG(I,J,2)-AVG(RHO1,I-1,J,2,2)
C      &      *UG(I-1,J,2)))/DELR
C
C      MGR9=(DBLAVG(ARVISZ,I,J+1,1)*(AVG(RHO1,I,J+1,2,1)
C      &      *UG(I,J+1,2)-AVG(RHO1,I,J,2,1)*UG(I,J,2))
C      &      -DBLAVG(ARVISZ,I,J,1)*(AVG(RHO1,I,J,2,1)*UG(I,J,2)
C      &      -AVG(RHO1,I,J-1,2,1)*UG(I,J-1,2)))/DELZ
C
C      UG(I,J,1)=(AVG(RHO1,I,J,3,1)*UG(I,J,3)
C      &      +2.0*DELT*(-1.0/R*MGR1-MGR2+MUG(I,J)*(MGR3+MGR4
C      &      +1.0/3.0*MGR5)+MGR6-DRAGR(I,J)-MGR7+MGR8+MGR9))
C      &      /AVG(RHO1,I,J,1,1)
C
C      *****
C      * GAS MOMENTUM EQUATION *
C      *   AXIAL DIRECTION   *
C      *****
C
C      1000      R=DELR*(I-0.5)
C      MGZ1=(DBLAVG(RHO1,I+1,J,2)*(R+DELR/2.0)

```

```

&      *AVG(UG,I+1,J,2,2)*AVG(WG,I+1,J,2,1)
&      -DBLAVG(RHO1,I,J,2)*(R-DELR/2.0)
&      *AVG(UG,I,J,2,2)*AVG(WG,I,J,2,1))/DELR
C
MGZ2=(RHO1(I,J,2)*(AVG(WG,I,J+1,2,2))*2.0
&      -RHO1(I,J-1,2)*(AVG(WG,I,J,2,2))*2.0)/DELR
C
IF(TOGGLE.EQ.1) THEN
C
      IF(I.EQ.ENDR) THEN
C
          ** NO-SLIP BOUNDARY CONDITION **
C
          MGZ3=((R+DELR/2.0)*(-1.0*WG(I,J,2)
&              -1.0/3.0*WG(I-1,J,2))-(R-DELR/2.0)*(WG(I,J,2)
&              -WG(I-1,J,2)))/(R*DELR**2.0)
C
          ELSE
C
          MGZ3=((R+DELR/2.0)*(WG(I+1,J,2)-WG(I,J,2))
&              -(R-DELR/2.0)*(WG(I,J,2)-WG(I-1,J,2)))/(R*DELR**2.0)
C
          END IF
C
          MGZ4=(WG(I,J+1,2)+WG(I,J-1,2)-2.0*WG(I,J,2))/DELR**2.0
C
          MGZ5=((R+DELR/2.0)*(UG(I+1,J,2)-UG(I+1,J-1,2))
&              -(R-DELR/2.0)*(UG(I,J,2)-UG(I,J-1,2)))/(R*DELR*DELR)
&              +MGZ4
C
          ELSE
C
          MGZ3=0.0
C
          MGZ4=0.0
C
          MGZ5=0.0
C
          END IF
C
          MGZ6=(GAMMAC(I,J)+GAMMAC(I,J-1))/2.0*WP(I,J,2)
C
          MGZ7=(PGPHI(I,J)-PGPHI(I,J-1))/DELR
C
          IF(I.EQ.ENDR) THEN
C
              MGZ8=(DBLAVG(ARVISR,I,J,1)*(AVG(RHO1,I,J,2,2)
&                  *WG(I,J,2)-AVG(RHO1,I-1,J,2,2)*WG(I-1,J,2))
&                  -DBLAVG(ARVISR,I-1,J,1)*(AVG(RHO1,I-1,J,2,2)
&                  *WG(I-1,J,2)-AVG(RHO1,I-2,J,2,2)*WG(I-2,J,2)))/DELR
C
              ELSE
C
              MGZ8=(DBLAVG(ARVISR,I+1,J,1)*(AVG(RHO1,I+1,J,2,2)

```



```

&      *WG(I+1,J,2)-AVG(RHO1,I,J,2,2)*WG(I,J,2))
&      -DBLAVG(ARVISR,I,J,1)*(AVG(RHO1,I,J,2,2)*WG(I,J,2)
&      -AVG(RHO1,I-1,J,2,2)*WG(I-1,J,2)))/DEL R
C
      END IF
C
      IF(J.EQ.1) THEN
        MGZ9=(ARVISZ(I,J+1)*(AVG(RHO1,I,J+2,2,2)
&      *WG(I,J+2,2)-AVG(RHO1,I,J+1,2,2)*WG(I,J+1,2))
&      -ARVISZ(I,J)*(AVG(RHO1,I,J+1,2,2)*WG(I,J+1,2)
&      -AVG(RHO1,I,J,2,2)*WG(I,J,2)))/DELZ
        ELSE
          MGZ9=(ARVISZ(I,J)*(AVG(RHO1,I,J+1,2,2)*WG(I,J+1,2)
&      -AVG(RHO1,I,J,2,2)*WG(I,J,2))-ARVISZ(I,J-1)
&      *(AVG(RHO1,I,J,2,2)*WG(I,J,2)-AVG(RHO1,I,J-1,2,2)
&      *WG(I,J-1,2)))/DELZ
          END IF
C
      WG(I,J,1)=(AVG(RHO1,I,J,3,2)*WG(I,J,3)
&      +2.0*DELT*(-1.0/R*MGZ1-MGZ2+MUG(I,J)*(MGZ3+MGZ4
&      +1.0/3.0*MGZ5)+MGZ6-DRAGZ(I,J)-MGZ7+MGZ8+MGZ9))
&      /AVG(RHO1,I,J,1,2)
C
C
C
C
C
C
      *****
      * PARTICLE MOMENTUM EQUATION *
      *   RADIAL DIRECTION   *
      *****
      R=DEL R*(I-1)
      IF(R.EQ.0.0) GO TO 2000
      MPR1=(RHO2(I,J,2)*(R+DEL R/2.0)
&      *(AVG(UP,I+1,J,2,1))*2.0-RHO2(I-1,J,2)
&      *(R-DEL R/2.0)*(AVG(UP,I,J,2,1))*2.0)/DEL R
C
      MPR2=(DBLAVG(RHO2,I,J+1,2)
&      *AVG(UP,I,J+1,2,2)*AVG(WP,I,J+1,2,1)
&      -DBLAVG(RHO2,I,J,2)*AVG(UP,I,J,2,2)
&      *AVG(WP,I,J,2,1))/DELZ
C
      MPR3=(GAMMAC(I,J)+GAMMAC(I-1,J))/2.0*UP(I,J,2)
C
      MPR4=(PP1MF(I,J)-PP1MF(I-1,J))/DEL R
C
      MPR5=(ARVISR(I,J)*(AVG(RHO2,I+1,J,2,1)*UP(I+1,J,2)
&      -AVG(RHO2,I,J,2,1)*UP(I,J,2))-ARVISR(I-1,J)
&      *(AVG(RHO2,I,J,2,1)*UP(I,J,2)-AVG(RHO2,I-1,J,2,1)
&      *UP(I-1,J,2)))/DEL R
C
      MPR6=(DBLAVG(ARVISZ,I,J+1,1)*(AVG(RHO2,I,J+1,2,1)
&      *UP(I,J+1,2)-AVG(RHO2,I,J,2,1)*UP(I,J,2))
&      -DBLAVG(ARVISZ,I,J,1)*(AVG(RHO2,I,J,2,1)*UP(I,J,2)
&      -AVG(RHO2,I,J-1,2,1)*UP(I,J-1,2)))/DELZ
C
      UP(I,J,1)=(AVG(RHO2,I,J,3,1)*UP(I,J,3)

```

```

&      +2.0*DELT*(-1.0/R*MPR1-MPR2-MPR3+DRAGR(I,J)-MPR4+MPR5
&      +MPR6))/AVG(RHO2,I,J,1,1)
C
C      *****
C      * PARTICLE MOMENTUM EQUATION *
C      *      AXIAL DIRECTION      *
C      *****
C
2000      R=DELR*(I-0.5)
          MPZ1=(DBLAVG(RHO2,I+1,J,2)*(R+DELR/2.0)
&          *AVG(UF,I+1,J,2,2)*AVG(WP,I+1,J,2,1)
&          -DBLAVG(RHO2,I,J,2)*(R-DELR/2.0)
&          *AVG(UF,I,J,2,2)*AVG(WP,I,J,2,1))/DELR
C
          MPZ2=(RHO2(I,J,2)*(AVG(WP,I,J+1,2,2)**2.0
&          -RHO2(I,J-1,2)*(AVG(WP,I,J,2,2)**2.0)/DELZ
C
          MPZ3=(GAMMAC(I,J)+GAMMAC(I-1,J-1))/2.0*WP(I,J,2)
C
          MPZ4=(PP1MF(I,J)-PP1MF(I,J-1))/DELZ
C
          MPZ5=(DBLAVG(ARVISR,I+1,J,1)*(AVG(RHO2,I+1,J,2,2)
&          *WP(I+1,J,2)-AVG(RHO2,I,J,2,2)*WP(I,J,2))
&          -DBLAVG(ARVISR,I,J,1)*(AVG(RHO2,I,J,2,2)*WP(I,J,2)
&          -AVG(RHO2,I-1,J,2,2)*WP(I-1,J,2)))/DELR
C
          IF(J.EQ.1) THEN
&              MPZ6=(ARVISZ(I,J+1)*(AVG(RHO2,I,J+2,2,2)
&              *WP(I,J+2,2)-AVG(RHO2,I,J+1,2,2)*WP(I,J+1,2))
&              -ARVISZ(I,J)*(AVG(RHO2,I,J+1,2,2)*WP(I,J+1,2)
&              -AVG(RHO2,I,J,2,2)*WP(I,J,2)))/DELZ
          ELSE
&              MPZ6=(ARVISZ(I,J)*(AVG(RHO2,I,J+1,2,2)*WP(I,J+1,2)
&              -AVG(RHO2,I,J,2,2)*WP(I,J,2))-ARVISZ(I,J-1)
&              *(AVG(RHO2,I,J,2,2)*WP(I,J,2)-AVG(RHO2,I,J-1,2,2)
&              *WP(I,J-1,2)))/DELZ
          END IF
C
          WP(I,J,1)=(AVG(RHO2,I,J,3,2)*WP(I,J,3)
&          +2.0*DELT*(-1.0/R*MPZ1-MPZ2-MPZ3+DRACZ(I,J)-MPZ4+MPZ5
&          +MPZ6))/AVG(RHO2,I,J,1,2)
C
C      *****
C      * GAS ENERGY EQUATION *
C      *****
C
          EG1=(AVG(RHO1,I+1,J,2,1)*UG(I+1,J,2)*(R+DELR/2.0)
&          *(AVG(EG,I+1,J,2,1)+((PGPHI(I+1,J)+PGPHI(I,J))/2.0)
&          /AVG(RHO1,I+1,J,2,1))-AVG(RHO1,I,J,2,1)
&          *UG(I,J,2)*(R-DELR/2.0)*(AVG(EG,I,J,2,1)
&          +((PGPHI(I,J)+PGPHI(I-1,J))/2.0)
&          /AVG(RHO1,I,J,2,1)))/DELR
C
          EG2=(AVG(RHO1,I,J+1,2,2)*WG(I,J+1,2)

```

```

&      *(AVG(EG,I,J+1,2,2)+((PGPHI(I,J+1)+PGPHI(I,J))/2.0)
&      /AVG(RHO1,I,J+1,2,2))-AVG(RHO1,I,J,2,2)
&      *WG(I,J,2)*(AVG(EG,I,J,2,2)
&      +((PGPHI(I,J)+PGPHI(I,J-1))/2.0)
&      /AVG(RHO1,I,J,2,2))/DELZ
C
      IF(TOGGLE.EQ.1) THEN
C
          EG3=(UG(I+1,J,2)-UG(I,J,2))/DELR
C
          EG4=AVG(UG,I+1,J,2,1)/R
C
          EG5=(WG(I,J+1,2)-WG(I,J,2))/DELZ
C
          EG6=(DBLAVG(WG,I+1,J+1,2)
&          -DBLAVG(WG,I,J+1,2))/DELR
&          +(DBLAVG(UG,I+1,J+1,2)
&          -DBLAVG(UG,I+1,J,2))/DELZ
C
      ELSE
C
          EG3=0.0
C
          EG4=0.0
C
          EG5=0.0
C
          EG6=0.0
C
      END IF
C
      EG7=(DRAGR(I+1,J)+DRAGR(I,J))*(UP(I+1,J,2)+UP(I,J,2))/4.0
&      +(DRAGZ(I,J+1)+DRAGZ(I,J))*(WP(I,J+1,2)+WP(I,J,2))/4.0
C
      EG8=GAMMAC(I,J)*(EGCHEM+AVG(UP,I+1,J,2,1)**2.0/2.0
&      +AVG(WP,I,J+1,2,2)**2.0/2.0)
C
      EG9=(AVG(ARVISR,I+1,J,1,1)*(RHO1(I+1,J,2)*EG(I+1,J,2)
&      -RHO1(I,J,2)*EG(I,J,2))-AVG(ARVISR,I,J,1,1)*(RHO1(I,J,2)
&      *EG(I,J,2)-RHO1(I-1,J,2)*EG(I-1,J,2)))/DELR
      IF(I.EQ.1)
&      EG9=(AVG(ARVISR,I+2,J,1,1)*(RHO1(I+2,J,2)*EG(I+2,J,2)
&      -RHO1(I+1,J,2)*EG(I+1,J,2))-AVG(ARVISR,I+1,J,1,1)
&      *(RHO1(I+1,J,2)*EG(I+1,J,2)-RHO1(I,J,2)*EG(I,J,2)))/DELR
      IF(I.EQ.ENDR)
&      EG9=(AVG(ARVISR,I,J,1,1)*(RHO1(I,J,2)*EG(I,J,2)
&      -RHO1(I-1,J,2)*EG(I-1,J,2))-AVG(ARVISR,I-1,J,1,1)
&      *(RHO1(I-1,J,2)*EG(I-1,J,2)-RHO1(I-2,J,2)*EG(I-2,J,2)))/DELR
C
      EG10=(AVG(ARVISZ,I,J+1,1,2)*(RHO1(I,J+1,2)*EG(I,J+1,2)
&      -RHO1(I,J,2)*EG(I,J,2))-AVG(ARVISZ,I,J,1,2)*(RHO1(I,J,2)
&      *EG(I,J,2)-RHO1(I,J-1,2)*EG(I,J-1,2)))/DELZ
      IF(J.EQ.1) EG10=(AVG(ARVISZ,I,J+2,1,2)*(RHO1(I,J+2,2)
&      *EG(I,J+2,2)-RHO1(I,J+1,2)*EG(I,J+1,2))

```

```

& -AVG(ARVISZ,I,J+1,1,2)*(RHO1(I,J+1,2)*EG(I,J+1,2)
& -RHO1(I,J,2)*EG(I,J,2))/DELZ
C
EG(I,J,1)=(RHO1(I,J,3)*EG(I,J,3)+2.0*DELT*(-1.0/R*EG1-EG2
& +MUG(I,J)*(2.0*(EG3**2.0+EG4**2.0+EG5**2.0)
& -2.0/3.0*(EG3+EG4+EG5)**2.0+EG6**2.0+AVG(UG,I+1,J,2,1)
& *(MGR3+MGR4+1.0/3.0*MGR5)+AVG(WG,I,J+1,2,2)
& *(MGZ3+MGZ4+1.0/3.0*MGZ5))
& -QDOT(I,J)-EG7+EG8+EG9+EG10))/RHO1(I,J,1)
C
C *****
C * PARTICLE ENERGY EQUATION *
C *****
C
EP1=(AVG(RHO2,I+1,J,2,1)*UP(I+1,J,2)*(R+DELR/2.0)
& *(AVG(EP,I+1,J,2,1)+((PP1MF(I+1,J)+PP1MF(I,J))/2.0)
& /AVG(RHO2,I+1,J,2,1))-AVG(RHO2,I,J,2,1)
& *UP(I,J,2)*(R-DELR/2.0)*(AVG(EP,I,J,2,1)
& +((PP1MF(I,J)+PP1MF(I-1,J))/2.0)
& /AVG(RHO2,I,J,2,1)))/DELR
C
EP2=(AVG(RHO2,I,J+1,2,2)*WP(I,J+1,2)
& *(AVG(EP,I,J+1,2,2)+((PP1MF(I,J+1)+PP1MF(I,J))/2.0)
& /AVG(RHO2,I,J+1,2,2))-AVG(RHO2,I,J,2,2)
& *WP(I,J,2)*(AVG(EP,I,J,2,2)
& +((PP1MF(I,J)+PP1MF(I,J-1))/2.0)
& /AVG(RHO2,I,J,2,2)))/DELZ
C
EP3=EG7
C
EP4=GAMMAC(I,J)*(EPCHEM-AVG(UP,I+1,J,2,1)**2.0/2.0
& -AVG(WP,I,J+1,2,2)**2.0/2.0,
C
EP5=(AVG(ARVISR,I+1,J,1,1)*(RHO2(I+1,J,2)*EP(I+1,J,2)
& -RHO2(I,J,2)*EP(I,J,2))-AVG(ARVISR,I,J,1,1)*(RHO2(I,J,2)
& *EP(I,J,2)-RHO2(I-1,J,2)*EP(I-1,J,2)))/DELR
IF(I.EQ.1)
& EP5=(AVG(ARVISR,I+2,J,1,1)*(RHO2(I+2,J,2)*EP(I+2,J,2)
& -RHO2(I+1,J,2)*EP(I+1,J,2))-AVG(ARVISR,I+1,J,1,1)
& *(RHO2(I+1,J,2)*EP(I+1,J,2)-RHO2(I,J,2)*EP(I,J,2)))/DELR
IF(I.EQ.ENDR)
& EP5=(AVG(ARVISR,I,J,1,1)*(RHO2(I,J,2)*EP(I,J,2)
& -RHO2(I-1,J,2)*EP(I-1,J,2))-AVG(ARVISR,I-1,J,1,1)
& *(RHO2(I-1,J,2)*EP(I-1,J,2)-RHO2(I-2,J,2)*EP(I-2,J,2)))/DELR
C
EP6=(AVG(ARVISZ,I,J+1,1,2)*(RHO2(I,J+1,2)*EP(I,J+1,2)
& -RHO2(I,J,2)*EP(I,J,2))-AVG(ARVISZ,I,J,1,2)*(RHO2(I,J,2)
& *EP(I,J,2)-RHO2(I,J-1,2)*EP(I,J-1,2)))/DELZ
IF(J.EQ.1) EP6=(AVG(ARVISZ,I,J+2,1,2)*(RHO2(I,J+2,2)
& *EP(I,J+2,2)-RHO2(I,J+1,2)*EP(I,J+1,2))
& -AVG(ARVISZ,I,J+1,1,2)*(RHO2(I,J+1,2)*EP(I,J+1,2)
& -RHO2(I,J,2)*EP(I,J,2)))/DELZ
C
EP(I,J,1)=(RHO2(I,J,3)*EP(I,J,3)+2.0*DELT*(-1.0/R*EP1-EP2

```

```

&      +QDOT(I,J)+EP3+EP4+EP5+EP6))/RHO2(I,J,1)
C
C
      IF(COUNT.GE.00.AND.COUNT.LE.10) THEN
        WRITE(6,100) I,J
        WRITE(6,200) CG1,CG2,CG3,CG4,(RHO1(I,J,K),K=1,3)
        WRITE(6,200) CP1,CP2,CP3,CP4,(RHO2(I,J,K),K=1,3)
        WRITE(6,300) MGR1,MGR2,MUG(I,J),MGR3,MGR4,MGR5,MGR6,
&      DRAGR(I,J),MGR7,MGR8,MGR9,(UG(I,J,K),K=1,3)
        WRITE(6,300) MGZ1,MGZ2,MUG(I,J),MGZ3,MGZ4,MGZ5,MGZ6,
&      DRAGZ(I,J),MGZ7,MGZ8,MGZ9,(WG(I,J,K),K=1,3)
        WRITE(6,400) MPR1,MPR2,MPR3,MPR4,MPR5,(UP(I,J,K),K=1,3)
        WRITE(6,400) MPZ1,MPZ2,MPZ3,MPZ4,MPZ5,(WP(I,J,K),K=1,3)
        WRITE(6,500) EG1,EG2,EG3,EG4,EG5,EG6,EG7,EG8,EG9,EG10,
&      (EG(I,J,K),K=1,3)
        WRITE(6,600) EP1,EP2,EP3,EP4,EP5,EP6,(EP(I,J,K),K=1,3)
100      FORMAT(/,'POSITION ',1X,2(I3))
200      FORMAT(1X,7(2X,G10.4))
300      FORMAT(1X,10(2X,G10.4)/1X,4(2X,G10.4))
400      FORMAT(1X,8(2X,G10.4))
500      FORMAT(1X,10(2X,G10.4)/1X,3(2X,G10.4))
600      FORMAT(1X,9(2X,G10.4)//)
      END IF
C
C      TAUGGR(I,J)=MUG(I,J)*(MGR3+MGR4+1.0/3.0*MGR5)
C      TAUGGZ(I,J)=MUG(I,J)*(MGZ3+MGZ4+1.0/3.0*MGZ5)
C
20      CONTINUE
10      CONTINUE
C
C      CALL DUMP2
C
C      *****
C      * BOUNDARY CONDITIONS *
C      *****
C
C      ** AT Z=0   END WALL SYMMETRY CONDITIONS **
C
DO 30 I=0,ENDR+1
  RHO1(I,0,1)=RHO1(I,1,1)
  RHO2(I,0,1)=RHO2(I,1,1)
  UG(I,0,1)=UG(I,1,1)
  WG(I,1,1)=0.0
  WG(I,0,1)=WG(I,2,1)
  UP(I,0,1)=UP(I,1,1)
  WP(I,1,1)=0.0
  WP(I,0,1)=WP(I,2,1)
  EG(I,0,1)=EG(I,1,1)
  EP(I,0,1)=EP(I,1,1)
30  CONTINUE
C
C      ** AT R=0   CENTER LINE SYMMETRY CONDITIONS **
C
DO 40 J=1,ENDZ

```

```

      RHO1(0,J,1)=RHO1(1,J,1)
      RHO2(0,J,1)=RHO2(1,J,1)
      UG(1,J,1)=0.0
      UG(0,J,1)=UG(2,J,1)
      WG(0,J,1)=WG(1,J,1)
      UP(1,J,1)=0.0
      UP(0,J,1)=UP(2,J,1)
      WP(0,J,1)=WP(1,J,1)
      EG(0,J,1)=EG(1,J,1)
      EP(0,J,1)=EP(1,J,1)
40    CONTINUE
C
C      ** AT Z=ENDZ   END WALL RADIATIVE CONDITIONS **
C
DO 50 I=0,ENDR+1
      RHO1(I,ENDZ+1,1)=(5.0*RHO1(I,ENDZ,1)-4.0*RHO1(I,ENDZ-1,1)
&    +RHO1(I,ENDZ-2,1))/2.0
      RHO2(I,ENDZ+1,1)=(5.0*RHO2(I,ENDZ,1)-4.0*RHO2(I,ENDZ-1,1)
&    +RHO2(I,ENDZ-2,1))/2.0
      UG(I,ENDZ+1,1)=(5.0*UG(I,ENDZ,1)-4.0*UG(I,ENDZ-1,1)
&    +UG(I,ENDZ-2,1))/2.0
      WG(I,ENDZ+1,1)=(5.0*WG(I,ENDZ,1)-4.0*WG(I,ENDZ-1,1)
&    +WG(I,ENDZ-2,1))/2.0
      UP(I,ENDZ+1,1)=(5.0*UP(I,ENDZ,1)-4.0*UP(I,ENDZ-1,1)
&    +UP(I,ENDZ-2,1))/2.0
      WP(I,ENDZ+1,1)=(5.0*WP(I,ENDZ,1)-4.0*WP(I,ENDZ-1,1)
&    +WP(I,ENDZ-2,1))/2.0
      EG(I,ENDZ+1,1)=(5.0*EG(I,ENDZ,1)-4.0*EG(I,ENDZ-1,1)
&    +EG(I,ENDZ-2,1))/2.0
      EP(I,ENDZ+1,1)=(5.0*EP(I,ENDZ,1)-4.0*EP(I,ENDZ-1,1)
&    +EP(I,ENDZ-2,1))/2.0
50    CONTINUE
C
C      ** AT R=ENDR   CIRCUMFERENTIAL WALL NO-SLIP CONDITIONS **
C      **              CRACK OPENING CONDITIONS              **
C
      NOTE: NO-SLIP CONDITIONS ARE APPLIED ONLY IF
            THE VISCOUS GAS EFFECTS ARE TO BE INCLUDED.
            CONSEQUENTLY, ACTUAL BOUNDARY CONDITIONS
            ARE APPLIED VIA ONE SIDED DIFFERENCING IN
            THE MAIN INTEGRATION LOOP IF TOGGLE=1.
            CONDITIONS LISTED HERE ARE ONLY USED TO KEEP
            FALSE EXTERIOR NODES FILLED AND HENCE THE VALUES
            MAY OR MAY NOT BE CORRECT.
C
DO 60 J=1,ENDZ
      RHO1(ENDR+1,J,1)=RHO1(ENDR,J,1)
      RHO2(ENDR+1,J,1)=RHO2(ENDR,J,1)
      UG(ENDR+1,J,1)=0.0
      WG(ENDR+1,J,1)=WG(ENDR,J,1)
      UP(ENDR+1,J,1)=0.0
      WP(ENDR+1,J,1)=WG(ENDR,J,1)
      EG(ENDR+1,J,1)=EG(ENDR,J,1)
      EP(ENDR+1,J,1)=EP(ENDR,J,1)

```

```

60      CONTINUE
C
C      *****
C      * REDUCTION OF TRUNCATION ERRORS *
C      *****
C
DO 70 I=0,ENDR+1
    DO 75 J=0,ENDZ+1
        IF(ABS(UG(I,J,1)).LE.TOL) UG(I,J,1)=0.0
        IF(ABS(WG(I,J,1)).LE.TOL) WG(I,J,1)=0.0
        IF(ABS(UP(I,J,1)).LE.TOL) UP(I,J,1)=0.0
        IF(ABS(WP(I,J,1)).LE.TOL) WP(I,J,1)=0.0
75      CONTINUE
70      CONTINUE
C
C      *****
C      * TIME SMOOTHER *
C      *****
C
DO 80 I=0,ENDR+1
    DO 85 J=0,ENDZ+1
        EGRHO1=EG(I,J,2)*RHO1(I,J,2)+EPS*(EG(I,J,1)*RHO1(I,J,1)
&      -2.0*EG(I,J,2)*RHO1(I,J,2)+EG(I,J,3)*RHO1(I,J,3))
        EPRHO2=EP(I,J,2)*RHO2(I,J,2)+EPS*(EP(I,J,1)*RHO2(I,J,1)
&      -2.0*EP(I,J,2)*RHO2(I,J,2)+EP(I,J,3)*RHO2(I,J,3))
        UGRHO1=UG(I,J,2)*RHO1(I,J,2)+EPS*(UG(I,J,1)*RHO1(I,J,1)
&      -2.0*UG(I,J,2)*RHO1(I,J,2)+UG(I,J,3)*RHO1(I,J,3))
        WGRHO1=WG(I,J,2)*RHO1(I,J,2)+EPS*(WG(I,J,1)*RHO1(I,J,1)
&      -2.0*WG(I,J,2)*RHO1(I,J,2)+WG(I,J,3)*RHO1(I,J,3))
        UPRHO2=UP(I,J,2)*RHO2(I,J,2)+EPS*(UP(I,J,1)*RHO2(I,J,1)
&      -2.0*UP(I,J,2)*RHO2(I,J,2)+UP(I,J,3)*RHO2(I,J,3))
        WPRHO2=WP(I,J,2)*RHO2(I,J,2)+EPS*(WP(I,J,1)*RHO2(I,J,1)
&      -2.0*WP(I,J,2)*RHO2(I,J,2)+WP(I,J,3)*RHO2(I,J,3))
        RHO1(I,J,2)=RHO1(I,J,2)+EPS*(RHO1(I,J,1)-2.0*RHO1(I,J,2)
&      +RHO1(I,J,3))
        RHO2(I,J,2)=RHO2(I,J,2)+EPS*(RHO2(I,J,1)-2.0*RHO2(I,J,2)
&      +RHO2(I,J,3))
        UG(I,J,2)=UGRHO1/RHO1(I,J,2)
        WG(I,J,2)=WGRHO1/RHO1(I,J,2)
        UP(I,J,2)=UPRHO2/RHO2(I,J,2)
        WP(I,J,2)=WPRHO2/RHO2(I,J,2)
        EG(I,J,2)=EGRHO1/RHO1(I,J,2)
        EP(I,J,2)=EPRHO2/RHO2(I,J,2)
        IF(COUNT.GE.00.AND.COUNT.LE.10) THEN
            WRITE(6,700) I,J,RHO1(I,J,2),RHO2(I,J,2),UG(I,J,2),
&      WG(I,J,2),UP(I,J,2),WP(I,J,2),EG(I,J,2),EP(I,J,2)
700      FORMAT(1X,2(I3),8(G10.4))
            END IF
85      CONTINUE
80      CONTINUE
    RETURN
END
C
C

```

```

C
C      FUNCTION AVG (VALU, SITER, SITEZ, TIME, DIR)
C
C      ** LOCAL VARIABLES **
C
C      REAL VALU(0:6,0:61,3)
C      INTEGER SITER, SITEZ, TIME, DIR
C
C      IF (DIR.EQ.1) THEN
C          AVG=(VALU(SITER,SITEZ,TIME)+VALU(SITER-1,SITEZ,TIME))/2.0
C      ELSE IF (DIR.EQ.2) THEN
C          AVG=(VALU(SITER,SITEZ,TIME)+VALU(SITER,SITEZ-1,TIME))/2.0
C      END IF
C      RETURN
C      END
C
C
C      FUNCTION DBLAVG (VALU, SITER, SITEZ, TIME)
C
C      ** LOCAL VARIABLES **
C
C      REAL VALU(0:6,0:61,3)
C      INTEGER SITER, SITEZ, TIME
C
C      DBLAVG=(VALU(SITER,SITEZ,TIME)+VALU(SITER-1,SITEZ,TIME)
C      & +VALU(SITER,SITEZ-1,TIME)+VALU(SITER-1,SITEZ-1,TIME))/4.0
C      RETURN
C      END
C
C
C      SUBROUTINE DUMP
C
C      ** LOCAL VARIABLES **
C
C      REAL RLOC, ZLOC, PGSI, RADPSI, TIMOUT, DTOUT, PWALOT
C      INTEGER I, J
C
C      ** COMMON VARIABLES **
C
C      REAL RHO1(0:6,0:61,3), RHO2(0:6,0:61,3), UG(0:6,0:61,3),
C      & UP(0:6,0:61,3), WG(0:6,0:61,3), WP(0:6,0:61,3),
C      & EG(0:6,0:61,3), EP(0:6,0:61,3)
C      REAL RHOG(0:6,0:61), RHOP(0:6,0:61), PG(0:6,0:61), PP(0:6,0:61),
C      & PGPHI(0:6,0:61), PPIMF(0:6,0:61), TG(0:6,0:61), TP(0:6,0:61),
C      & PHI(0:6,0:61), RADP(0:6,0:61), MUG(0:6,0:61),
C      & GAMMAC(0:6,0:61), DRAGR(0:6,0:61), DRAGZ(0:6,0:61),
C      & QDOT(0:6,0:61), ARVISR(0:6,0:61), ARVISZ(0:6,0:61)
C      INTEGER IGN(0:6,0:61)
C      REAL RLEN, ZLEN, DELR, DELZ, DELT, STEP, EPS, ARV, TOL, R, TIME,
C      & CVG, CVP, RO, MW, B1, TGO, TPO, TCH, TIGN, B, BMT, EPT, RHOPO,

```



```

& PHIO, PGO, PCH, PWALL, RADPO, KO, MUGG, PR
  INTEGER INIT, TOGGLE, ENDR, ENDZ, STOPIT, COUNT, MAX,
& RPRINT, ZPRINT, TPRINT, NTGR, NTGZ, NTPR, NTPZ, NPGR, NPGZ
  COMMON /PRI/ RHO1, RHO2, UG, UP, WG, WP, EG, EP
  COMMON /SEC/ RHOG, RHOP, PG, PP, PGPHI, PPIMF, TG, TP, PHI,
& RADP, IGN, MUG, GAMMAC, DRAGR, DRAGZ, QDOT, ARVISR, ARVISZ
  COMMON // RLEN, ZLEN, DELR, DELZ, DELT, STEP, EPS, ARV, TOL, R,
& TIME, CVG, CVP, RO, MW, B1, TGO, TPO, TCH, TIGN, B, BNT, EPT,
& RHOPG, PHIO, PGO, PCH, PWALL, RADPO, KO, MUGO, PR, INIT, TOGGLE,
& ENDR, ENDZ, STOPIT, COUNT, MAX,
& RPRINT, ZPRINT, TPRINT, NTGR, NTGZ, NTPR, NTPZ, NPGR, NPGZ

```

C
C

```

EXTERNAL AVG
PRINT 100
DO 10 I=1,ENDR
  RLOC=I*DELR-DELR/2.0
  DO 20 J=1,ENDZ
    ZLOC=J*DELZ-DELZ/2.0
    PGSI=PG(I,J)*1.0E-10
    RADPSI=RADP(I,J)*1.0E4
    UGPRT=AVG(UG,I,J,2,1)
    WGPRT=AVG(WG,I,J,2,2)
    UPPRT=AVG(UP,I,J,2,1)
    WPPRT=AVG(WP,I,J,2,2)
    IF (((J.EQ.0).OR.(J.EQ.ENDZ)).OR.((J/ZPRINT)*ZPRINT.EQ.J))
& .AND.(((I.EQ.0).OR.(I.EQ.ENDR)).OR.((I/RPRINT)*RPRINT.EQ.I)))
    PRINT 200,RLOC,ZLOC,UGPRT,UPPRT,WGPRT,WPPRT,
& PGSI,TG(I,J),TP(I,J),RHOG(I,J),RHOP(I,J),PHI(I,J),RADPSI,
& GAMMAC(I,J),QDOT(I,J),DRAGR(I,J),DRAGZ(I,J)
20  CONTINUE
    PRINT 400
10  CONTINUE
    PWALOT=PWALL*1.0E-10
    TIMOUT=TIME*1.0E6
    DTOUT=DELT*1.0E6
    PRINT 300,TIMOUT,COUNT,DTOUT,PWALOT

```

C
C

```

100  FORMAT(' ',1X,'RLOC',3X,'ZLOC',5X,'UG',6X,'UP',6X,'WG',6X,'WP',
& 3X,'GAS PRESS',3X,'TG',5X,'TP',4X,'RHOG',3X,'RHOP',3X,'PHI',
& 2X,'RADIUS',2X,'GAMMA',5X,'QDOT',5X,'DRAGR',3X,'DRAGZ'/
& 3X,2('CM',5X),4('CM/S',4X),'GPA',5X,2('DEG K',3X),'G/CC',
& 3X,'G/CC',10X,'UM'/134(' '))
200  FORMAT(' ',2(F5.3,1X),4(F7.0,1X),F8.5,1X,2(F6.0,1X),2(F6.4,1X),
& F5.3,1X,F6.2,4(1X,G8.2))
300  FORMAT('/' DATA IS RECORDED AT ',F8.4,' MICRO-SECONDS',6X,
& 15,' INTEGRATIONS AT THIS TIME'/' CURRENT TIME STEP IS ',
& F8.4,' MICRO-SECONDS',6X,'MAXIMUM WALL PRESSURE IS ',
& F8.5,' GPA')
400  FORMAT(' ')
      RETURN
      END

```

C

```

SUBROUTINE DUMP2(TAUGGR,TAUGGZ,DRAGR,DRAGZ,ENDR,ENDZ,DELR,DELZ)
REAL TAUGGR(0:6,0:61),TAUGGZ(0:6,0:61),DRAGR(0:6,0:61),
& DRAGZ(0:6,0:61),DELR,DELZ,LAMR,LAMZ,RLOC,ZLOC
INTEGER I,J,ENDR,ENDZ
WRITE(7,100)
DO 10 I=0,ENDR
  RLOC=I*DELR
  DO 20 J=0,ENDZ
    ZLOC=J*DELZ
    LAMR=TAUGGR(I,J)/DRAGR(I,J)
    LAMZ=TAUGGZ(I,J)/DRAGZ(I,J)
    WRITE(7,200) RLOC,ZLOC,TAUGGR(I,J),TAUGGZ(I,J),DRAGR(I,J),
&    DRAGZ(I,J),LAMR,LAMZ
20  CONTINUE
    WRITE(7,300)
10  CONTINUE
100 FORMAT('1',1X,'RLOC',3X,'ZLOC',3X,'TAUGGR',3X,'TAUGGZ',3X,
& 'DRAGR',4X,'DRAGZ',4X,'LAM R',4X,'LAM Z'/3X,'CM',5X,'CM',
& 4X,4('DYN/CC',3X)/68('-'))
200 FORMAT(2(1X,F6.3),6(1X,G8.2))
300 FORMAT(' ')
RETURN
END

```

LIST OF SYMBOLS

Symbol	Definition	Units
a	speed of sound in gas	cm/s
b	burning rate coefficient	$(\text{cm/s})/(\text{dyn/cm}^2)^n$
h_1	non-ideal gas equation of state co-volume	cm^3/g
C_{vg}	gas specific heat at constant volume	$\text{erg/g}\cdot\text{K}$
C_{vp}	particle specific heat at constant volume	$\text{erg/g}\cdot\text{K}$
D_r	gas-particle interaction drag, radial component	dyn/cm^3
D_z	gas-particle interaction drag, axial component	dyn/cm^3
E_g	gas total energy	erg/g
E_p	particle total energy	erg/g
E_g^{chem}	gas chemical energy released during combustion	erg/g
E_p^{chem}	particle chemical energy released during combustion	erg/g
E_{ign}	particle ignition energy	erg/g
f_{pg}	interphase friction factor	
h_{pg}	convective heat transfer coefficient	$\text{erg/s}\cdot\text{cm}^2\cdot\text{K}$
k_g	gas thermal conductivity	$\text{erg/s}\cdot\text{cm}\cdot\text{K}$
K_0	bulk modulus of solid	$\text{g/cm}\cdot\text{s}^2$
L	total length of bed	cm
n	burning rate index	
P_g	gas phase pressure	dyn/cm^2
P_p	particle phase pressure	dyn/cm^2

LIST OF SYMBOLS (continued)

Symbol	Definition	Units
P_{g0}	initial gas phase pressure	dyn/cm^2
P_{p0}	initial particle phase pressure	dyn/cm^2
Pr	gas Prandtl number	
\dot{Q}	interphase convective heat transfer	$\text{erg/cm}^3 \cdot \text{s}$
r	radial coordinate	
r_p	particle radius	μm
r_{p0}	initial particle radius	μm
\dot{r}	surface burning rate	cm/s
R	total bed radius	cm
R'	gas constant	$\text{erg/K} \cdot \text{gmol}$
Re	Reynolds number	
t	time	s
T_g	gas temperature	K
T_p	particle temperature	K
T_{g0}	initial gas temperature	K
T_{p0}	initial particle temperature	K
u_g	radial component of gas velocity	cm/s
u_p	radial component of particle velocity	cm/s
w_g	axial component of gas velocity	cm/s
w_p	axial component of particle velocity	cm/s
z	axial coordinate	
z_c	location of opening in outer wall	cm
Γ_c	gas production rate during combustion	$\text{g/cm}^3 \cdot \text{s}$

LIST OF SYMBOLS (concluded)

Symbols	Definition	Units
δ	finite differencing operator	
Δr	radial distance between nodes	cm
Δz	axial distance between nodes	cm
Δz_c	length of opening in outer wall	cm
ϵ	time filter coefficient	
μ_g	gas viscosity	poise
μ_{g0}	initial gas viscosity	poise
ρ_g	gas phase density	g/cm^3
ρ_p	particle phase density	g/cm^3
ρ_{g0}	initial gas phase density	g/cm^3
ρ_{p0}	initial particle phase density	g/cm^3
ρ_1	bulk gas density	g/cm^3
ρ_2	bulk particle density	g/cm^3
τ	shear stress components	dyn/cm^2
ϕ	porosity	